University of Alberta

Characterization of GBF1, Arfs and COPI at the ER-Golgi Intermediate Compartment and Mitotic Golgi Clusters

by

Justin Chun

A thesis submitted to the Faculty of Graduate Studies and Research
in partial fulfillment of the requirements for the degree of

Doctor of Philosophy

Department of Cell Biology

Fall 2009
Edmonton, Alberta

Examining Committee

Dr. Paul Melançon, Department of Cell Biology

Dr. Richard Rachubinski, Department of Cell Biology

Dr. Gary Eitzen, Department of Cell Biology

Dr. Michael Hendzel, Department of Oncology

Dr. John Bergeron, Department of Anatomy and Cell Biology, McGill University

ABSTRACT

Protein trafficking between the endoplasmic reticulum (ER) and Golgi complex is regulated by the activity of ADP-ribosylation factors (Arfs). Arf activation by guanine nucleotide exchange factors (GEFs) leads to the recruitment of the coatomer protein COPI and vesicle formation. By using fluorescently-tagged proteins in live cells, we have been able to identify novel functions for Arfs and the Arf-GEF GBF1 at the ER-Golgi intermediate compartment (ERGIC) and mitotic Golgi clusters. We first focused on Arf function at the ERGIC after observing both class I (Arf1) and class II (Arfs 4 and 5) Arfs at this structure. We discovered that class II Arfs remain bound to ERGIC membranes independently of GBF1 activity following treatment with brefeldin A (BFA). Further characterization of the class II Arfs using additional pharmacological agents such as Exo1 and inactive mutant forms of Arf4 demonstrated that the class II Arfs associate with the ERGIC membrane via receptors distinct from GBF1. Our work suggests that GBF1 accumulation on membranes in the presence of BFA is due to loss of Arfs from the membrane rather than the formation of an abortive complex with Arf and GBF1. Next, while studying GBF1 in live cells, we unexpectedly observed GBF1 localizing to large fragmented structures during mitosis. We identified these structures as mitotic Golgi fragments that are positive for GBF1 and COPI throughout mitosis. Again using live cells treated with BFA and Exo1, we demonstrated that GBF1 concentrates on these mitotic fragments suggesting that they are derived from Golgi membranes. By colocalization studies and

fluorescence recovery after photobleaching, we demonstrated that these mitotic fragments maintain a *cis-to-trans* subcompartmental Golgi polarization and membrane dynamics of GBF1 similar to interphase cells. Interestingly, inactivation of GBF1 and loss of COPI from the membranes of the mitotic Golgi fragments did not delay progressing through mitosis. Our results from our second project indicate for the first time that the mitotic Golgi clusters are bona fide Golgi structures that exist throughout mitosis with a functional COPI machinery.

ACKNOWLEDGEMENTS

Many thanks to my supervisor Dr. Melançon for giving me the opportunity to train in a stimulating and productive environment. I appreciate all the support and guidance he has provided for me during my graduate studies in his laboratory. Also, I could not have asked for a better supervisory committee. Drs. Rachubinski and Eitzen have provided me with excellent feedback and advice. I could not have completed my graduate work without their expertise and faith in my abilities. I would like to thank Drs. Hendzel and Bergeron for their constructive criticisms and challenging me to perform to the highest standards.

I will definitely miss the Department of Cell Biology including the office staff, graduate students, technicians, post-docs and professors. I will especially miss both past and present members of the Melançon lab including Xinhua, Ileana, Lisa, Zoya, Anh, Florin, Nathan, and Douglas. In particular, Florin has been a great "pal" ever since we first met. The members of this world-class department have made graduate school an unforgettable experience.

Lastly, I dedicate this thesis to my wife, family and friends who have been very supportive and encouraging. Their support enabled me to overcome some of the most exhausting months of my life.

TABLE OF CONTENTS

LIST OF TABLES

LIST OF FIGURES

LIST OF SYMBOLS AND ABBREVIATIONS

ADP	adenosine diphosphate
AP	adaptor protein
Arf	ADP-ribosylation factor
Arl	ADP-ribosylation factor-like
ARNO	ARF nucleotide-binding site opener
ATCC	American type culture collection
ATP	adenosine triphosphate
BFA	brefeldin A
BIG	BFA-inhibited GEF
C	Cytosol
CCD	charge-coupled device
CHO	Chinese hamster ovary
COP	coatomer protein
COS	CV-1 (simian) in Origin, and carrying the SV40 genetic material
ddH_2O	double distilled water
DMSO	dimethyl sulfoxide
E	glutamate
ECL	enhanced chemiluminescence
EM	electron microscopy
ER	endoplasmic reticulum
ERES	ER exit sites
ERGIC	ER-Golgi intermediate compartment
Exo1	2-(4-fluorobenzoylamino)-benzoic acid methyl ester
FBS	fetal bovine serum
FRAP	fluorescence recovery after photobleaching
g	gram
GalT	galactosyltransferase
GAP	GTPase activating protein
GBF1	Golgi-specific BFA resistance factor 1
GDP	guanosine diphosphate
GEF	guanine nucleotide exchange factor
GFP	green fluorescent protein
GGA	gamma-ear-containing, ARF-binding protein
GTP	guanosine triphosphate
h	hour(s)
HA	hemagglutinin
HRP	horseradish peroxidase
I	isoleucine
IF	immunofluorescence
IP	immunoprecipitation
K	lysine
KD	knockdown

L	leucine
M	microsomal
Man II	mannosidase II
mCherry	monomeric Cherry (red fluorescent protein)
min	minute(s)
NA	numerical aperture
NOZ	nocodazole
NRK	normal rat kidney
PBS	phosphate buffered saline
PCR	polymerase chain reaction
PFA	paraformaldehyde
PH	pleckstrin homology
PM	plasma membrane
PS	phosphoserine
Q	glutamine
s	second(s)
SDS-PAGE	sodium dodecyl sulphate-polyacrylamide gel electrophoresis
Sec7d	Sec7 domain
SNARE	soluble *N*-ethylmaleimide sensitive factor attachment receptor
TGN	*trans*-Golgi network
VSV	vesicular stomatitis virus
VSV-G	VSV-glycoprotein
VTC	vesicular tubular cluster
WT	wild type
w/v	weight per volume

CHAPTER ONE: INTRODUCTION

1.1 Overview of the secretory pathway: ER to Golgi transport

The secretory pathway of eukaryotic cells is a highly organized endomembrane system consisting of several independent organelles including the endoplasmic reticulum (ER), the ER-Golgi intermediate compartment (ERGIC), the sub-compartments of the Golgi complex, and the *trans*-Golgi network (TGN) (Figure 1.1). Quantitative proteomic analysis has established that over 1400 proteins maintain the secretory pathway (Gilchrist *et al.*, 2006). Proteins involved in ER-to-Golgi transport distribute to organelles of the secretory pathway and work cooperatively to synthesize, modify, sort, and secrete newly synthesized proteins. Organelles within this pathway have very discrete roles and function sequentially to transport and secrete proteins.

1.1.1 Protein synthesis and transport in the ER

Protein synthesis begins in the ER as ribosomes dock onto a protein pore in the ER membrane and release newly synthesized polypeptides into the lumen of the ER (Lee *et al.*, 2004). The chaperones of the ER lumen facilitate the folding of a new protein to its proper conformation. Also, the ER is the site for the first post-translational modifications of nascent chains, including the addition of N-linked glycan chains and hydroxylation of prolines. Next, secretory proteins ready for transport from the ER are sorted into specialized subdomains of the ER called ER exit sites (ERES) or transitional ER (tER). The ERES are long-lived, ribosome-free structures devoted to generating anterograde transport vesicles (Palade, 1975; Bannykh *et al.*, 1996; Bannykh and Balch, 1997). Nascent cargo

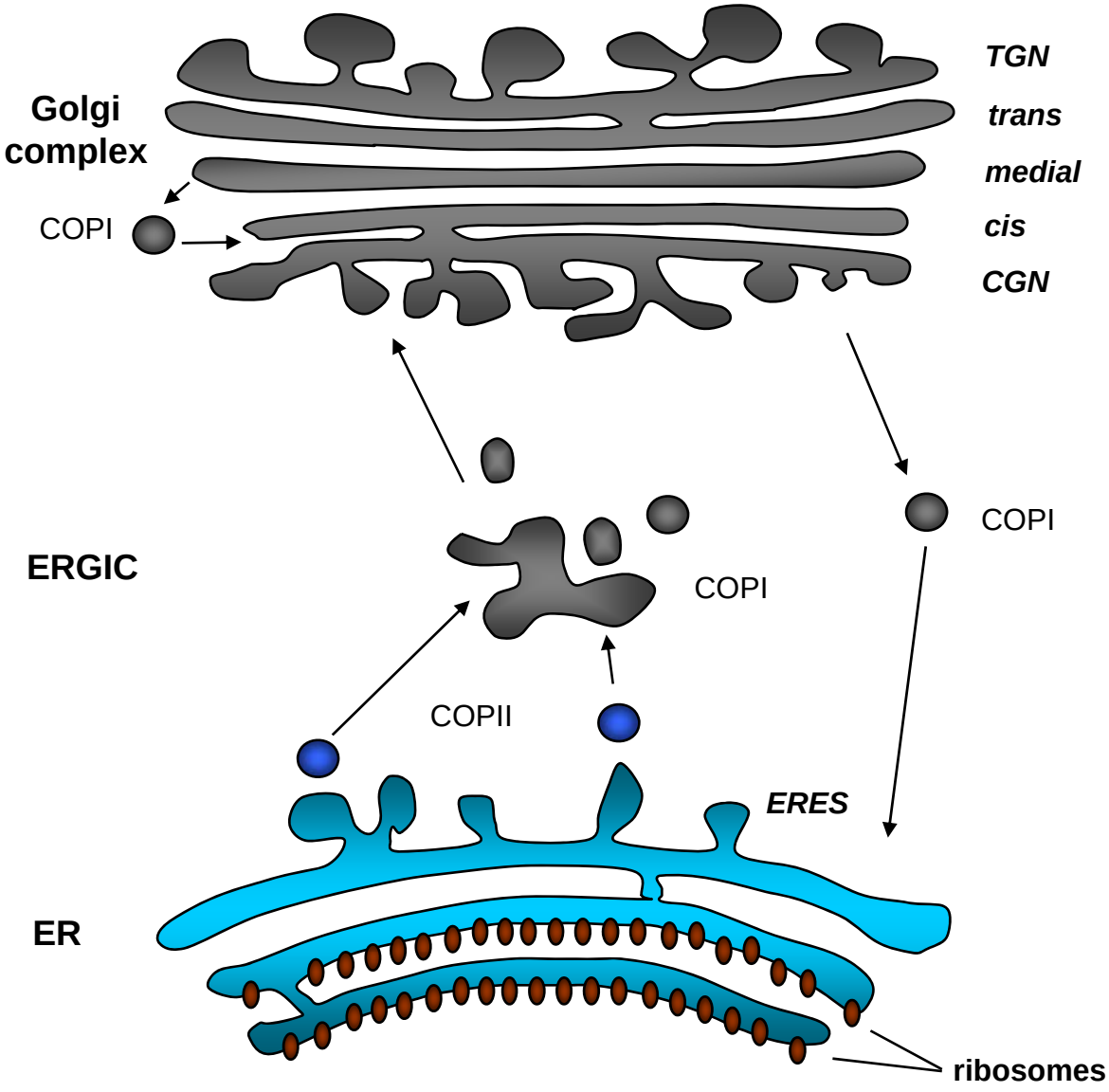

Figure 1.1 Schematic depicting the organelles and coats involved in ER-to-Golgi trafficking. Depiction of vesicle transport pathways from the ER to the ERGIC and the Golgi complex. COPII and COPI mediate anterograde and retrograde transport carriers, respectively, from the ER to the ERGIC and Golgi complex. COPI is also involved in retrograde trafficking of resident Golgi enzymes within the Golgi stack.

proteins and a variety of cellular machinery proteins required for vesicle formation are selectively packaged into transport vesicles.

1.1.2 Protein transport to the ERGIC

In animal cells, proteins sorted into ERES are packaged into vesicles and transported from the ERES to the ERGIC. The ERGIC, also known as pre-Golgi intermediates and vesicular tubular clusters (VTCs), was originally identified as a complex membrane system consisting of vesicles and tubules (Hauri and Schweizer, 1992; Saraste and Kuismanen, 1992; Bannykh *et al.*, 1996). A hexameric, 58 kDa protein (now known as p58 in rats and ERGIC-53 in humans) was first characterized by Saraste *et al*. in rat pancreatic exocrine cells as a major component of pre- and *cis*-Golgi elements (Saraste *et al.*, 1987; Lahtinen *et al.*, 1992). ERGIC-53 is now a well characterized cargo receptor that functions as a mannose-specific leguminous type lectin (Hauri *et al.*, 2000). p58 is a hallmark protein used to identify the ERGIC, but p58-GFP has been shown to localize to the ER, Golgi complex, and the ERGIC. p58-GFP localizes to two types of peripheral structures that consist of relatively stable punctate structures and fast moving tubules (Ben-Tekaya *et al.*, 2005). Interestingly, peripheral ERGIC structures appear in close proximity to, but remain distinct from, ERES. Although the ERGIC cannot be fully resolved from ERES by light microscopy, it is clearly resolved by electron microscopy (Schweizer *et al.*, 1988; Schweizer *et al.*, 1990; Appenzeller-Herzog and Hauri, 2006).

ERGIC-53 facilitates the transport of many proteins from the ER to the Golgi complex. Early work by Hauri's group demonstrated that the transport of

the lysosomal enzymes, cathepsin C and cathepsin Z, are mediated by ERGIC-53 and suggested that ERGIC-53 is a receptor facilitating ER-to-ERGIC transport (Vollenweider *et al.*, 1998; Appenzeller, *et al.*, 1999). The same group also demonstrated that mutations of ERGIC-53 cause combined deficiency of blood coagulation factors V and VIII (Nichols *et al.*, 1998; Zhang *et al.*, 2003). The multiple coagulation factor deficiency 2 gene (MCFD2) is a protein with EF-hand domains that interacts with ERGIC-53 and important for the selective binding of ERGIC-53 to factors V and VIII (Zhang *et al*., 2003; Nyfeler *et al.*, 2006). Recent work by Nyfeler *et al*. has identified α_1-antitrypsin as another soluble secretory protein transported by ERGIC-53 (Nyfeler *et al*., 2008). These studies examining ERGIC-53 in ER-to-Golgi transport have provided good evidence for active receptor-mediated ER export of secretory proteins.

In contrast to our reasonably good understanding of ERGIC-53 and its cargoes, very little is known about the cargo receptors for many soluble secretory proteins and the proteins functioning at the ERGIC. In addition to the cargo transported by ERGIC-53, proteins that have been localized to the ERGIC include β-COP, p115, syntaxin 5 (Sed5 in yeast), GM130, p23 and p25 of the p24 family and Surf4 (Erv29 in yeast) (Schindler *et al.*, 1993; Banfield *et al.*, 1994; Rojo *et al.*, 1997; Orci *et al.*, 1998; Mitrovic *et al.*, 2008). The functions of these proteins at the ERGIC are not well understood, but at least Surf4, ERGIC-53 and p25 have been demonstrated to be required to maintain the architecture of the ERGIC and Golgi complex (Mitrovic *et al.*, 2008).

There is still an ongoing debate as to whether the ERGIC forms by homotypic fusion of COPII vesicles or if it is a pre-formed structure that accepts newly synthesized COPII vesicles by heterotypic fusion (Bethune *et al.*, 2006b). Though the ERGIC was initially thought to be either a specialized domain of the ER (Sitia and Meldolesi, 1992) or the *cis*-Golgi (Mellman and Simons, 1992), recent studies now support the notion that the peripheral ERGIC constitutes independent structures (Appenzeller-Herzog and Hauri, 2006). Also, observations from live cell microscopy suggest that the peripheral ERGIC consists of a population of stable structures that may have a sorting function or a function in quality control (Zuber *et al.*, 2001; Ben-Tekaya *et al.*, 2005; Appenzeller-Herzog and Hauri, 2006). Based on recent studies, two models have been proposed to describe protein trafficking from the ER to the Golgi complex (Figure 1.2). The first model, called the transport complex model, proposes that anterograde transport vesicles that bud from the ERES tether and fuse to form pleiomorphic carriers that are transported along the microtubule cytoskeleton (Bannykh *et al.*, 1998; Stephens and Pepperkok, 2001). This model was derived from studies using fluorescently tagged overexpressed viral protein (tsO45-VSV-G) in live cells (Presley *et al.*, 1997; Scales *et al.*, 1997). These live cell imaging experiments showed that tsO45-VSV-G-GFP moves from ERES to the Golgi along microtubules using the minus-end directed motor dynein. However, one problem with the transport complex model is that overexpressed tsO45-VSV-G-GFP was the only marker used and assumed to be identical to the ERGIC clusters. Since overexpression of the viral protein can lead to an exaggeration of membrane

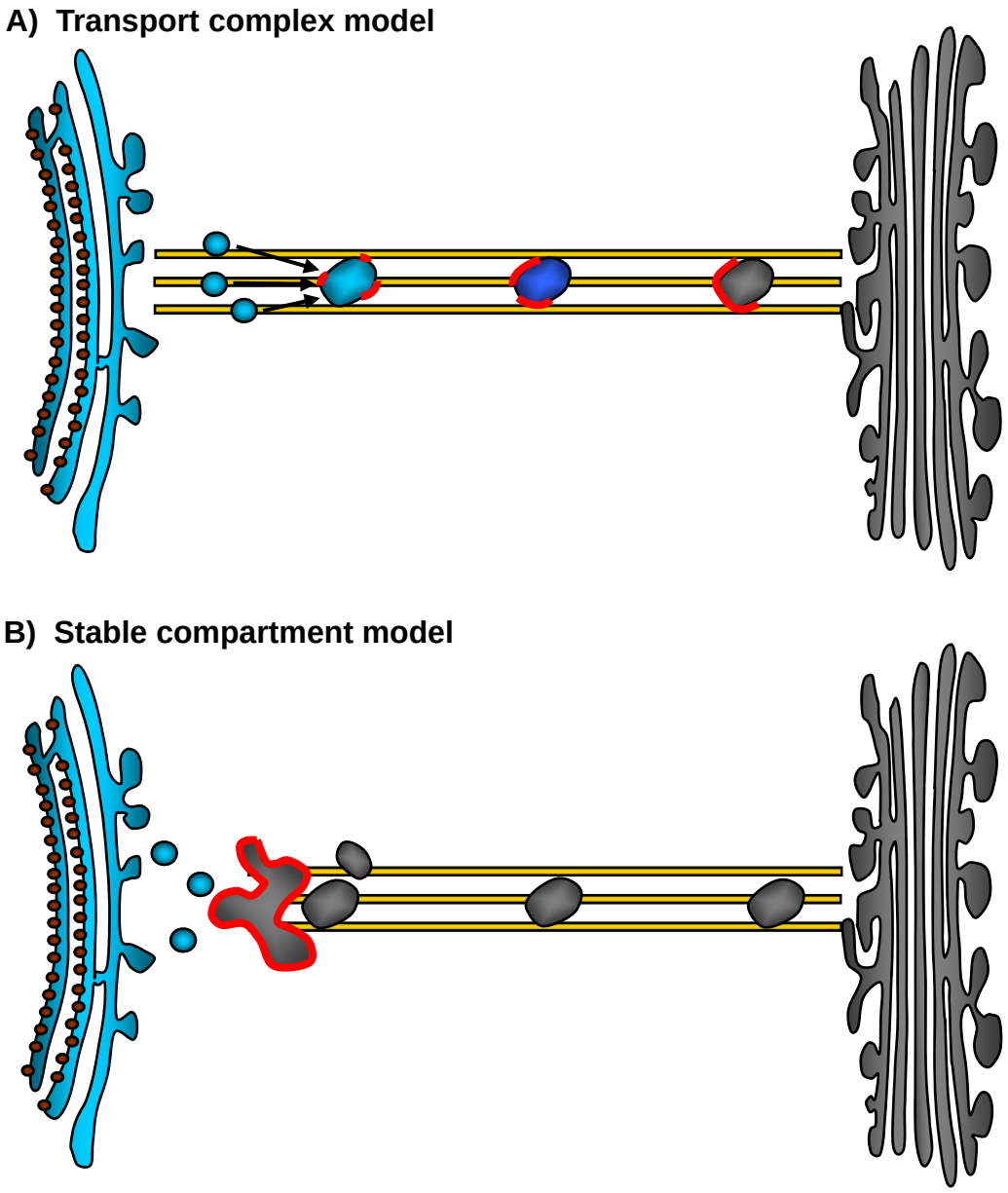

Figure 1.2 Role of the ERGIC in ER-Golgi transport.
A) Transport complex (TC) model. COPII vesicles bud from ERES and then fuse to form pleiomorphic TCs. The TCs, thought to be identical to the ERGIC, are transported down a microtubule highway (yellow lines) by a process dependent on the motor dynein. COPI (red areas) functions to segregate an anterograde cargo-rich domain from a retrograde cargo-rich domain. The TCs are thought to fuse with the *cis*-most cisterna of the Golgi complex or form a new *cis*-Golgi cisterna.
B) Stable compartment model. Vesicle transport from the ERES to the ERGIC is regulated by COPII but microtubule-independent. Long-range transport from the ERGIC to the Golgi complex requires the activity of a dynein motor and the presence of microtubules. COPI (red outline) may be involved in sorting of cargo at the ERGIC and the fission of anterograde cargo carriers from the ERGIC. The ERGIC generates anterograde carriers destined to the *cis*-Golgi cisterna.

movement or the suppression of ER quality control mechanisms, future studies using additional proteins will be necessary. Another concern with the transport complex model is the observation that the majority of peripheral ERGIC clusters are in close proximity to ERES rather than being randomly located between the ER and Golgi complex. Lastly, incubating cells at 15^{o}C, which is known to block ERGIC-to-Golgi but not ER-to-ERGIC trafficking of ERGIC-53, does not increase the number of ERGIC clusters as would be predicted by the transport complex model (Klumperman *et al.*, 1998).

In contrast to the transport complex model, recent live cell imaging of GFP-tagged ERGIC-53 by Hauri's group has suggested the presence of long-lived membrane compartments (Ben-Tekaya *et al.*, 2005). Using dual label live cell imaging, they demonstrated that stationary peripheral ERGICs are sites of repeated sorting of a secretory marker, signal-sequence-tagged DsRed (ssDsRed) (Ben-Tekaya *et al.*, 2005). Their work supports the stable compartment model, which proposes that anterograde carriers leave from the ERGIC compartment when moving towards the Golgi complex. Also, their results are consistent with the notion that the ERGIC represents the first sorting station that discriminates between anterograde and retrograde transport (Martinez-Menarguez *et al.*, 1999). Thus protein exported from the ER may be packaged directly into carriers for transport towards the *cis*-Golgi (transport complex model) or alternatively sorted into anterograde carriers derived from the ERGIC following modification (stable compartment model).

1.1.3 Protein transport through the Golgi stack

Anterograde carriers from the ERGIC are thought to transport folded secretory proteins to the Golgi complex, the primary location for protein and lipid modification and sorting. The Golgi complex is the central organelle of the secretory pathway that functions as a hub for secreted proteins to be delivered to the plasma membrane or lysosomes (Pfeffer, 2001). This organelle consists of usually four to six membrane-bound sacks called cisternae that are readily visible by conventional electron microscopy (EM) studies of thin sections of cells (Mogelsvang *et al.*, 2004; Bethune *et al.*, 2006b). Recently, advanced tools for 3D visualization called EM tomography have provided insight into the structure and function of the Golgi complex (Mogelsvang *et al.*, 2004). The Golgi stack is actually a continuous ribbon of cisternae that can be classified as *cis*, *medial* and *trans* based on biochemical and structural criteria. Material packaged in the ER into vesicles of approximately 50 nm or VTCs advance to the highly fenestrated *cis*-face of the Golgi ribbon to fuse with a pre-existing *cis*-cisterna or to form a new cisterna using the existing *cis*-cisterna as a template (Marsh *et al.*, 2001). Next, the proteins move from the *cis*-Golgi through the *medial*-Golgi and exit from the *trans*-Golgi. Finally, the TGN functions as a sorting station that sends proteins to the plasma membrane or redirects proteins to additional compartments of the endomembrane system.

The organization of the Golgi stack into *cis*-, *medial*-, and *trans*-compartments allows compartmentalization of enzymes that function in glycan side chain modification of glycoproteins and proteolytic cleavage. Each cisterna

is the site of distinct Golgi enzymes including glycosyltransferases, Golgi matrix proteins, and GTPases (Pfeffer, 2001). For example, the proteins p115, mannosidase II, and BIG1/2 can be resolved by confocal or electron microscopy to the *cis*-, *medial*-, and *trans*-cisternae, respectively, of the Golgi stack (Velasco *et al.*, 1993; Nelson *et al.*, 1998; Zhao *et al.*, 2002). In addition, many kinases act on proteins localized to the Golgi complex. For example, protein kinase D (PKD) is a well characterized kinase that regulates fission of anterograde transport carriers at the TGN (Liljedahl *et al.*, 2001; Ghanekar and Lowe, 2005). Also, several mitotic kinases, including Cdc2, MEK1, and Polo-like kinase 1, have important roles in the disassembly-reassembly of the Golgi complex (Acharya *et al.*, 1998; Lowe *et al.*, 1998; Sutterlin *et al.*, 2001).

1.2 The molecular mechanisms involved in ER-to-Golgi trafficking

Membrane traffic between the ER and Golgi complex is regulated by the collaborative effort of a plethora of proteins (Bonifacino and Glick, 2004). The directionality of protein transport from one organelle to another involves three well defined events. First, cargo recruitment and vesicle budding are mediated by cargo carriers and coat proteins. Next, cargo-containing vesicles associate with microtubule motors to transit along the microtubules to the acceptor compartment. Lastly, vesicles docking and fusion are controlled by tethering factors and SNAREs (soluble *N*-ethylmaleimide sensitive factor attachment receptors). In addition to the coat proteins, motors, and SNAREs, tethering factors such as p115 and the Rab proteins also play important roles. Rabs are thought to regulate both

the activity of motors as well as the recruitment of tethering factors and SNAREs (Beraud-Dufour and Balch, 2002). Although the collaborative efforts of all the proteins at each step are required for transport from one organelle to another, the focus of this thesis will be the regulation of vesicle budding and formation. Therefore, emphasis will be placed on the coat proteins involved in vesicle formation at each organelle involved in ER-to-Golgi transport.

1.2.1 COPII machinery for protein export from the ERES

Formation of transport vesicles and cargo sorting between the organelles of the secretory pathway are bidirectional and microtubule-dependent processes generally regulated by the COPII and COPI coats (Lee *et al.*, 2004). Newly synthesized proteins are collected and exported as COPII-coated vesicles from ERES. The COPII coat acts at ERES for the formation of anterograde transport vesicles that sort and transport cargo to the ERGIC. The first step of COPII assembly requires recruitment of the small GTPase Sar1 from the cytosol to the ERES by Sec12, a transmembrane protein (Figure 1.3). Sec12 is a guanine nucleotide exchange factor that promotes release of GDP from Sar1 and allows binding of GTP (Futai *et al.*, 2004). Upon binding to GTP, Sar1 becomes activated, tightly binds to the ER membrane by a GTP-triggered membrane anchor and recruits the heterodimers adaptor complex Sec23/24 (Yoshihisa *et al.*, 1993; Bi *et al.*, 2002; Fromme *et al.*, 2008). The Sec13/31 coat protein complex then binds Sec23/24, and polymerizes to form the coat lattice (Barlowe *et al.*, 1994; Stagg *et al.*, 2006). The hydrolysis of Sar1-GTP to produce Sar1-GDP is catalyzed by Sec23, which acts as a GAP (GTPase activating protein) whose

A) COPII coat formation

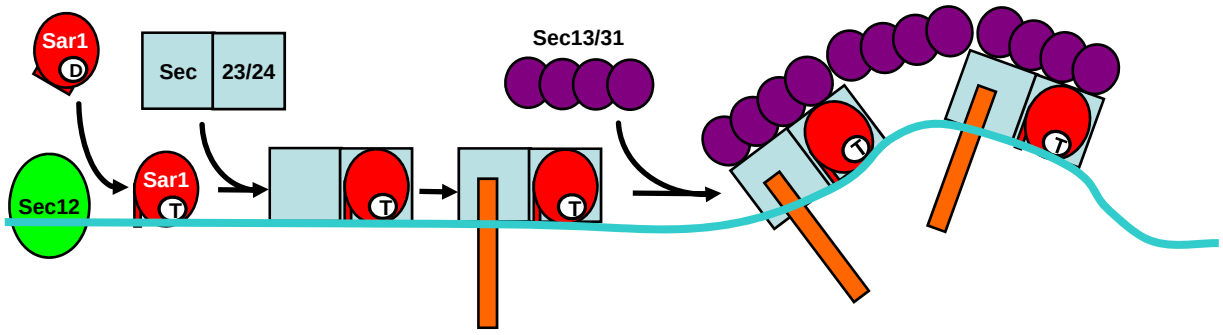

B) COPI coat formation

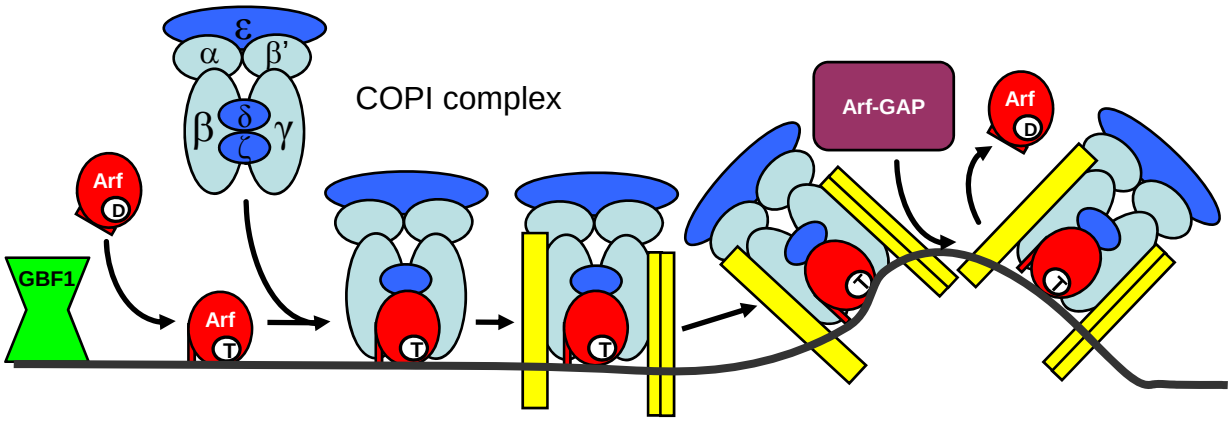

Figure 1.3 COPII and COPI coat assembly for vesicle formation.
A) COPII coat complex for anterograde vesicle transport from ERES. Sec12, a GEF for Sar1, initiates COPII coat assembly by stimulating the exchange of GDP (D) for GTP. (T). GTP binding to Sar1 exposes an amphipathic α-helix that aides in ER membrane binding. Next, a heterodimer of Sec23/24 is recruited by Sar1 forming a Sar1-Sec23/24 complex that interacts with cargo proteins (orange rectangle). A heterotetramer of Sec13/31 is thought to be recruited to polymerize the COPII coat and drive vesicle budding.
B) COPI coat complex for retrograde vesicle transport at ERGIC and Golgi membranes. An Arf-GEF (GBF1) initiates the exchange of GDP (D) for GTP (T) on Arf1 at ERGIC and Golgi membranes. Activated, membrane-bound Arf1 recruits the preassembled heptameric COPI complex. Specific subunits of the COPI coatomer complex contain cargo recognition sites that bind to different cargo proteins (yellow rectangles). The COPI coat polymerizes by an unknown mechanism. Arf-GAP recruitment to the budding membrane stimulates the hydrolysis of Arf-GTP resulting in release of Arf-GDP and the dissociation of the COPI coat from the membrane.

activity is stimulated upon recruitment of the Sec13/31 heterodimer (Yoshihisa *et al.*, 1993; Antonny *et al.*, 2001).

Reconstitution experiments have demonstrated that Sar1, Sec23/24, and Sec13/31 make up the minimal COPII machinery (Barlowe, 2003). However, additional factors regulate the proper assembly and disassembly of COPII-coated vesicles. For example, in addition to the well established molecular players for the COPII coat, Sec16 interacts with multiple components of the COPII machinery including Sar1, Sec23, Sec24, and Sec31 (Espenshade *et al.*, 1995; Gimeno *et al.*, 1996; Shaywitz *et al.*, 1997; Supek *et al.*, 2002). It appears that Sec16 plays an important role in nucleating and regulating COPII vesicle formation (Shaywitz *et al.*, 1997; Supek *et al.*, 2002). A recent study in *Pichia pastoris* has suggested that Sec16 functions in ERES organization by helping to organize COPII into clusters that make up the ERES (Connerly *et al.*, 2005). Many studies have established the general players for COPII coat formation, but it remains unclear as to how ERES are made and maintained or the mechanism by which COPII vesicle budding is restricted to ERES.

1.2.2 The COPI machinery at the ERGIC and Golgi complex

COPI-coated vesicles are involved in intra-Golgi traffic to maintain the structure of the Golgi complex and mediate the retrograde transport of proteins such as escaped ER proteins and machinery proteins. The 700 kDa, heptameric COPI coat, originally identified as having a role in coating vesicles formed at the periphery of the Golgi complex and within the Golgi stack, is molecularly distinct from the COPII coat (Orci *et al.*, 1986; Lee *et al.*, 2004). An obvious difference

between the COPII and COPI coats is that whereas the Sar1 GAP is an integral part of the COPII coat, the GTP hydrolysis on Arf1 is stimulated by a separate Arf-GAP that may function as a coat component during cargo selection and vesicle formation (Lee *et al.*, 2005). Also, unlike the COPII coat, COPI is composed of seven subunits: α-, β-, β'-, γ-, δ-, ε-, and ζ-COPs (Figure 1.3). Four subunits of the COPI, β, γ, δ, ζ , have sequence homology to the clathrin-binding adaptor protein (AP) complexes, and the α, β', ε subunits may function similarly to clathrin as a structural scaffold (Lee *et al.*, 2004). The genes encoding each coatomer subunit except for ε-COP (a structural component of the COPI coat) have been demonstrated to be essential for cell viability in yeast.

The forward transport of secretory proteins from the ER is balanced by a retrograde transport pathway regulated by COPI. In mammalian cells, COPI localizes predominantly to the *cis*-Golgi and the ERGIC (Duden *et al.*, 1991; Scales *et al.*, 1997). The retrograde transport from the Golgi complex and the ERGIC by COPI functions to recycle components required for ERES-derived vesicle formation and to retrieve proteins containing a dilysine retrieval signal (Cosson and Letourneur, 1994). During coat formation, the seven subunits of COPI are recruited *en bloc* to the Golgi membrane and directly bind to dilysine motifs at the C-terminus of cargo proteins (Cosson and Letourneur, 1994; Hara-Kuge *et al.*, 1994; Letourneur *et al.*, 1994; Elsner *et al.*, 2003). Many proteins, including ER resident proteins and the p24 family of proteins, have been shown to bind COPI. Interestingly, ER resident proteins bind to coatomer on the α and β' subunits, while transmembrane proteins of the p24 family of proteins require

dimerization and bind to γ-COP (Bethune *et al.*, 2006a). The ability of the different subunits of COPI to bind different cargo protein suggests that each subunit has a specific function in cargo sorting.

In addition to its role in the retrograde transport of ER resident proteins and other transmembrane proteins, COPI may play an important role in sorting retrograde cargo from anterograde cargo at the ERGIC and structural maintenance of the ERGIC and the Golgi complex. It appears that the ERGIC discriminates between anterograde and retrograde cargo, since recycling membrane proteins are concentrated in COPI-positive structures while secretory cargo is mainly found in COPI-negative regions of the ERGIC (Martinez-Menarguez *et al.*, 1999). Interestingly, a very recent study by Hauri's group has revealed the importance of Surf4 (human orthologue of the yeast cargo receptor Erv29p) in maintaining the architecture of the ERGIC and the Golgi complex. Knockdown of Surf4 with ERGIC-53 caused a partial redistribution of COPI but not of Golgi matrix proteins to the cytosol (Mitrovic *et al.*, 2008). Taken together, these studies show the importance of COPI in protein sorting and maintenance of the ERGIC and Golgi structure.

1.2.3 Current models for COPI activity and protein trafficking at the Golgi complex

COPI has a crucial function in retrograde cargo transport and in maintaining the structure of the Golgi complex but the exact role of COPI in intra-Golgi trafficking remains controversial. The role of COPI at the Golgi complex is debatable as evident in the existence of several models for intra-Golgi. The first

model, called the vesicular transport model, proposes that cargo is transported anterogradely between static cisternae by coordinated budding and fusion reactions, while the retrograde-directed COPI vesicles transport Golgi resident enzymes (Rothman and Wieland, 1996). The vesicular transport model favours the notion of a stable Golgi complex. The vesicular transport model has fallen out of favour since it cannot account for many experimental observations. For example, the vesicular transport model cannot explain the transport of larger molecules such as procollagen that cannot fit in COPI vesicles nor why small proteins such as VSV-G move synchronously with procollagen at indistinguishable rapid rates (Bonfanti *et al.*, 1998; Mironov *et al.*, 2001). Also Martinez-Menarguez *et al*. demonstrated that purified intra-Golgi COPI vesicles contain retrograde proteins rather than anterograde proteins (Martinez-Menarguez *et al.*, 2001). A second model called the cisternal maturation model is now the favoured model since it better addresses the inconsistencies between the predictions of the vesicular transport model and experimental data for intra-Golgi transport.

The cisternal maturation model proposes that anterograde cargo is transported *en bloc* with cisternae (Glick and Malhotra, 1998). This model postulates that pre-Golgi carriers fuse at the *cis*-Golgi to assemble into new cisternae. COPI vesicles are thought to transport Golgi processing enzymes from late cisternae to earlier cisternae closer to the *cis*-Golgi to maintain the distinct compositions of each cisterna resulting in the maturation of each cisterna. As Golgi processing enzymes are transported from *trans*-compartments to *cis*-

compartments, early compartments containing cargo progress through the Golgi stack as they mature. In the past, the cisternal maturation model has been criticized for not accounting for the presence of anterograde cargo within COPI vesicles (Nickel *et al.*, 1998; Pepperkok *et al.*, 2000) nor the different transport rates of anterograde cargo (Bonfanti *et al.*, 1998). However, recent data obtained by the laboratories of Glick and Nakano have provided good evidence for the cisternal maturation model. Independently, both laboratories demonstrated by direct visualization in real time using yeast that early Golgi markers are replaced by later Golgi markers on the same membrane (Losev *et al.,* 2006; Matsuura-Tokita *et al.*, 2006). Their work provides direct evidence that a single Golgi membrane can undergo a transition from a *cis* composition to a *trans* composition over time. Based on these landmark papers, the cisternal maturation model is now the preferred model for intra-Golgi transport.

In addition to the cisternal maturation model and the vesicular transport model, other models have also been proposed. First, the percolating vesicle model (Orci *et al.*, 2000; Pelham and Rothman, 2000) combines aspects of both the cisternal maturation model and the vesicular transport model. In this model, one population of COPI vesicles would mediate the fast transport of anterograde cargo between all cisternae in a bidirectional manner, while a second COPI vesicle population would allow recycling back to the ER. Next, studies based on electron tomography revealing tubular inter-cisternal connections (Trucco *et al.*, 2004) led to the development of a continuity-based model (Mironov *et al.*, 2005). This model proposes that polymorphic carriers with the ability to bridge adjacent

cisternae mediate the transport of cargo. Since intra-Golgi transport of protein would be achieved by tubules, COPI vesicles would function to control inter-cisternal fusion events and to establish Golgi morphology (Bethune *et al.*, 2006b). Lastly, the most recent model of intra-Golgi trafficking proposed appears to be completely different from the major prevailing models. Lippincott-Schwartz and colleagues have proposed a new model called the rapid-partitioning model that can account for their results demonstrating that cargo exits the Golgi complex with exponential kinetics instead of having a lag or transit time (Patterson *et al.*, 2008). They propose a model that involves the partitioning of transmembrane cargo and enzymes within a two-phase membrane system that sorts lipids into different domains of the Golgi complex and association of proteins with their preferred lipid environment. Intra-Golgi transport is suggested to occur by rapid partitioning of enzymes and cargo between two lipid phases combined with rapid exchange between cisternae. Unlike previous models, this model postulates bidirectional trafficking of cargo and processing enzymes within the Golgi complex. Furthermore, the rapid-partitioning model emphasizes the importance of lipid-trafficking pathways. With the proposal of this challenging model, it appears that the model to best describe intra-Golgi transport and the role of COPI at the Golgi complex remains unclear. Therefore, future studies will be required to determine the prevailing model for intra-Golgi transport.

1.3 ADP ribosylation factors (Arfs)

ADP ribosylation factors (Arfs) are small, ubiquitous, GTPases belonging to the Ras superfamily. Contrary to their name, which was coined based on the identification of Arfs as protein cofactors required for cholera toxin to ADP-ribosylate the G_s heterotrimeric G protein (Kahn and Gilman, 1986), the endogenous role of Arfs does not involve ADP-ribosylation. Instead, Arfs play important roles in regulating membrane traffic and cytoskeleton organization. Arfs act as switches to regulate protein activity by cycling between their active GTP-bound and inactive GDP-bound states. Recruitment of Arf-GDP from cytosol to a membrane allows activation by a guanine nucleotide exchange factor (GEF). Subsequent inactivation of Arf-GTP by a GTPase activating protein completes the cycle and releases Arf-GDP to cytosol (Donaldson and Jackson, 2000).

Arfs are unique members of the Ras superfamily, since they are myristoylated at the second glycine residue of the amphipathic N-terminal helix (Antonny *et al.*, 1997) (Figure 1.4). Inactive, GDP-bound Arfs are primarily cytosolic since the amphipathic N-terminal helix is retracted in a hydrophobic groove on the protein. However, it has been postulated that myristoylated Arf1-GDP weakly associates with membranes through this myristoyl moiety before guanine nucleotide exchange (Antonny *et al.*, 1997). As GDP is replaced by GTP, Arf undergoes a conformational change causing the opening of switch 1 and switch 2 domains and rearrangement of the N-terminal helix and the interswitch region of Arf-GTP (Renault *et al.*, 2003) (Figure 1.4). The conformational

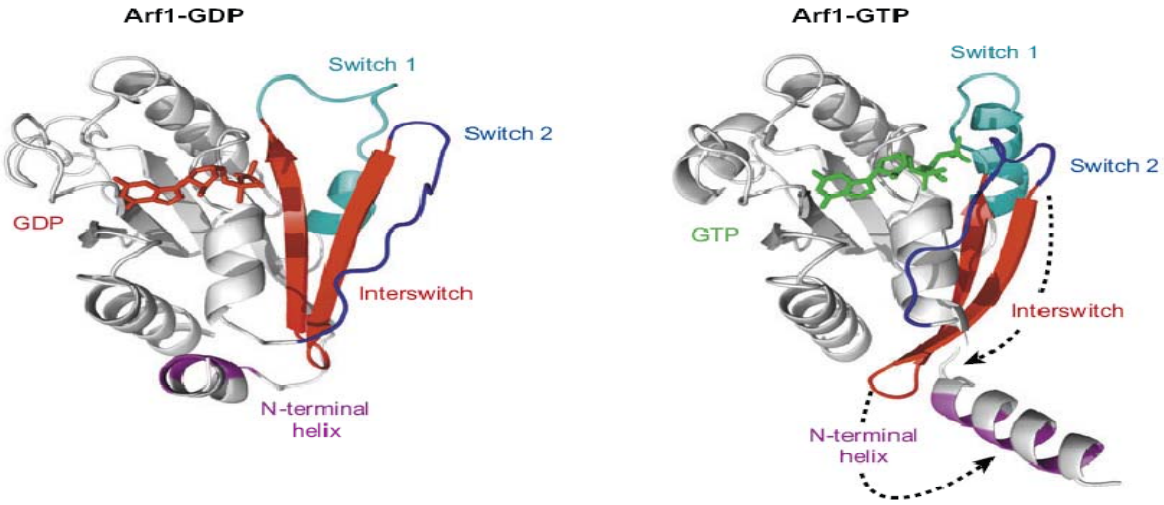

Figure 1.4 Structures of Arf1 in its GDP- and GTP-bound states.
Arf1-GDP contains an N-terminal, amphipathic helix that is buried in a pocket. When GTP binds to Arf1, a conformation change causes the interswitch to move away from Switch 1 and Switch 2. As a result, the N-terminal helix is displaced and available to interact with the membrane lipid bilayer. Adapted from Gillingham and Munro, 2007.

change requires displacement of the amphipathic N-terminal helix from the protein core and promotes tight association of active Arf-GTP with the membrane.

The myristoylated N-terminal helix is thought to mediate the stable interaction of the activated Arf with the membrane (Antonny *et al.*, 1997; Goldberg, 1998). However, there is evidence that myristoylation of the N-terminal helix may not be necessary for weak membrane interaction. For example, Arf1 can bind to membranes even without the myristoyl group, and Arf6 can associate with membranes even in the GDP-bound conformation (Franco *et al.*, 1993; Macia *et al.*, 2004).

1.3.1 Classes of Arfs

Relative to other GTPases, the Arf family of GTPases appears to have a distinct and early eukaryotic origin. Interestingly, the protist *Giardia lamblia*, which represents an early diverging lineage, has six Arf family members but no representative members of the Ras and heterotrimeric G-proteins (D'Souza-Schorey and Chavrier, 2006). Mammals express six Arf isoforms, Arf1-6 (Arf2 has been lost in primates), which are grouped into three classes based on primary sequence and gene organization (Kahn *et al.*, 2006).

Class I consists of Arfs 1-3 which share 96% sequence identity and are the most abundantly expressed in cells and tissues examined (Cavenagh *et al.*, 1996). Class I Arfs play critical roles in membrane traffic within eukaryotic cells by initiating the recruitment of various coat proteins and by modulating the activity of several lipid modifying enzymes (Donaldson and Jackson, 2000). The class II

Arfs, Arf4 and Arf5, are 90% identical to each other, occur at much lower abundance and remain poorly characterized. Arf6, the only class III Arf, shares the least degree of sequence identity to the other Arfs. Arf6 is thought to function in endosomal membrane traffic and structural organization at the plasma membrane (D'Souza-Schorey *et al.*, 1995; Peters *et al.*, 1995).

1.3.2 Distinct cellular localization and function of the Arfs

Based on *in vitro* studies using biochemical assays, Arf proteins were thought to have redundant roles since they shared common effector functions. Such functions include activation of phospholipase D (Liang *et al.*, 1997), activation of phosphatidylinositol 4-phosphate 5-kinase (Honda *et al.*, 1999), COPI recruitment to Golgi membranes (Liang and Kornfeld, 1997), and binding to Golgi-localized, gamma-ear-containing, ARF-binding proteins (GGAs) (Takatsu *et al.*, 2002). In addition, *in vitro* assays suggested a role for Arf1 in ER-to-Golgi transport (Balch *et al.*, 1992), intra-Golgi transport (Taylor *et al.*, 1992), nuclear vesicle dynamics (Boman *et al.*, 1992), and endosome fusion (Lenhard *et al.*, 1992). Lastly, compartmentalization of the Arfs within the cellular environment may be necessary for maintaining the unique function of each Arf since the majority of Arf effector molecules identified can bind with more than one Arf protein *in vitro* (D'Souza-Schorey and Chavrier, 2006). A major concern with reconstitution assays is that an Arf with a specific function within the cell would be able to complement a function played by a different Arf. Also, within a cell, Arf proteins may have specific functions based on their

distinct cellular localization or compartmentalization, which allows interaction with specific molecules.

The best characterized Arfs, Arf1 and Arf6, often localize to distinct compartments where they perform different functions (Peters *et al.*, 1995). While Arf1 localizes primarily to the Golgi complex to regulate the assembly of several types of coat complexes, Arf6 has been shown to regulate endosomal membrane traffic and structural organization at the plasma membrane (D'Souza-Schorey and Chavrier, 2006). *In vivo*, Arf6 has been shown to have a very selective effect for endocytic structures and no effect on regulating COPI coated vesicles at the Golgi complex (Peters *et al.*, 1995). Also, although little is known about Arf4, it has been implicated in the sorting of rhodopsin into post-Golgi carriers (Deretic *et al.*, 2005). Therefore, the few *in vivo* studies to date have suggested more specific and defined roles for each of the Arfs. It appears that there may be protein or lipid determinants at specific locations in the cell that ensure compartment identity (D'Souza-Schorey and Chavrier, 2006).

In addition to the distinct cellular localization of Arfs, there may also be differences in the intrinsic activity of Arfs. For example, although Arf1 is less abundant than Arf3 in bovine brain extract, Arf1 had a three- to five-fold greater specific activity than Arf3 in a transport inhibition assay (Taylor *et al.*, 1992). Furthermore, when Golgi-enriched membranes and either purified Arf1 or Arf3 were incubated in the presence of GTPγS, more Arf1 bound than Arf3 (Tsai *et al.*, 1992). These results are surprising, since Arf1 and Arf3 belong to the same class and have 96% sequence identity (Cavenagh *et al.*, 1996). Nevertheless, they

suggest that subtle differences in amino acid sequence between the Arfs may result in a specific function or signal for specific localization.

Despite apparently unique roles for each Arf, recent reports suggest that they may not function independently of each other. Arf knockdown (KD) studies by Kahn and colleagues revealed that distinct pairs of Arfs may be required at each step of protein traffic (Volpicelli-Daley *et al.*, 2005). For example, disruption of ER to Golgi traffic resulted only from double KD of Arf1 and Arf4. Requirement for specific Arf pairs suggests that even though there may be some functional redundancy between individual Arfs, each Arf must play some distinct and critical roles. Consistent with this notion, a recent study by Donaldson and colleagues revealed a mechanism in which activated Arf6 promotes recruitment of the ARF nucleotide-binding site opener (ARNO) protein for subsequent activation of Arf1 on endosomes (Cohen *et al.*, 2007). Therefore, the cooperative role or cross-talk between different Arf members may serve as a potential mechanism for mediating activities in a specific sequence.

1.3.3 The Arf-like (Arl) proteins involved in protein trafficking

In addition to the Arfs and Sar1, there are a number of other Arf-like (Arl) proteins that have the typical features of Arf GTPases (Munro, 2005). Arl1 and Arl3 have been shown to be localized to the *trans*-side of the Golgi complex (Lowe *et al.*, 1996; Lu *et al.*, 2001; Panic *et al.*, 2003). Interestingly, the recruitment of Arl1 to the Golgi complex requires the activity of Arl3, indicating that one Arl regulates the recruitment of a second Arl (Panic *et al.*, 2003; Setty *et*

al., 2003). Arl3-GTP may be required for regulating the recruitment or activation of the unidentified GEF for Arl1 (Munro, 2005).

Arl1 appears to be important for the regulation of Golgi structure and function. Overexpression of Arl1(Q71L), a mutant locked in its GTP-bound form, causes a stable association of COPI, Arfs and AP-1 coats to an expanded Golgi complex (Lu *et al.*, 2001). How Arl1 is regulated at the Golgi complex remains unknown. Also, neither the GEF nor the GAP for the Golgi-localized Arl1 have been identified. It may be possible that the GEFs or GAPs for Arf1 act on Arl1 (Munro, 2005).

1.3.4 Arf receptor(s)

Myristoylation of the N-terminal helix of Arfs only allows weak association of the GDP-bound proteins with membranes. Therefore, for tight association of Arf1 with the membrane, several groups have proposed the existence of an Arf1 receptor. The first proposal for a proteinaceous receptor for Arf-GTP was suggested by Rothman's group based on binding studies that demonstrated that two distinct populations of Arf bound to Golgi membranes, with only one population being saturable on membranes (Helms *et al.*, 1993). In addition, biochemical studies examining Arf recruitment and Arf1-mediated GTP hydrolysis provided evidence that Arf1-GDP associates with membranes. First, membrane recruitment of Arf1 was demonstrated to be necessary prior to nucleotide exchange (Beraud-Dufour *et al.*, 1999). Second, multiple cycles of GDP to GTP exchange were proposed to occur based on the results demonstrating the requirement for Arf1-mediated GTP hydrolysis for efficient uptake of cargo

by COPI vesicles (Nickel *et al.*, 1998; Malsam *et al.*, 1999; Pepperkok *et al.*, 2000).

Much effort has been made to identify Arf receptors. Several studies have now identified potential proteins that act as Arf1 receptors. For example, the p24 family of type I transmembrane proteins were the first proteins proposed to be Arf1 receptors shown to bind to Arf1 (Gommel *et al.*, 2001; Majoul *et al.*, 2001). Arf1 binds to the cytoplasmic region of p23, a member of the p24 family thought to function as a Golgi-cargo receptor. Also, several ER-Golgi SNAREs that are present on COPI-coated membranes such as membrin can function as receptors for Arf1-GDP and potentially increase Arf-GDP levels at the membrane (Rein *et al.*, 2002; Honda *et al.*, 2005). In contrast to the receptors identified for Arf1-GDP, receptors for class II and III Arfs have not yet been reported.

1.4 Activation of Arf by Arf-GEFs of the Sec7 family

The functions of Arfs depend on guanine nucleotide exchange which is stimulated by GEFs. The family of Arf-GEFs now make up a diverse group with unique properties (Cox *et al.*, 2004). Six subfamilies of Arf-GEFs that range in size from small (40-80 kDa, including CYH/ARNO and EFA6) to intermediate (100-150 kDa, including BRAG and SYT1) and large (160-230 kDa, including GBF/GEA and BIG/SEC7) (Cox *et al.*, 2004; Mouratou *et al.*, 2005) (Figure 1.5). All Arf-GEFs contain a central catalytic Sec7 domain (Sec7d) that is approximately 200 amino acids in size and stimulates Arf guanine nucleotide exchange. While the smaller Arf-GEFs have coiled-coiled domains and pleckstrin

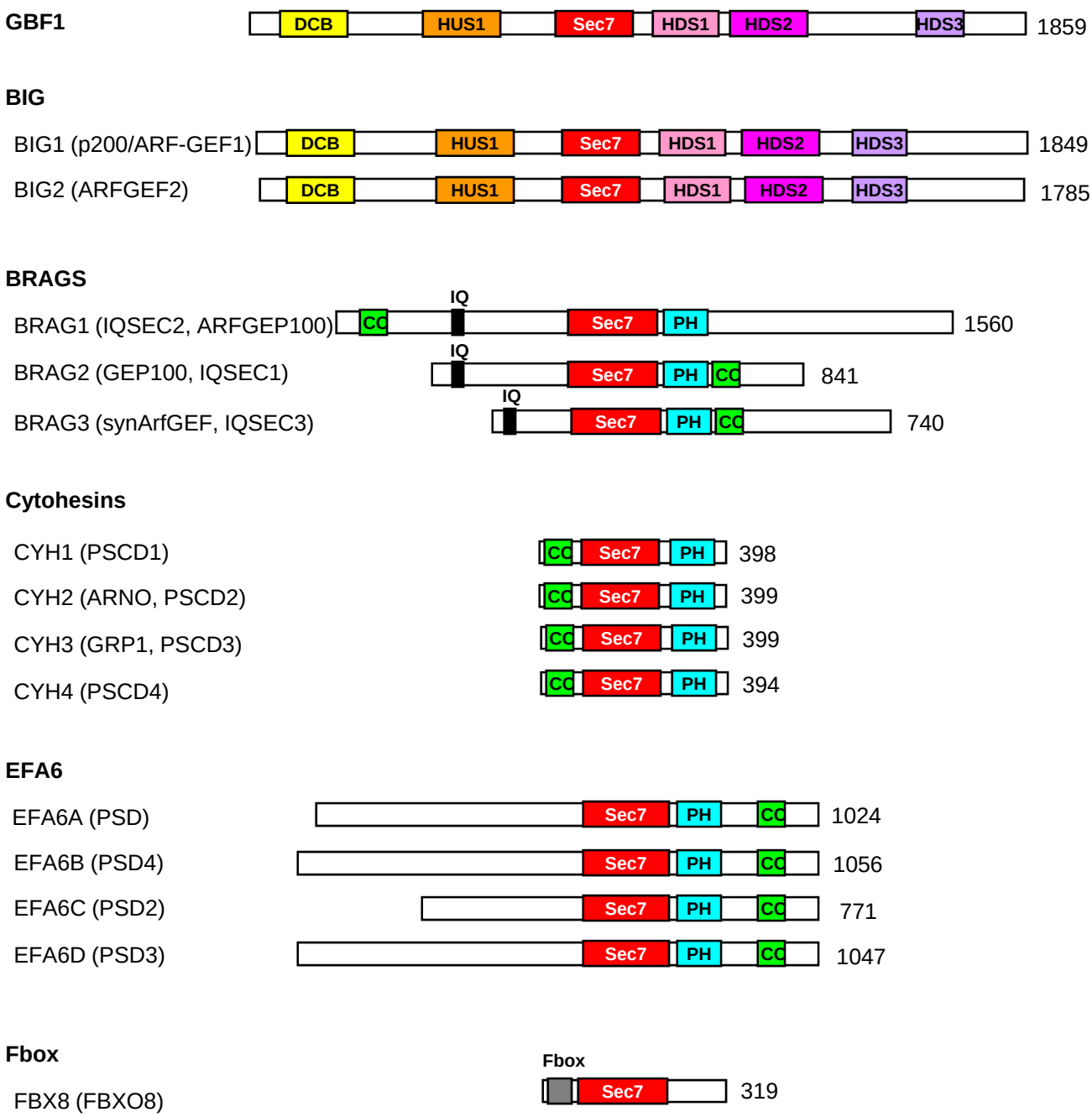

Figure 1.5 Human members of the Sec7 family of Arf-GEFs.
The six different subfamilies of Arf-GEFs of *Homo sapiens* are shown with their protein names, corresponding sizes (number of amino acids) and domain organization. The colored bars represent domain organization common to GEFs of each subfamily. These domains include Sec7: Sec7 domain common to all Arf-GEFs; DCB: Dimerization and Cyclophilin Binding domain; HUS: Homology Upstream of Sec7 domain; HDS1-3: Homology Downstream of Sec7 domains 1-3; PH: pleckstrin homology domain; CC: coiled-coil domain; IQ: IQ domain; Fbox: Fbox motif.

homology (PH) domains, the coiled coil domains are absent in the intermediate Arf-GEFs. Also, both the PH domains and coiled-coil domains are absent in the large Arf-GEFs.

1.4.1 The Sec7 domain

The main feature of the Sec7d that is responsible for the catalytic activity of the GEFs for Arf nucleotide exchange is the presence of an invariant glutamate residue that is commonly referred to as a glutamate finger. Based on crystal structure studies, nucleotide exchange is proposed to occur by a series of ordered steps (Renault *et al.*, 2003). First, the binding of Arf-GDP to the Sec7d opens the Arf switch 1 and switch 2 domains causing a rotation of the Arf protein core (Figure 1.4). This allows the negative charge of the glutamate finger to be inserted near the nucleotide phosphates to destabilize the crucial magnesium and β-phosphate of the bound nucleotide (Beraud-Dufour *et al.*, 1998). Also, this rotation of the core leads to the ejection of the N-terminal helix of Arf to move away from the protein core. The nucleotide-free Arf bound to the Sec7d of the GEF then undergoes a conformational change to a GTP-like state. Lastly, the Arf-Sec7d complex accepts GTP causing the dissociation of the Sec7d.

A charge reversal mutation of glutamate to lysine of all Arf-GEFs tested has been shown to prevent nucleotide exchange activity. For example, mutation of the glutamate finger in ARNO (E156K) stabilizes the interaction between the mutant GEF and Arf-GDP resulting in Arf inactivation (Beraud-Dufour *et al.*, 1998). Similarly, the equivalent mutation in GBF1 (E794K) causes the redistribution of Golgi proteins and disassembly of the Golgi complex (Garcia-

Mata *et al.*, 2003). The EK mutant GEF is thought to form an inactive, stable complex with Arf-GDP under low magnesium conditions in which the lysine residue stabilizes bound GDP thus preventing the conformational change required for nucleotide exchange (Shin and Nakayama, 2004).

1.4.2 GBF1 is a large Arf-GEF with a crucial function in ER-to-Golgi traffic

Each GEF is thought to function in specific subcellular compartments or subcompartments within an organelle. For example, it has been well documented that the large Arf-GEFs Golgi-specific brefeldin A (BFA) resistance factor 1 (GBF1) and the BFA-insensitive Arf-GEFs (BIGs) localize to the *cis*- and *trans*-Golgi compartments, respectively (Zhao *et al.*, 2002). Distinct localization of Arf-GEFs suggests the possibility that different Arfs may be regulated at specific cisternae within the Golgi complex. Consistent with this notion, GBF1 mediates the recruitment of COPI to the ERGIC and *cis*-Golgi membranes, whereas BIG2 regulates the activities of AP-1 and GGAs at the TGN (D'Souza-Schorey and Chavrier, 2006).

GBF1 is an Arf-GEF with an indispensible role for ER-to-Golgi traffic. In mammalian cells, GBF1 is the only known Arf-GEF localized to the ERGIC and *cis*-Golgi complex with an activity on class I and II Arfs (Claude *et al.*, 1999; Kawamoto *et al.*, 2002; Zhao *et al.*, 2002; Garcia-Mata *et al.*, 2003). GBF1 has been demonstrated to have specificity for class II Arfs *in vitro* and *in vivo*, but has also been suggested to act on Arf1 and Arf3 *in vivo* (Claude *et al.*, 1999; Kawamoto *et al.*, 2002). Using microinjection of antibodies to GBF1 and knockdown of GBF1, several studies have established that GBF1 has a critical

role in COPI-dependent cargo transport from the ER to the Golgi complex (Zhao *et al.*, 2006; Szul *et al.*, 2007; Manolea *et al.*, 2008). Depletion of GBF1 prevents cargo transport from the ERGIC (Manolea *et al.*, 2008) and activation of the unfolded protein response ultimately resulting in cell death (Citterio *et al.*, 2008). Furthermore, GBF1 has been well established as a target of the enteroviruses of the picornavirus family. The viral 3A protein specific to coxsackievirus B3 and poliovirus but not other picornavirus 3A proteins is able to bind to and inhibit the function of GBF1 thus interfering with Arf1-mediated COPI recruitment (Wessels *et al.*, 2006a; Wessels *et al.*, 2006b; Belov *et al.*, 2007). Taken together, these studies show the specific and crucial function of GBF1 in the early secretory pathway.

1.4.3 The putative GBF1 receptor

How GBF1 is targeted to specific compartments of the Golgi complex remains unclear. However, it appears that the presence of a membrane receptor is highly likely. Based on the ability of brefeldin A to trap GBF1 on membranes, it has been proposed that an integral membrane protein that acts as a compartment specific receptor for GBF1 likely exists (Niu *et al.*, 2005; Zhao *et al.*, 2006). A membrane receptor for GBF1 has not been identified, but several integral membrane proteins have been identified as interacting partners of GBF1. hGmh1 was the first Golgi transmembrane domain partner of the yeast homolog of GBF1 to be identified (Chantalat *et al.*, 2003). The tethering factor p115 (Garcia-Mata and Sztul, 2003) and Rab1b (Monetta *et al.*, 2007) have also been identified as interacting partners that may contribute to membrane recruitment of GBF1.

Although several binding partners have been identified for GBF1, no interacting partner has been established as the canonical receptor for GBF1. Further studies will be necessary to identify the proteins and possibly lipids that function as specific receptors for GBF1 at the ERGIC and the Golgi complex.

1.5 Arf-GAPs in the early secretory pathway

Similar to other small GTPases, the Arf family binds tightly to GTP and has a very low intrinsic rate of hydrolysis. Stimulation of GTP hydrolysis on Arfs is achieved by several Arf-GAPs that share an essential zinc finger domain and a conserved arginine residue (Lee *et al.*, 2004). The specificity of Arf-GAPs localized to early secretory compartments remains largely uncharacterized. However, it has been well established that GTP hydrolysis of Arf1 is required for the dissociation of COPI from vesicles (Tanigawa *et al.*, 1993). ArfGAP1 appears to be a component of the COPI coat and may function to couple cargo sorting with vesicle formation (Lee *et al.*, 2005). Consistent with this notion, incorporation of cargo requires GTP hydrolysis of Arf1-GTP (Nickel *et al.*, 1998; Lanoix *et al.*, 1999; Pepperkok *et al.*, 2000). Also, the increased membrane curvature of COPI-coated vesicles stimulates the activity of Arf-GAP1 (Bigay *et al.*, 2003; 2005). It appears that Arf-GAP1 may be excluded from regions of negative curvature, thus restricting its activity to late in the budding process. However, the mechanism by which Arf-GAP1 catalyzes GTP hydrolysis on COPI vesicles is not fully understood.

1.6 Experimental approaches used to characterize Arfs

Several experimental approaches have been developed to characterize Arf-GEFs both *in vitro* and *in vivo*. These include drugs, viral proteins, as well as mutations in Arfs that interfere with the exchange of GDP for GTP or stabilize an abortive Arf-GEF complex (Beraud-Dufour *et al.*, 1998; Goldberg, 1998; Mossessova *et al.*, 1998: 2003; Peyroche *et al.*, 1999; Niu *et al.*, 2005; Szul *et al.*, 2005; Wessels *et al.*, 2006). Each of these experimental tools that advanced our understanding of the mechanisms regulating Arf function will be described in detail below.

1.6.1 BFA, an uncompetitive inhibitor that inactivates Arf function at the Golgi complex

BFA is a fungal metabolite with a rapid and dramatic effect on the structure and function of the Golgi complex (Klausner *et al.*, 1992). Ever since the initial discovery of its effect on the secretory pathway, BFA has been extensively used as a tool to interfere with transport steps and study the mechanisms regulating the organization of intracellular compartments. BFA is now known to specifically inhibit the GEF activity for Arf1 by targeting the catalytic Sec7d (Mansour *et al.*, 1999; Peyroche *et al.*, 1999; Robineau *et al.*, 2000; Mossessova *et al.*, 2003). BFA inserts at the interface between Arf and the Sec7d, prevents GDP displacement and causes the formation of an Arf-GDP-BFA-Sec7d complex (Mossessova *et al.*, 2003; Renault *et al.*, 2003; Zeghouf *et al.*, 2005). Based on crystallographic studies, this complex is thought to be an abortive complex that is stabilized before the GDP can be released. However, no

sound *in vivo* evidence exists to date showing the formation and accumulation of a stable Arf-GDP-BFA-Sec7d complex.

1.6.2 Arf mutants

Arf1(T31N), a dominant-negative mutant of Arf1 that has a low affinity for GTP, has been proposed to also form such a complex and prevent activation of endogenous Arfs. Interestingly, treatments with BFA, as well as expression of GBF1(E794K) or Arf1(T31N), greatly reduce the dynamic exchange between free and membrane-bound GBF1 (Niu *et al.*, 2005; Szul *et al.*, 2005; Zhao *et al.*, 2006). These observations suggest that trapping an Arf-GBF1 complex prevents GBF1 release from membranes and led to the conclusion that nucleotide exchange is linked to release of GBF1 from its membrane receptor (Cherfils and Melançon, 2005; Niu *et al.*, 2005; Szul *et al.*, 2005; Zhao *et al.*, 2006). This conclusion appears consistent with the demonstration that the enterovirus 3A protein blocks protein traffic to the Golgi complex and can form a complex with Arf1(T31N) and GBF1 (Wessels *et al.*, 2006b).

1.6.3 Other pharmacological agents used to study Arfs

In addition to BFA, several other chemical agents have been used separately or in combination with BFA to study the secretory pathway. Such pharmacological agents that have been well characterized and relevant to this thesis include Exo1, LM11, H89 and coumermycin A1. Exo1 is a cell-permeable, methylanthranilate analog that rapidly releases Arf1 from Golgi membranes (Feng *et al.*, 2003). In contrast to the effect of BFA on the GEF, Exo1 is thought to act on Arf-GAP to stimulate the release of COPI from membranes. Next, LM11 is a

small molecule inhibitor recently identified by structure-based screening that inhibits the catalytic activity of GEFs that are both BFA sensitive and BFA resistant by binding to a pocket near the ARNO/Arf1 interface (Viaud *et al.*, 2007). LM11 appears to target the class I and II, but not class III, Arfs. Similar to BFA, LM11 prevents conformational changes required for nucleotide exchange. However, in contrast to the uncompetitive mechanism used by BFA, LM11 is a non-competitive inhibitor. Lastly, H89, a small chemical inhibitor of PKA and other kinases, was shown to block Golgi disassembly caused by Arf1 inactivation in BFA-treated cells (Lee and Linstedt, 2000). The mechanism by which H89 blocks Golgi disassembly is unclear owing to the fact that H89 has many cellular targets. BFA has vastly improved our understanding of ER-to-Golgi traffic, and the pharmacological agents mentioned above are expected to dissect the specific mechanisms involved in COPI-mediated trafficking.

1.7 Partitioning of the Golgi complex during mitosis

During mitosis, protein traffic is dramatically altered, and there have been contradictory roles proposed for Arf1. In mammalian cells, the ribbon of interconnected cisternae of the Golgi complex is first fragmented into "Golgi blobs", which further vesiculate to become very small dispersed vesicles as mitosis progresses (Colanzi and Corda, 2007). Between the stages of prometaphase and anaphase, the morphology of the Golgi appears to be a haze by light microscopy (Colanzi *et al.*, 2003). The ambiguity of fate of the Golgi

complex during mitosis has been a topic of intense debate leading to two competing models that have attempted to describe the Golgi haze.

1.7.1 Competing models for the fate of the Golgi complex during mitosis

Although the fragmentation of the Golgi complex is well characterized, there have been inconsistent interpretations for the fate of the Golgi fragments during mitosis (Colanzi and Corda, 2007). Whether the haze represents small dispersed Golgi remnants or Golgi enzymes redistributed to the ER remains controversial and has spawned two models that differ greatly. The autonomous model states that Golgi fragments remain as autonomous structures and are remnants that breakdown/reassemble independently of the ER (Shima *et al.*, 1997; Jesch and Linstedt, 1998; Pecot and Malhotra, 2004; Axelsson and Warren, 2004). The autonomous model supports the idea that Arf1 and COPI would remain active on the Golgi fragments throughout mitosis and that the Golgi and ER membranes remain separate without communicating. The second model, the ER-dependent model, states that the Golgi membrane fuses with the ER during mitosis (Thyberg and Moskalewski 1992; Zaal *et al.*, 1999, Altan-Bonnet *et al.*, 2003, 2006). This model proposes that the inhibition of anterograde trafficking of proteins and membranes out of the ER and acceleration of retrograde transport results in the rapid absorption of Golgi proteins into the ER (Zaal *et al.*, 1999; Lippincott-Schwartz and Zaal, 2000). At the onset of mitosis, the ER-dependent model assumes that Golgi proteins redistribute to the ER based on the assumption that Arf1 and the COPI machinery are inactivated.

There is overwhelming support for the autonomous model. Early work using EM documented Golgi fragments persisting throughout mitosis (Maul and Brinkley, 1970). Also, the ability of the Golgi membranes to break down into smaller fragments during mitosis has been mimicked by using drugs such as ilimaquinone (Takizawa *et al.*, 1993) or okadaic acid (Lucocq *et al.*, 1995) or in cell-free assays with purified Golgi membranes (Misteli and Warren, 1995a,b). The fragmentation of the Golgi by these treatments is argued to be the general process that underlies Golgi fragmentation during mitosis. In contrast, similar treatments that perturb the Golgi structure using different pharmacological agents have been used to support the ER-dependent model. For example, treatment with nocodazole or BFA or the expression of dominant negative Sar1 or Arf1 mutants causes the Golgi to fragment as a result of Golgi membrane proteins redistributing to the ER (Lippincott-Schwartz *et al*., 1989; Cole *et al*., 1998; Storrie *et al*., 1998; Zaal *et al*., 1999). Proponents of the ER-dependent model believe that depolymerization of microtubules or the inhibition of ER export are sufficient causal factors for mediating Golgi disassembly during mitosis.

In 2004, two studies by the Warren and Malhotra groups attempted to settle the debate of whether the haze during mitosis represents Golgi remnants or Golgi enzymes redistributed to the ER (Axelsson and Warren, 2004; Pecot and Malhotra, 2004). Both groups developed assays and convincingly established that Golgi membranes do not fuse with the ER during mitotic progression in mammalian cells. However, a recent study addressing the fate of the Golgi during mitosis has rekindled the debate, since the authors argue that the ER-dependent

model is the predominant model (Altan-Bonnet *et al.*, 2006). Although the rationales for some of their experiments may be flawed and some of their results may be inconsistent with current literature, this study tips the scale once again in favour of the ER-dependent model.

1.7.2 Role of Arf1 and the COPI machinery during mitosis

The ER-dependent model postulates that Arf inactivation plays a central role in Golgi fragmentation and redistribution to the ER. Altan-Bonnet *et al.* (2003) have demonstrated that cells expressing a constitutively active form of Arf1 or an inhibitor of PKA, H89, can prevent Golgi complex fragmentation during mitosis by preventing Arf1 inactivation. Furthermore, the Golgi and ER membranes are proposed to be linked by continuously communicating during mitosis without the activity of COPI (Altan-Bonnet *et al.*, 2006). In contrast to the ER-dependent model, two very recent publications have suggested a role for the COPI machinery during mitosis. They provide *in vitro* evidence that Arf1 is active during mitosis and its activity is required for mitotic Golgi fragmentation (Xiang *et al.*, 2007; Tang *et al.*, 2008). Tang *et al.* (2008) demonstrated that vesiculation of the "Golgi blobs" is mediated by Arf1 and the coatomer complex. The biochemical studies examining Arf1 provide good evidence for examining the potential roles of COPI and GBF1 during mitosis.

1.8 Rationales for this thesis

1.8.1 Rationale for project #1: GDP-bound class II Arfs associate with the ERGIC independently of GBF1

In contrast to the detailed information available on the Arf-GEFs that regulate the secretory pathway, much less is known about the function of class I and class II Arfs. The hindered progress for the characterization of class I and class II Arfs is due primarily to the limited number of antibodies available that are able to detect class II Arfs and the extensive biochemical overlap of different Arf isoforms. For my first project, we exploit live cell imaging methods in combination with a variety of pharmacological agents. Our working hypothesis was that class I and class II Arfs would have distinct localizations and behaviors at the ERGIC and the Golgi complex.

1.8.2 Rationale for project #2: Characterization of GBF1 and COPI at mitotic Golgi fragments

To date, the interpretations for the fate of the Golgi complex during mitosis are inconsistent and have led to two models that greatly differ. The autonomous model and ER-dependent model make opposite predictions for the morphology of mitotic Golgi fragments and the role of COPI during mitosis. While the ER-dependent model predicts that the Golgi and ER membranes remain linked by continuously communicating during mitosis without a requirement for COPI, the autonomous model predicts active COPI at mitotic Golgi fragments.

We hypothesize that an active COPI machinery exists during mitosis based on the recent *in vitro* evidence suggesting that Arf1 is active during mitosis and its activity is required for mitotic Golgi fragmentation (Xiang *et al.*, 2007; Tang *et al.*, 2008). Again we use live cell imaging and immunofluorescence to study the fate of the Golgi complex during mitosis and to examine the potential roles of COPI and GBF1 during mitosis.

CHAPTER TWO: MATERIALS AND METHODS

2.1 Reagents

During the course of this work, the chemicals, reagents, enzymes, and commercial kits were used according to the instructions provided by the respective manufacturer unless otherwise stated. BFA, nocodazole, and Exo1 were stored in DMSO as 10 mg/ml, 5 mg/ml and 25 mg/ml (91.5 mM) stock solutions, respectively. All use of reagents was in accordance with procedures set out by the Environmental Health and Safety of the University of Alberta and Workplace Hazardous Materials Information System.

Table 2.1 List and source of chemicals and reagents

Reagent	Supplier
acetic acid, glacial	Fisher Scientific
6X load dye	Promega
acrylamide/bis (30%; 29:1)	Bio-rad
agarose (UltraPure™)	Invitrogen
agarose (UltraPure™; low melting point)	Gibco (Invitrogen)
ammonium chloride	Caledon
ammonium persulfate	Bio-rad
ampicillin	Novopharm
bactotryptone	BD
bacto-yeast	BD
blasticidin	Invitrogen
bovine serum albumin	Sigma
brefeldin A	Sigma
Brilliant blue R-250	Sigma
bromophenol blue	Sigma
calcium chloride	BDH
calf intestinal alkaline phosphatase (CIAP)	Invitrogen
CO_2-independent medium	Gibco (Invitrogen)
Complete, EDTA-free protease inhibitor cocktail tablets	Roche
Coumermycin A1	Sigma
deoxycholic acid sodium salt	Sigma
DTT (dithiothreitol)	Fisher Scientific
DMEM (Dulbecco's Modified Eagle Medium)	Gibco (Invitrogen)

DMSO (dimethyl sulfoxide)	Sigma
dNTP (deoxyribonucleotide triphosphate)	Invitrogen
doxycycline	Sigma
EDTA (ethylenediamine-tetraacetic acid)	Sigma
Exo1	Calbiochem
Fermentas PageRuler™ Prestained Protein Ladder Plus	Fermentas
Fetal bovine serum (FBS)	Gemini Bio-Products
Fibronectin	Sigma
FuGENE 6 transfection reagent	Roche
gelatin	Fisher Scientific
GeneRuler 1 kb DNA Ladder	Fermentas
glycerol	Fisher Scientific
glycine	Roche
H89	Sigma
hydrochloric acid	Fisher Scientific
hygromycin	Invitrogen
Igepal CA-630 (NP-4)	Sigma
isopropanol	Fisher Scientific
kanamycin	Sigma
L-glutamine	Gibco
magnesium chloride	BDH
magnesium sulphate	Fisher Scientific
methanol	Fisher Scientific
nocodazole	Sigma
O-phenanthroline	Sigma
Opti-MEM	Gibco (Invitrogen)
paraformaldehyde	Sigma
penicillin/streptomycin	Gibco (Invitrogen)
phosphatase cocktail I	Sigma
phosphatase cocktail II	Sigma
PBS (phosphate buffered saline; Dulbecco's)	Gibco (Invitrogen)
phosphate-free DMEM	Invitrogen
Platinum® Pfx DNA polymerase	Invitrogen
Ponceau S	Sigma
potassium chloride	BDH
Precision Plus protein standard	Bio-rad
Prolong® Gold with DAPI antifade reagent	Molecular Probes
protein A sepharose CL-4B	GE Healthcare
restriction endonuclease	Invitrogen or NEB
sodium bicarbonate	Caledon
sodium chloride	Fisher Scientific
SDS (sodium dodecyl sulfate)	Bio-rad
sodium fluoride	Sigma
sodium hydroxide	Fisher Scientific
sucrose	Sigma
SYBR Safe DNA gel stain	Molecular probes

	(Invitrogen)
T4 DNA ligase	Invitrogen
TEMED (tetramethylethylenediamine)	OmniPur
thymidine	Sigma
TransIT-LTI transfection reagent	Mirus
Tris	Roche
Triton X-100	VWR
Trypsin-EDTA	Gibco (Invitrogen)
Tween	Fisher Scientific

Table 2.2 Commercial Kits

Kit	Supplier
ECL Plus Western Blotting Detection System	GE Healthcare
GeneJET Plasmid miniprep kit	Fermentas
QIAGEN Plasmid Maxi kit	QIAGEN
QIAGEN Plasmid Midi kit	QIAGEN
QIAprep spin miniprep kit	QIAGEN
QIAquick gel extraction kit	QIAGEN
QIAquick PCR purification kit	QIAGEN
Silver stain plus	Bio-rad

Table 2.3 Commonly used buffers and solutions

Solution	Composition
Coomassie Blue staining solution	0.25% Brilliant blue R-250, 45% (v/v) methanol, 10% acetic acid
Coomassie Blue destaining solution	40% (v/v) methanol, 10% (v/v) acetic acid
Luria-Bertani (LB) Broth	1% bactotryptone, 0.5% bacto-yeast extract, 1% (w/v) NaCl, pH 7.0
Paraformaldehyde (3%)	3% paraformaldehyde, 0.1 mM $CaCl_2$, 0.1 mM $MgCl_2$
Permeabilization buffer	0.1% (v/v) Triton X-100, 0.05% SDS in

Phosphate buffered saline (PBS)	PBS 2.7 mM KCl, 1.5 mM KH_2PO_4, 137.9 mM NaCl, 8.1 mM Na_2HPO_4
Quench buffer	50 mM NH_4Cl in PBS
RIPA buffer	150 mM NaCl, 1% (v/v) NP-40, 0.5% Na-deoxycholate, 2 mM EDTA, 2 mM $MgCl_2$, 50 mM Tris-HCl, pH 8.0
Running buffer	25 mM Tris-HCl, 190 mM glycine, 0.1% SDS
SDS-PAGE sample buffer (6X)	30% (v/v) glycerol, 1% SDS, 0.6 M DTT, 0.012% bromophenol blue, 70% (v/v) 4X Tris-HCl/SDS buffer, pH 6.8)
Separating gel (4X Tris-HCl/SDS, pH 8.8)	0.4% SDS, 1.5 M Tris-HCl, pH 8.8
SOC medium	2% bactotryptone, 0.5% bacto-yeast extract, 10 mM NaCl, 2.5 mM KCl, 10 mM $MgCl_2$, 10 mM $MgSO_4$, 20 mM glucose
Stacking gel (4X Tris-HCl/SDS, pH 6.8)	0.4% SDS, 0.5 M Tris-HCl, pH 6.8
TAE (50X)	2 M Tris, 5.71% (v/v) glacial acetic acid, 50 mM EDTA, pH 8.0
Transfer buffer	25 mM Tris-HCl, 190 mM glycine, 20% (v/v) methanol, 2.5% (v/v) isopropanol
TTBS	50 mM NaCl, 0.5% (v/v) Tween-20, 20 mM Tris-HCl, pH 7.5

2.2 Cell culture

The cell lines used for the work described in this thesis include HeLa (ECACC; Sigma-Aldrich, 93021013), NRK-52E cells (ATCC CRL-1571), NRK

cells stably expressing GFP tagged GBF1 (described in Zhao *et al.*, 2006), COS1 cells (ATCC CRL-1650), T-Rex™-293 (Invitrogen), and CHO (Pro-5; ATCC CRL-1781). Vero and A549 cells were gifts from Dr. Tom Hobman (University of Alberta, Canada).

Cell monolayers were maintained in Dulbecco's modified Eagle's medium (DMEM) supplemented with 10% FBS, 100 μg penicillin/ml medium, 100 μg streptomycin/ml medium and 2 mM *L*-glutamine at 37^{o}C in a 5% CO_2 incubator. For live cell imaging, cells were grown in CO_2 independent DMEM supplemented with 10% FBS.

2.3 Antibodies

The source and dilution for primary antibodies used in the work for this thesis are listed below in Tables 2.4 and 2.5 for immunofluorescence (IF) and Table 2.6 for immunoblotting. For IF, secondary goat antibodies conjugated with either Alexa 488 or Alexa 594 were purchased from Molecular Probes (Eugene, OR) and used at 1:600 dilution. For immunoblots, proteins were detected using a horseradish peroxidase (HRP)-conjugated goat anti-rabbit IgG secondary antibody that was purchased from Bio-Rad Laboratories (Mississauga, ON) and used at 1:2500 dilution.

Table 2.4 Polyclonal antibodies used for IF

Antibody	Dilution	Source
anti-Arf1 (2048)	1:400	Dr. Bernd Helms; University of Utrecht, The Netherlands

anti-Arf4,5 (9D6; affinity- purified)	1:25	(Berger *et al.*, 1988) for preparation. Antibody preparation and characterization performed by Anita Gilchrist and Mary Schneider, respectively
anti-BIG1 (9D3)	1:200	(Zhao *et al.*, 2002, Claude *et al.*, 2002)
anti-GBF1 9D2 IgG	1:400	(Zhao *et al.*, 2006)
anti-GBF1 9D4 (final bleed)	1:2500	(Manolea *et al.*, 2008)
anti-calnexin	1:200	Dr. Thomas Simmen; University of Alberta, Edmonton, Canada
anti-giantin	1:1000	(Claude, 1999, Zhao, 2006)
anti-mannosidase II	1:800	Dr. Kelley Moremen; University of Georgia, Athens, USA
anti-p58 (Molly6)	1:400	Dr. Jaakko Saraste; University of Bergen, Bergen, Norway; (Saraste *et al.*, 1987)
anti-Sec31	1:500	Dr. Bor Luen Tang; Institute of Molecular and Cell Biology, Singapore, Republic of Singapore; (Tang *et al.*, 2000)

Table 2.5 Monoclonal antibodies used for IF

Antibody	Dilution	Source
anti-β-coatomer protein (clone M3A5)	1:200	Dr. T. Kreis; University of Geneva, Geneva, Switzerland; (Allan and Kreis, 1986)
anti-GBF1 (clone 25)	1:400	BD Biosciences (Mississauga, Canada)
anti-hemagglutinin (HA) (clone 3F10, rat)	1:100	Roche Diagnostics (Laval, Canada)
anti-mannosidase II (clone 53FC3)	1:100	Dr. Brian Burke; University of Florida, Gainesville, USA; (Burke *et al.*, 1982)

anti-p115 (clone 7D1)	1:1000	Dr. Gerry Waters; Princeton University, Princeton, USA
anti-α-tubulin (clone DM1A)	1:1000	Sigma-Aldrich (St. Louis, USA)

Table 2.6 Antibodies used for immunoblotting

Antibody	Dilution	Source
anti-GFP (rabbit)	IB: 1:1000	Dr. Gary Eitzen; University of Alberta, Edmonton, Canada

2.4 Construction of plasmids

2.4.1 GBF1 tagged with mCherry

A plasmid encoding GBF1 tagged at the N-terminus with monomeric Cherry (mCherry) was constructed in the backbone of pcDNA™5/TO (Invitrogen. pcDNA™5/TO was first modified to include an NheI site by insertion of a synthetic duplex (5'-GTGCTAGC-3'; NheI site underlined) between the HindIII and KpnI sites (sense oligo 5'-AGCTTGTGCTAGCGGTAC-3' and antisense oligo 5'-CGCTAGCACA-3'). An inducible plasmid encoding the GFP-GBF1 chimera was then constructed by transferring the NheI-NotI fragment from pIND-GFP-GBF1 (Zhao *et al.*, 2006) into pcDNA™5/TO-NheI. Construction of pcDNA™5/TO-mCherry-GBF1 entailed two sequential steps. A fragment encoding mCherry amplified by polymerase chain reaction (PCR) from pRSETB-mCherry (Dr. Roger Tsien; University of California San Diego, CA) was first inserted between the NheI and XhoI sites of pcDNA™5/TO-NheI; an XhoI

fragment encoding GBF1 was then transferred from pcDNA™5/TO-GFP-GBF1 into the XhoI sites of pcDNA™5/TO-NheI-mCherry. This approach yielded an mCherry-GBF1 with linker identical in length and sequence to that of the previously characterized GFP-GBF1 (Zhao *et al.*, 2006).

2.4.2 Arfs tagged with GFP

The plasmids used for Arf-GFP expression in this study were constructed by Zoya Shapovalova by inserting fragments encoding human Arf1, Arf3, Arf4 and Arf5 between the XhoI and KpnI sites of pEGFP-N1 (Clontech, Mountain View, CA). Fragments were obtained by PCR amplification from vectors harboring human Arf sequences using forward primers that introduced an XhoI site upstream of the ATG, and reverse primers that changed the TGA stop codon to CGC and introduced a KpnI site immediately downstream that allowed in-frame translation of GFP following a 12 residue linker (AVPRARDPPVAT). The templates used for isolation of fragments encoding wild type Arfs were previously described (Berger *et al.*, 1988). The Arf4(T31N) mutant was created by site-directed mutagenesis using the QuickChange kit (Stratagene, La Jolla, CA), as per manufacturer's instructions. The Arf1(T31N) fragment was amplified using a plasmid encoding HA-tagged bovine Arf1(T31N) (Peters *et al.*, 1995) obtained from Dr. V. Hsu (Harvard Medical School, Boston, MA). Mutagenesis of Arf4 was performed by Assad Omar, an AHFMR summer student under the supervision of Mary Schneider.

2.4.3 Arfs tagged with mCherry

The plasmid for Arf1-mCherry was derived from one encoding Arf1-RFP constructed by Dr. J. Donaldson (NIH, Bethesda, MD) by inserting the complete bovine Arf1 cDNA between the BglII and EcoR1 sites of RFP-N1 (Cohen *et al.*, 2007). To generate Arf1-mCherry, Zoya Shapovalova exchanged the BamHI-NotI fragment encoding RFP with a similar one encoding mCherry. This procedure introduced a 13-residue linker (GILQSTVPRARDP) between the terminal Lys of Arf1 and the initiating Met of mCherry. To generate mCherry tagged forms of Arf3, Arf4 and Arf5, I substituted a BamHI-NotI fragment encoding mCherry into pEGFP-N1 into which human Arf cDNAs amplified by PCR from vectors encoding Arf3-HA, Arf4-HA and Arf5-HA (Peters *et al.*, 1995) had been inserted between the XhoI and KpnI sites. This procedure yielded chimeras containing an 8-residue linker (AVPRARDP) between the terminal Arf residue and the initiating Met of mCherry.

Table 2.7 Chimeras of Arfs with GFP, RFP or mCherry and their linkers

Chimera	Linker	MCS point of insertion	Reference
hArf1-GFP	DPPVAT	BamH1	Dr. Guillermo Romero; University of Pittsburgh, Pittsburgh, USA; (Vasudevan *et al*., 1998)
bArf1-RFP	GILQSTVPRARDPPVAT	EcoR1	Dr. Julie Donaldson; National

			Institutes of Health, Bethesda, USA; (Cohen *et al*., 2007)
bArf1-GFP	GILQSTVPRARDPPVAT	EcoR1	This study
bArf1-mCherry	GILQSTVPRARDP	EcoR1	This study
hArf4/5-GFP	AVPRARDPPVAT	Kpn1	Dr. John Presley; McGill University, Montreal, Canada
hArf3/4/5-mCherry	AVPRARDP	Kpn1	This study
hArf1/3/4/5-GFP	AVPRARDPPVAT	Kpn1	This study

2.5 NRK cell line expressing GFP tagged GBF1

The isolation and characterization of the stable NRK cell line expressing the N-terminal GFP-tagged GBF1 (NRK-GFP-GBF1) has been previously described (Zhao *et al.*, 2006).

2.6 Plating cells and transient transfections

Most experiments were performed with cells grown on glass coverslips either in 6-well plates or 12-well plates. Prior to plating out A549, CHO, and Vero cells shown in Figure 4.8, each 22 mm square coverslip was coated with 2 μg fibronectin/ml PBS (Sigma) for at least 1 h at 37^{o}C. For transient expression from plasmids, cell were grown on coverslips to 40-50% confluency, transfected with the designated plasmids using FuGENE 6 (Roche Diagnostics, Indianapolis,

IN) or TransIT-LTI transfection reagent (Mirus, Madison, WI) according to manufacturer's instructions and cultured for 16 to 24 hrs prior to fixation.

2.7 Immunofluorescence

IF was carried out on cells grown on glass coverslips sterilized by ethanol and flaming. Usually after drug treatment, cells were washed once with PBS and fixed with 3% paraformaldehyde (with 100 μM calcium chloride and 100 μM magnesium chloride in PBS) at either room temperature or 37^{o}C for 20 min. Fixation was terminated by incubation with quench buffer (50 mM ammonium chloride in PBS) for 10 min and this was followed by incubation with a permeabilization buffer (0.1% Triton X-100, 0.05% SDS in PBS). Prior to incubation with antibodies, cells were blocked using three, 5 min incubations with 0.2% gelatin in PBS. Cells double labeled with mouse and rabbit antibodies were processed as described (Zhao *et al.*, 2002).

2.8 Fluorescence microscopy

2.8.1 Epifluorescence microscopy

Epifluorescence images were obtained using an Axioskop II microscope (Carl Zeiss, Thornwood, NY) equipped with a 63X objective (plan-Apocromat, NA=1.4) and a CoolSNAP HQ monochrome CCD Photometrics camera (Tucson, AZ). The images were exported as 12 bit images using Image Pro 5.1.

2.8.2 Confocal microscopy

Confocal images from fixed cells were obtained using a Zeiss Axiovert 200M confocal microscope equipped with an UltraVIEW ERS 3E spinning disk (PerkinElmer, Waltham, MA) and 63X objective lens (plan-Apocromat, NA=1.4). Images were captured with a 9100-50 electron multiplier CCD digital camera (Hamamatsu Photonics, Bridgewater, NJ) and processed with Ultraview Image Suite. Images with dual labeling were captured from the same cells by exciting each fluorophore and detecting sequentially (multitrack mode) to avoid channel bleed-through. Laser intensity and filters were adjusted to give maximum signal but avoid saturation.

2.8.3 Live cell, time-lapse imaging

For live cell imaging, cells were grown in glass bottom microwell dishes (Plastek Cultureware, MatTek corporation, Ashland, MA). The medium was switched to CO_2 independent DMEM (Gibco Laboratories, Grand Island, NY) supplemented with 10% FBS immediately before imaging on a temperature-controlled (37ºC) stage of a Zeiss Axiovert 200M confocal microscope equipped with an UltraVIEW ERS 3E spinning disk (PerkinElmer) and 100X objective lens (plan-Apocromat, NA=1.4). Live cell imaging was performed in a room maintained either at 23ºC or 35^{o}C; a thermocouple placed in the glass coverslip registered a few degrees above room temperature even when the heated stage was set at 37ºC. Images were captured with a 9100-50 electron multiplier CCD digital camera and processed with Ultraview Image Suite. Experiments involving drug addition were performed by adding 500 µl of medium containing 4 times drug

concentration to a dish containing 1.5 ml medium. For BFA washout experiments (Figure 3.7), medium was twice aspirated and replaced with medium lacking drug at the indicated time. Focus was adjusted immediately following manipulation as required.

2.9 Fluorescence recovery after photobleaching (FRAP)

FRAP experiments were performed with glass bottom microwell dishes using a temperature controlled stage and objective warmer set at 37^{o}C. 8-bit confocal images were obtained with a LSM 510 confocal microscope (Carl Zeiss, Thornwood, NY) equipped with a 63X objective (plan-Apochromat, NA=1.4) using 488 nm laser excitation and a 500-550 nm bandpass filter for GFP. The filters and intensity of the laser (exposure and gain) were adjusted to give maximum signal without saturation. To measure FRAP, three prebleach images were taken at low laser intensity prior to photobleaching. Next, the region of interest (ROI; outlined red in the figures) within a cell was bleached using 15 iterations at 100% laser power (488 nm line). The recovery of fluorescence signal into the bleached areas was monitored at 2.2 s intervals immediately after the bleach by time-lapse imaging at low-intensity illumination. Since no significant focal level change was observed, focus was not adjusted. For Figures 4.5A-C, the cells were photobleached prior to BFA treatment and after BFA to illustrate GFP-GBF1 recovery at the Golgi complex and mitotic Golgi clusters within the same cells. For quantification of recovery kinetics of GFP-GBF1 signal (Figure 4.6A), fresh, naïve cells were treated for 2 min with either DMSO or 5 μg BFA/ml medium and then subjected to photobleaching.

Quantitative analysis of recovery kinetics of GFP-GBF1 signal in the ROI (either the juxtanuclear Golgi region of interphase cells or one half of the mitotic Golgi clusters in metaphase cells) was performed using NIH ImageJ processing software (version 1.62 downloaded from http://rsbweb.nih.gov/ij/). The signal intensity (integrated density) was measured for the ROI and total cell signal for each time point from 50 frames per movie. For mitotic cells that progressed through the stages of mitosis, the area of recovery for the photobleached mitotic Golgi fragments was adjusted accordingly. Next, GFP-GBF1 signal in the ROI was expressed as a fraction of total cell fluorescence for each time point. Ratios at each time point were expressed as a fraction of the initial value before bleach and plotted against time. Time zero was set to equal the third prebleach scan prior to photobleaching. Graphs were obtained by averaging FRAP values for three experiments per curve using Microsoft Excel software. Standard deviations were calculated and plotted on curves using Microsoft Excel.

2.10 Cell fractionation and preparation of cell extracts

BFA-mediated membrane recruitment of endogenous GBF1 was assayed using T-Rex™-293 cells (Invitrogen). T-Rex™-293 cells were grown on 100 mm plates and transfected with plasmids encoding Arf1-GFP or Arf4-GFP for 17 to 22 h (Figure 3.6D).

Cells grown on a 100 mm plate were scraped into 500 µl of buffer (10 mM Tris-HCl pH 8.0, 150 mM NaCl, protease inhibitor cocktail (Roche), pepstatin A and O-phenanthroline) and then recovered by centrifugation at 1500xg for 3 min,

4°C. Buffer was removed and 250 µl of fresh buffer was added to each pellet. Cells were treated in suspension with vehicle control (DMSO) or 10 µg BFA/ml homogenate for T-Rex™-293 cells (Figure 3.6D). Following 2 min incubation at 37°C, cells were homogenized by 15 passages through a 23-gauge needle. Low speed supernatants acquired after centrifugation at 8000xg for 3 min, 4°C, were subsequently centrifuged at 107,400xg for 25 min at 4°C using a Beckman Coulter TLA 120.1 rotor. Resultant supernatants (cytosol) were retained and Igepal added to 1%. High-speed pellets (microsomes) were resuspended with equivalent volume of wash buffer containing 1% Igepal. Samples in sample buffer were heated for 10 min at 100°C prior to freezing at -80°C. Equivalent amounts of cytosolic and microsomal fractions were separated by SDS-PAGE as described below in section 2.11.1.

2.11 Analysis of protein samples

2.11.1 SDS-polyacrylamide gel electrophoresis (SDS-PAGE)

Proteins samples were analyzed by electrophoresis on tris-glycine sodium dodecyl sulfate-polyacrylamide gels calibrated with pre-stained molecular weight standards (Bio-rad Laboratories or Fermentas). Processed frozen protein samples were thawed at room temperature and subjected to centrifugation for 5 min at 13,000 rpm at room temperature. 25 µl of each sample was loaded per lane on either a 5% or a 5%/15% step gradient slab SDS gel. Samples were separated on a 6.5 inch wide slab gel apparatus (CBS Scientific, Del Mar, CA), first at 80V for 30 min through the stacking gel, then at 120-150V through the resolving gel.

2.11.2 Immunoblotting

Following electrophoresis of samples by SDS-PAGE, protein analysis by immunoblotting was carried out essentially as previously described (Harlow and Lane, 1988). Proteins were transferred to nitrocellulose membranes at 100 V for 2 h or 26 V overnight in a transfer buffer (25 mM Tris-HCl, 190 mM glycine, 20% methanol, 2.5% isopropanol). The protein transfer was assessed by incubating membranes with Ponceau S (0.1% (w/v) Ponceau S, 5% acetic acid) followed by two rinses with Milli-Q ddH_2O. Nitrocellulose membranes were blocked for 1 h in TTBS (50 mM NaCl, 0.5% Tween, 20 mM Tris-HCl, pH 7.5) containing 5% skim milk. Membranes were then incubated for 1 h in primary antibodies in TTBS containing 2% milk for anti-GFP. Following 3 x 10 min washes with TTBS, the membranes were incubated with HRP-conjugated secondary antibodies that were detected by enhanced chemiluminescence (ECL) using the ECL-plus system (GE Healthcare) following the manufacturer's instructions. The membranes were exposed to Super RX medical X-ray film (Fujifilm) in a FBXC 810 autoradiography cassette (Fisher Scientific) for 5 s to 10 min and then the films were developed using a X-OMAT 2000A processor (Kodak).

2.12 Image quantification and analysis

2.12.1 Quantification of fluorescence signal overlap for Arf-mCherry with GFP-GBF1 or p58-GFP

Quantification of the extent of signal overlap between Arf-mCherry and either GFP-GBF1 or p58-GFP (Figure 3.2) was performed essentially as previously described (Zhao *et al.*, 2002). Briefly, NIH ImageJ was used to generate separate masks for the green and red signal using a range of threshold values that retained all discernable peripheral structures. At least 5 cells were analyzed. Results are expressed as percentage of total spots chosen for analysis in the green mask that were concentric with spots in the red mask.

2.12.2 Quantification of COPI positive mitotic structures

Mitotic cells in prometaphase, metaphase, and anaphase were identified using the DAPI channel on an epifluorescence microscope for NRK cells stained with DAPI and a β-COP antibody (clone M3A5). Membrane-associated COPI at mitotic Golgi structures were identified by the presence of β-COP labeling of mitotic structures following treatment of cells with DMSO or 5 μg BFA/ml medium for 20 min. Quantification of COPI positive mitotic structures was from three different experiments for each treatment.

2.12.3 Quantification of fluorescence signal overlap for GBF1 with Man II or BIG1.

Quantification of the extent of signal overlap between GBF1 and either Man II or BIG1 (Figure 4.7C) was performed essentially as previously described (Chun *et al.*, 2008) using Metamorph software (version 6.1). The signal intensities exclusively at the mitotic Golgi fragments were analyzed by using an inclusive threshold set to include total membrane signal without saturation. A median filter of 2 pixels was chosen to eliminate background signal. The

integrated intensities for GBF1 overlapping with either Man II or BIG1 after 1.5 min BFA treatment are reported as a percentage of overlap.

2.12.4 Quantification of fluorescence signal intensities

Signal intensities for GFP-GBF1 and Arf-mCherry in Figure 3.6B were quantified using Metamorph software (version 6.1). The signal intensities exclusively at the Golgi and ERGIC membranes were analyzed by using an inclusive threshold set between 80 and 100 to include total membrane signal without saturation. A median filter of 2 pixels was chosen to eliminate background signal. The integrated intensities exported to Microsoft Excel were plotted as a function of time.

Signal intensities for Figure 4.6B were quantified using using NIH ImageJ processing software. The signal intensity of GFP-GBF1 was measured for membranes (Golgi complex and puncta for interphase cells and mitotic Golgi clusters for mitotic cells) and expressed relative to total GFP-GBF1 signal as a ratio. The integrated intensities were exported to Microsoft Excel and plotted for each drug treatment.

CHAPTER THREE: GDP-BOUND CLASS II ARFS ASSOCIATE WITH THE ER-GOLGI INTERMEDIATE COMPARTMENT INDEPENDENTLY OF GBF1

A version of this chapter has previously been published as "Characterization of class I and II ADP-ribosylation factors (Arfs) in live cells: GDP-bound class II Arfs associate with the ER-Golgi intermediate compartment independently of GBF1" (Chun *et al.*, 2008 Molecular Biology of the Cell 19: 3488-3500).

Overview

Despite extensive work on Arf1 at the Golgi complex, the functions of Arfs 2-5 in the secretory pathway, or for that of any Arf at the endoplasmic reticulum-Golgi intermediate compartment (ERGIC) remain uncharacterized. Here, we examined the recruitment of fluorescently tagged Arfs 1, 3, 4, and 5 onto peripheral ERGIC. Live cell imaging detected Arfs on peripheral puncta that also contained GBF1 and the ERGIC marker p58. Unexpectedly, brefeldin A did not promote co-recruitment of Arfs with GBF1 either at the Golgi complex or the ERGIC, but uncovered striking differences between Arf1/3 and Arf4/5. While Arf1 and Arf3 quickly dissociated from all endo-membranes following BFA addition, Arf4 and Arf5 persisted on ERGIC structures, even after redistribution of GBF1 to separate compartments. The GDP-arrested Arf4(T31N) mutant localized to the ERGIC, even in the presence of BFA. Lastly, loss of Arf-GTP following treatment with Exo1 caused rapid release of all Arfs from the Golgi complex and led to GBF1 accumulation on both Golgi and ERGIC membranes. Our results demonstrate that GDP-bound Arf4 and Arf5 associate with ERGIC membranes through receptors distinct from those responsible for GBF1 recruitment. Furthermore, they provide the first evidence that GBF1 accumulation on membranes may be caused by loss of Arf-GTP, rather than the formation of an Arf-GDP-BFA-GBF1 complex.

3.1 Arf1 and class II Arfs localize to peripheral ERGIC

GBF1 has been detected at peripheral punctate structures and implicated in the maturation of cargo carriers necessary for assembly and maintenance of the Golgi complex (Garcia-Mata *et al.*, 2003; Szul *et al.*, 2005; Zhao *et al.*, 2006; Manolea *et al.*, 2008). GBF1 likely activates one or more Arf isoforms on these punctate structures to initiate recruitment of COPI but no Arfs have yet been reported to localize at the ERGIC. The limited availability of selective antibodies to detect endogenous Arfs in fixed cells likely accounts for the lack of information. Antibodies that detect specifically endogenous Arf1 and Arf5 at the Golgi complex in fixed cells are available but did not permit further characterization of weak peripheral structures. As shown in Figure 3.1A, several puncta are observed with antibodies directed against both endogenous Arf1 and Arf5. However, the signal from these puncta was weak and often appeared to be masked by high levels of non-specific background staining. Therefore, these peripheral structures could not be unambiguously characterized. To overcome these issues, NRK cells were transfected with plasmids encoding untagged Arf1 and Arf5. As shown in Figure 3.1B, overexpressed Arf1 and Arf5 are readily detected at the Golgi complex as well as peripheral puncta.

To examine in more detail the potential function of both class I and class II Arfs at peripheral ERGIC structures, we tagged Arfs 1, 3, 4, and 5 with both green (GFP) and red (mCherry) fluorescent proteins. We chose not to examine the class III Arf6 since it has been well documented to function in the endo-lysosomal system. A GFP-tagged form of Arf1 has been characterized in detail

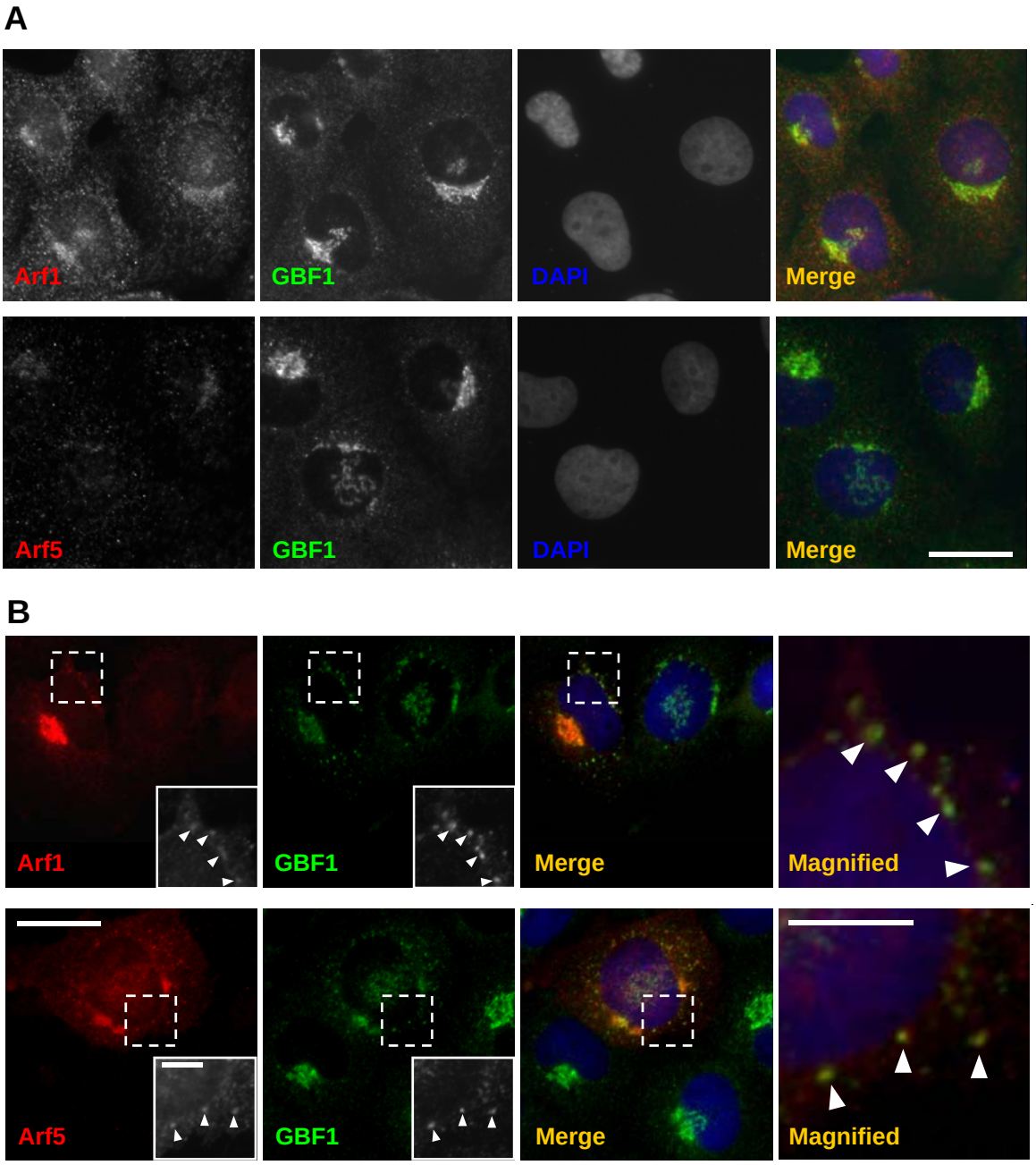

Figure 3.1 Arf1 and Arf5 localize to both the Golgi complex and peripheral puncta positive for GBF1.

A) NRK cells were processed for indirect immunofluorescence (IF) with antibodies directed against GBF1 (green channel) and either Arf1 or Arf5 (red channel). DNA (blue channel) was revealed by DAPI staining. Bar, 20 µm.

B) NRK cells were transfected with plasmids encoding untagged Arf1 or Arf5, fixed and then processed for indirect IF in the presence of DAPI with antibodies directed against GBF1 (green channel) and either Arf1 or Arf5 (red channel). Arrowheads indicate some peripheral puncta positive for Arf1/Arf5 and GBF1. Bar, 20 µm for full image and 5 µm for insets and magnified images.

and was shown to exhibit properties identical to those of the untagged protein (Vasudevan *et al.*, 1998; Presley *et al.*, 2002).

A well characterized NRK cell line stably expressing low levels of GFP-GBF1 [NRK-GFP-GBF1; (Zhao *et al.*, 2006)] was transfected with plasmids encoding either Arf1-mCherry, Arf3-mCherry, Arf4-mCherry or Arf5-mCherry. As shown in Figure 3.2, all four Arfs localized to the Golgi complex. The higher magnification images shown in Figure 3.2 demonstrate that all four Arfs were also readily detected at peripheral punctate structures (arrowheads). Similar results were obtained with Arfs tagged with GFP in live HeLa cells (Figure 3.3), or untagged Arf5 in NRK, COS1 and HeLa cells (Figure 3.4). Further examination of images such as those shown in Figure 3.2 confirmed that Arf-positive puncta were observed in the vast majority of live transfected cells; all cells ($n > 31$) expressing Arf4 or Arf5 displayed Arf-positive puncta, while 91% of Arf1 transfectants ($n = 34$) and 76% of Arf3 transfectants ($n = 29$) displayed puncta.

To examine in more detail the nature of Arf-positive puncta, NRK cells were co-transfected with plasmids encoding mCherry-tagged Arfs and the ERGIC marker p58 tagged with GFP. As shown in Figure 3.2A, most Arf4- and Arf5-positive puncta, as well as a significant fraction of Arf1 puncta, also contained p58-GFP. Similar experiments performed in HeLa cells expressing a GFP-tagged form of Sec16L (Connerly *et al.*, 2005) confirmed that, as expected of ERGIC structures, Arf-positive puncta often appeared next to but separate from ERES (Figure 3.5).

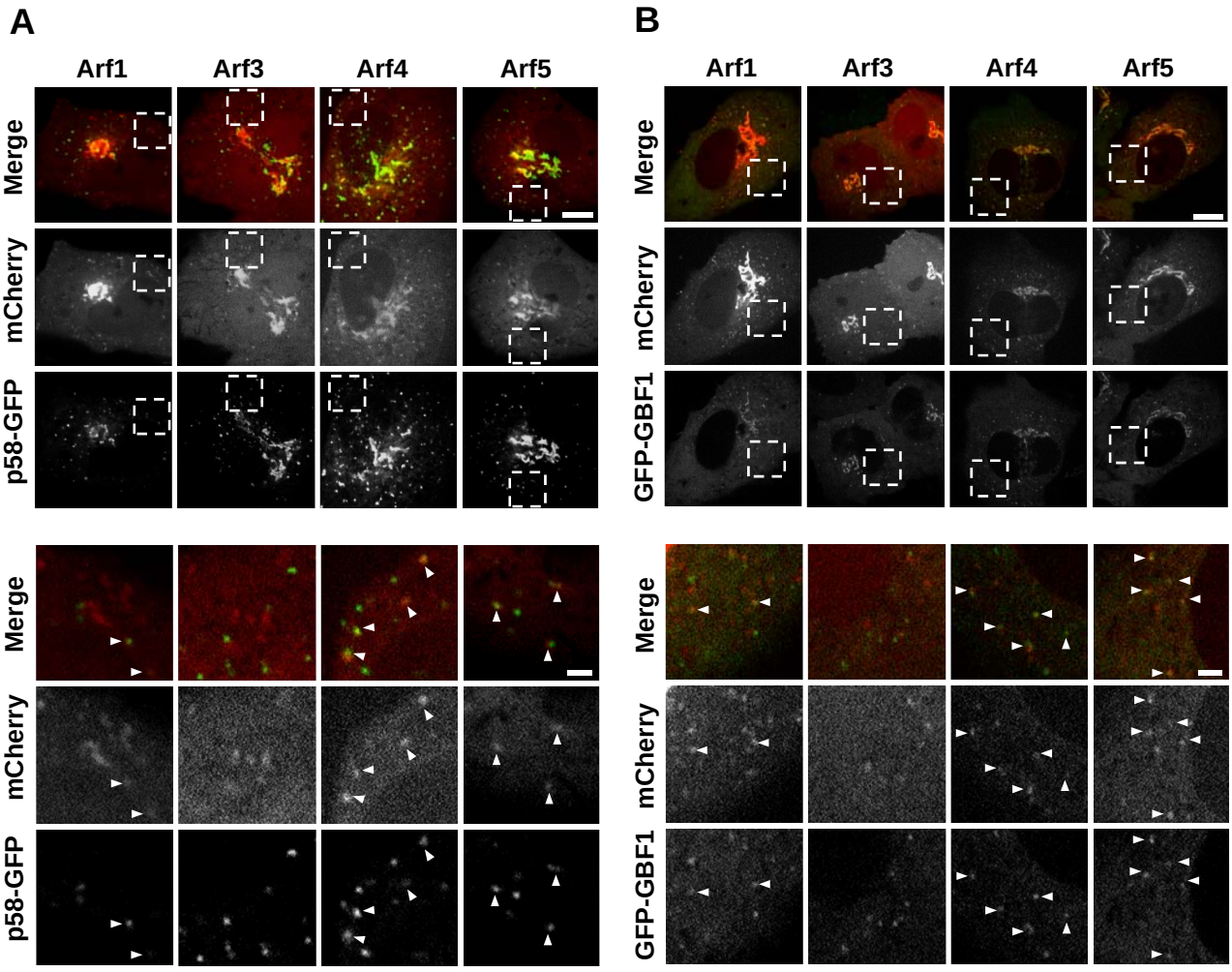

Figure 3.2 Class II Arf-positive puncta correspond to peripheral ERGIC that also contain GFP-GBF1.

A) NRK cells were co-transfected with plasmids encoding p58-GFP and mCherry-tagged forms of either Arf1, Arf3, Arf4, or Arf5. Images were acquired from live cells using a spinning disk confocal microscope. The upper, middle and lower rows display merged still images, mCherry-tagged Arfs and p58-GFP corresponding to a single confocal slice representative of at least 3 experiments. The lower sets of images show enlargement of the boxed area for single channel and merged images acquired from the mCherry and GFP channels. The majority of cells expressing Arf1 (91%), Arf3 (76%), Arf4 (100%) and Arf5 (100%) contain mCherry-positive puncta. Arrowheads indicate overlapping signal of the red and green channels at punctate structures. Bar, 10 µm for full images and 2 µm for magnified images.

B) NRK cells stably expressing low levels of GFP-GBF1 (NRK-GFP-GBF1) were transfected with plasmids encoding mCherry tagged forms of either Arf1, Arf3, Arf4 or Arf5. Live cells were imaged as described for panel A. Arrowheads indicate overlapping signal of the red (mCherry-tagged Arfs) and green (GFP-GBF1) channels at punctate structures. Bar, 10 µm for full image and 2 µm for magnified image.

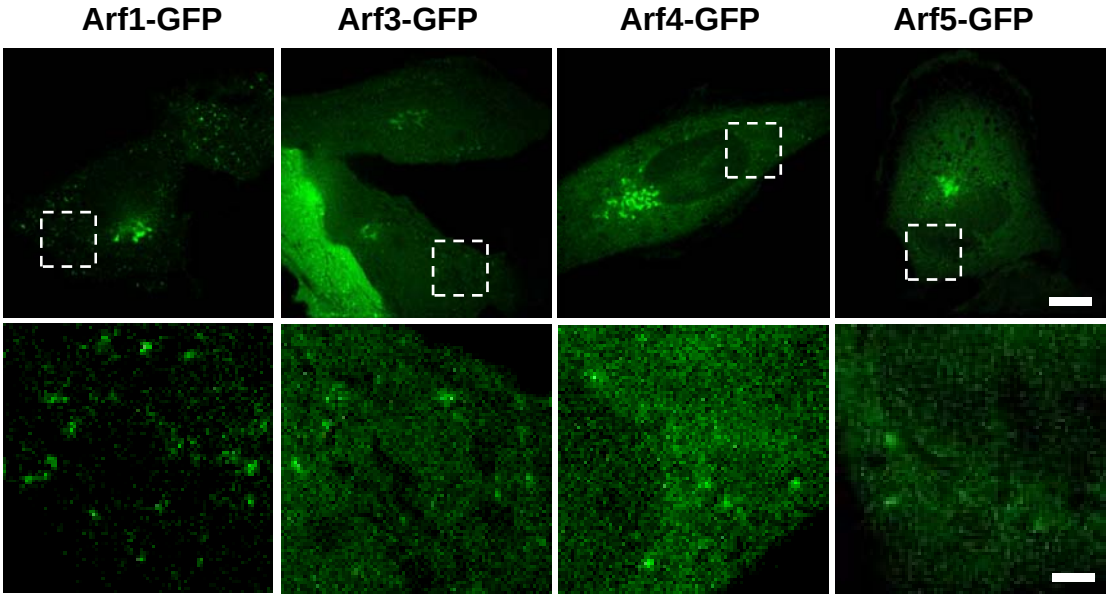

Figure 3.3 Class I and II Arfs tagged with GFP localize to the Golgi complex and peripheral puncta in HeLa cells.
HeLa cells were transfected with plasmids encoding GFP-tagged forms of one of Arfs 1, 3, 4 and 5 and imaged for GFP signal. Single frames of a movie acquired from live cells are shown. Bars represent 5 μm full images and 1 μm for magnified images.

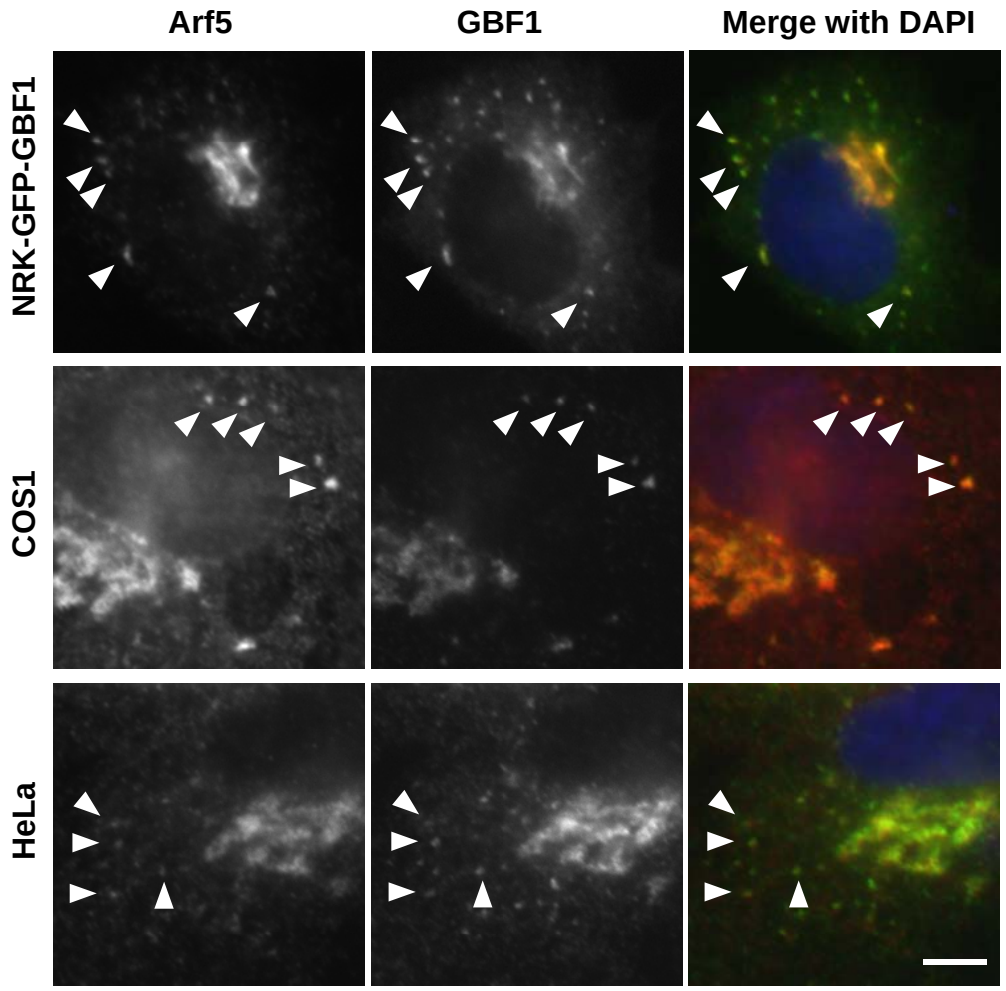

Figure 3.4 Untagged Arf5 localizes to peripheral puncta that are positive for GBF1.
NRK-GFP-GBF1, COS1 and HeLa cells were transfected with a plasmid encoding untagged Arf5, fixed, and then processed for indirect IF with antibodies directed against GBF1 (green channel) and Arf5 (red channel). DNA (blue channel) was revealed by DAPI staining. Arrowheads indicate some peripheral puncta positive for Arf5 and GBF1. Bar, 5 μm.

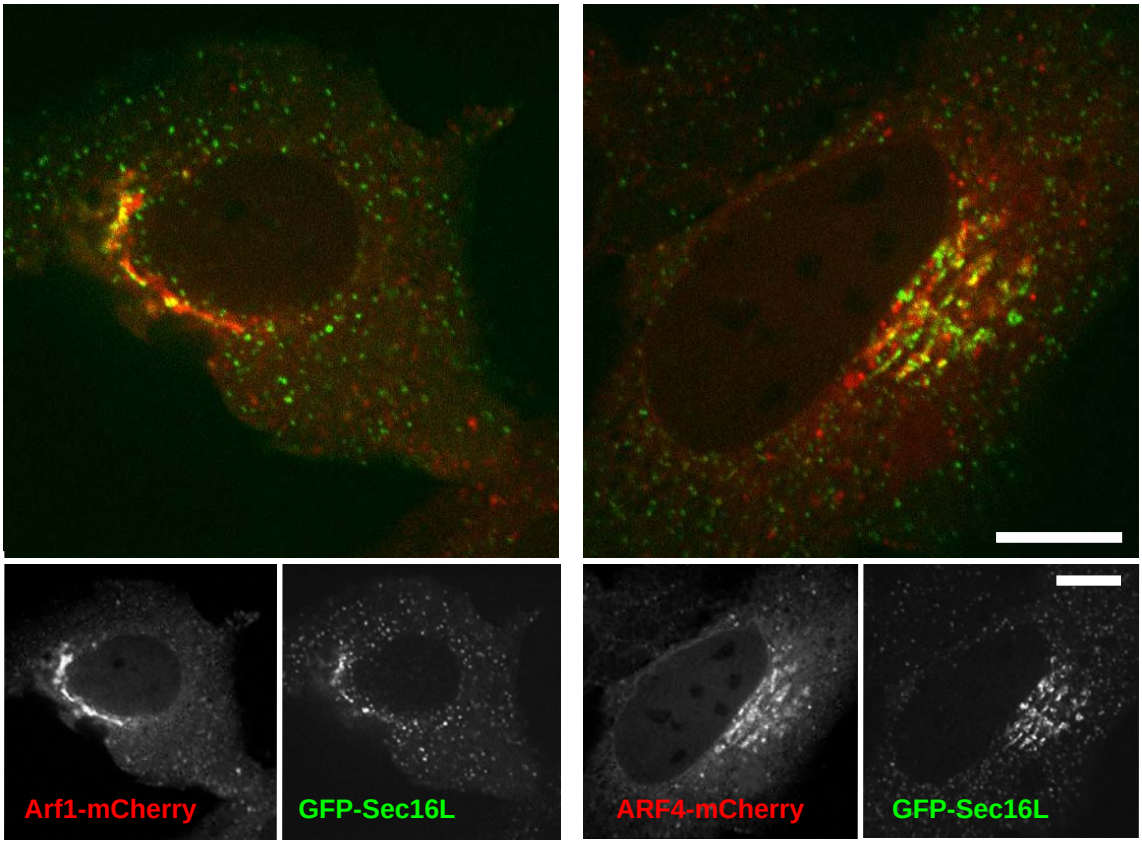

Figure 3.5 Arf1-mCherry and Arf4-mCherry localize to peripheral puncta that are not ERES.

HeLa cells were co-transfected with plasmids encoding Arf1-mCherry or Arf4-mCherry and GFP-Sec16L. Images were acquired from live cells using a spinning disk confocal microscope as described in Chapter 2. Bar, 10 µm.

Comparison with the distribution of GFP-GBF1 revealed that a significant fraction of the Arf 1, 4, and 5-positive structures also contained GBF1 (Figure 3.2B).

Quantitative analysis of images acquired from live cells (similar to those shown in Figure 3.2A), revealed that while the majority of the Arf4 (84 ± 4%; n=169) and Arf5 (78 ± 2%; n=195) positive structures contained the ERGIC marker p58-GFP, this fraction was reproducibly smaller for Arf1 (44 ± 4%; n=255) and Arf3 (27 ± 6%; n=123) puncta. Similar analysis of cells co-expressing Arfs-mCherry and GFP-GBF1 confirmed that most (> 80%) class II Arf-positive puncta also contained GBF1. We conclude that class II Arfs-positive peripheral structures correspond to peripheral ERGIC structures.

3.2 Arfs do not accumulate on membranes with GBF1 following BFA treatment

The dissociation of GBF1 from membranes has been proposed to be tightly linked to nucleotide exchange and to occur only following the release of GDP and binding of GTP on the Arf substrate. This model is derived from the observation that BFA treatment or overexpression of exchange-deficient mutants of Arf1 or GBF1 greatly reduces the kinetics of GBF1 release from membranes and causes its accumulation on a limited subset of intracellular membranes (Niu *et al.*, 2005; Szul *et al.*, 2005; Zhao *et al.*, 2006). We set out to exploit these observations in order to identify the preferred Arf substrate of GBF1 at the ERGIC. The model predicted that immediately after BFA addition, GBF1 would

accumulate at the membrane with concomitant retention of a corresponding Arf signal. We reasoned that formation of the 1:1 Arf-GBF1 complex would be best detected using proteins modified with similar fluorescent tags to avoid differences in signal strength resulting from the use of antibodies with varying affinities.

Analysis of mCherry-tagged Arfs revealed that the majority of all four Arfs quickly redistributed from the Golgi complex upon treatment with BFA (Figure 3.6). Contrary to expectation, little class I Arf signal remained on either the Golgi complex or the ERGIC, even as GBF1 signal dramatically increased on these structures (Figure 3.6A). Furthermore, the response of class II Arfs on the ERGIC matched neither our expectation nor the behavior of class I Arfs. The level of Arf4-mCherry and Arf5-mCherry at puncta remained relatively constant and did not increase to match the signal observed with GFP-GBF1 (Figure 3.6B). Further testing to validate the outcome by exchange of fluorescent tags (i.e. Arf-GFP) in different cell lines yielded identical results. Interestingly, several class II Arf-positive puncta displayed limited motion and appeared stable (Figure 3.6A), as reported by Hauri and colleagues (Ben-Tekaya *et al.*, 2005; Appenzeller-Herzog and Hauri, 2006).

Quantification of membrane-associated GBF1 and Arf signal from the movies shown in Figure 3.6A confirmed that whereas GBF1 accumulated on membranes and reached a maximum around 1 min, none of the Arfs increased in signal following BFA treatment (Figure 3.6B). Quantitative analysis of membrane-bound Arf and GBF1 fluorescence signal after 1 min treatment in several similar experiments confirmed these observations (Figure 3.6C).

Figure 3.6 BFA treatment does not cause co-recruitment of Arfs with GBF1 on Golgi and ERGIC membranes.
A) NRK-GFP-GBF1 cells were transfected with plasmids encoding the indicated mCherry-tagged Arfs. Images were acquired every 5 s after the addition of 5 µg BFA/ml medium. Images shown are from single frames at the indicated time points. Bar, 10 µm.

B) Quantification of the change in Arf-mCherry and GFP-GBF1 signal intensities at the Golgi and peripheral puncta membranes in response to BFA. The signal intensities from stills obtained from each experiment shown in panel A were measured at the indicated times as described in Chapter 2 section 2.12.4 and then expressed as a percentage of maximum Arf and GBF1 values.

C) Quantification of GFP-GBF1 and Arf-mCherry relative signal intensities (percentage of maximum) at the Golgi and peripheral puncta membranes after 1 min treatment with BFA. Values correspond to averages with standard error obtained from at least 3 different sets of experiments. For each cell examined, maxima for Arfs were defined as values measured before BFA addition, while maxima for GBF1 were values measured 1 min after BFA addition.

D) TRex^{TM}-293 cells were transfected with plasmids encoding Arf1-GFP or Arf4-GFP and treated with carrier DMSO or 10 µg BFA/ml homogenate for 2 min at 37ºC. Homogenates were prepared and then separated into cytosolic (C) and membrane (M) fractions as described in Chapter 2 section 2.10. Panels show analysis of fractions following SDS-PAGE and immunoblotting with GBF1 (top) and GFP (bottom) antibodies.

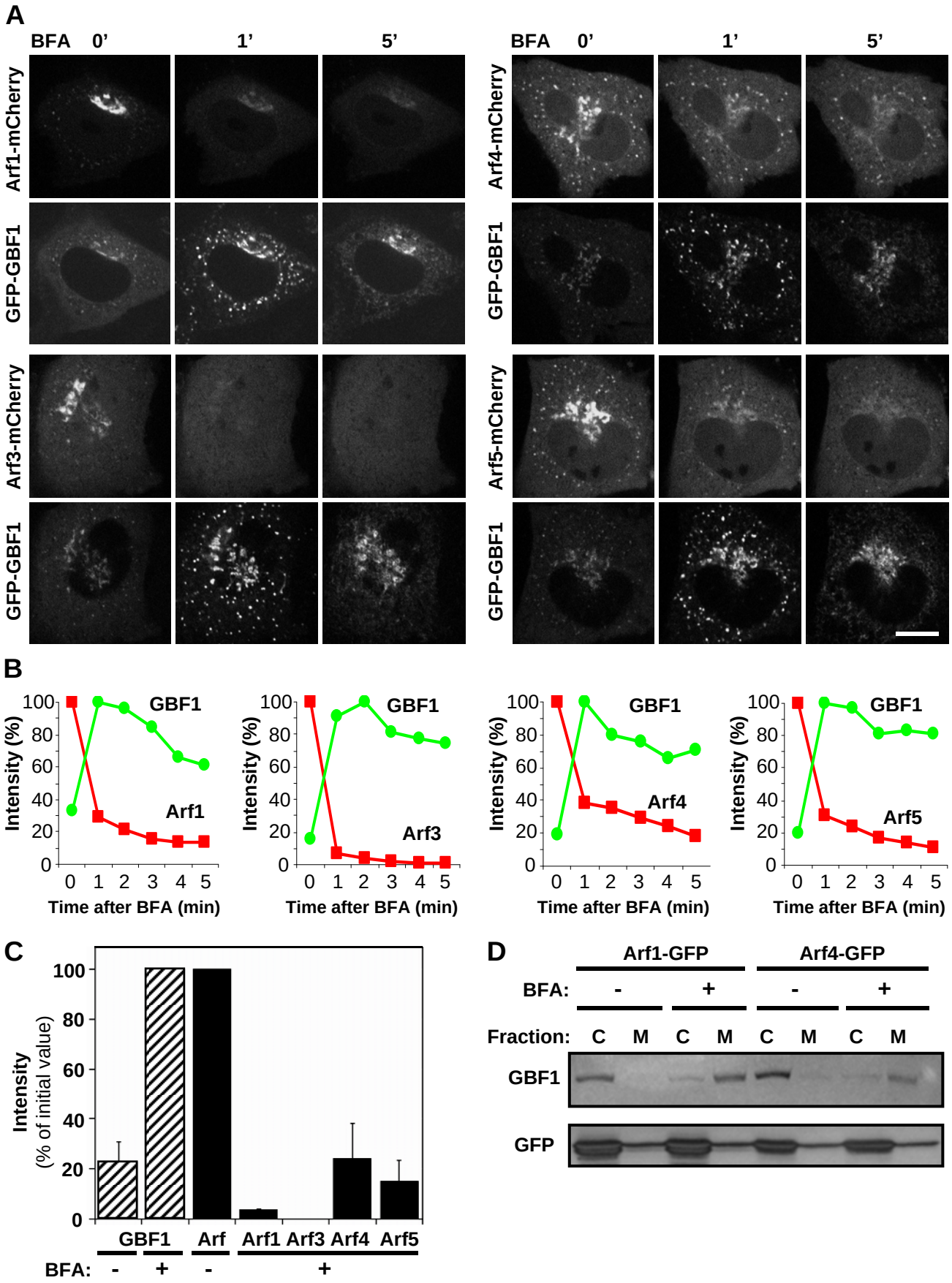

Figure 3.6 BFA treatment does not cause co-recruitment of Arfs with GBF1 on Golgi and ERGIC membranes.

Complementary analysis of sub-cellular fractions further confirmed that BFA does not lead to Arf accumulation in the membrane fraction (Figure 3.6D). Whereas GBF1 dramatically accumulated on membranes (M), Arfs remained largely in the cytosol fraction (C) with no increase in the membrane fraction obtained from cells treated briefly with BFA. These results suggest that contrary to expectation, BFA does not trap Arfs with GBF1 in an abortive complex on membranes *in vivo*.

The dramatically different behavior of class I and class II Arfs prompted us to examine their response to BFA in more detail. COS1 cells were co-transfected with plasmids encoding Arf1 and Arf4 tagged with either mCherry or GFP in order to directly compare the response of Arf1 and Arf4 to BFA treatment. Both Arf1-GFP and Arf4-mCherry could be readily detected on peripheral puncta in COS1 prior to drug addition (Figure 3.7A). To confirm that Arf1 and Arf4 localization to peripheral puncta was not an artifact of the cell line used or the fluorescent tag used, we repeated our analysis using Arf1-mCherry with Arf4-GFP in HeLa cells (Figure 3.8). Using Arfs on which the fluorescent tags had been flipped (i.e. Arf1-mCherry and Arf4-GFP instead of Arf1-GFP and Arf4-mCherry) in HeLa cells, we confirmed localization of Arf1-mCherry and Arf4-GFP at peripheral puncta. As observed before, when cells were treated with BFA, Arf1-GFP/Arf1-mCherry rapidly dissociated from membranes, while Arf4-mCherry/Arf4-GFP clearly remained associated on peripheral puncta (Figures 3.7A and Figure 3.8). Interestingly, unlike what was observed in NRK-GFP-GBF1 cells (Figure 3.6A), Arf4-mCherry/Arf4-GFP signal significantly increased

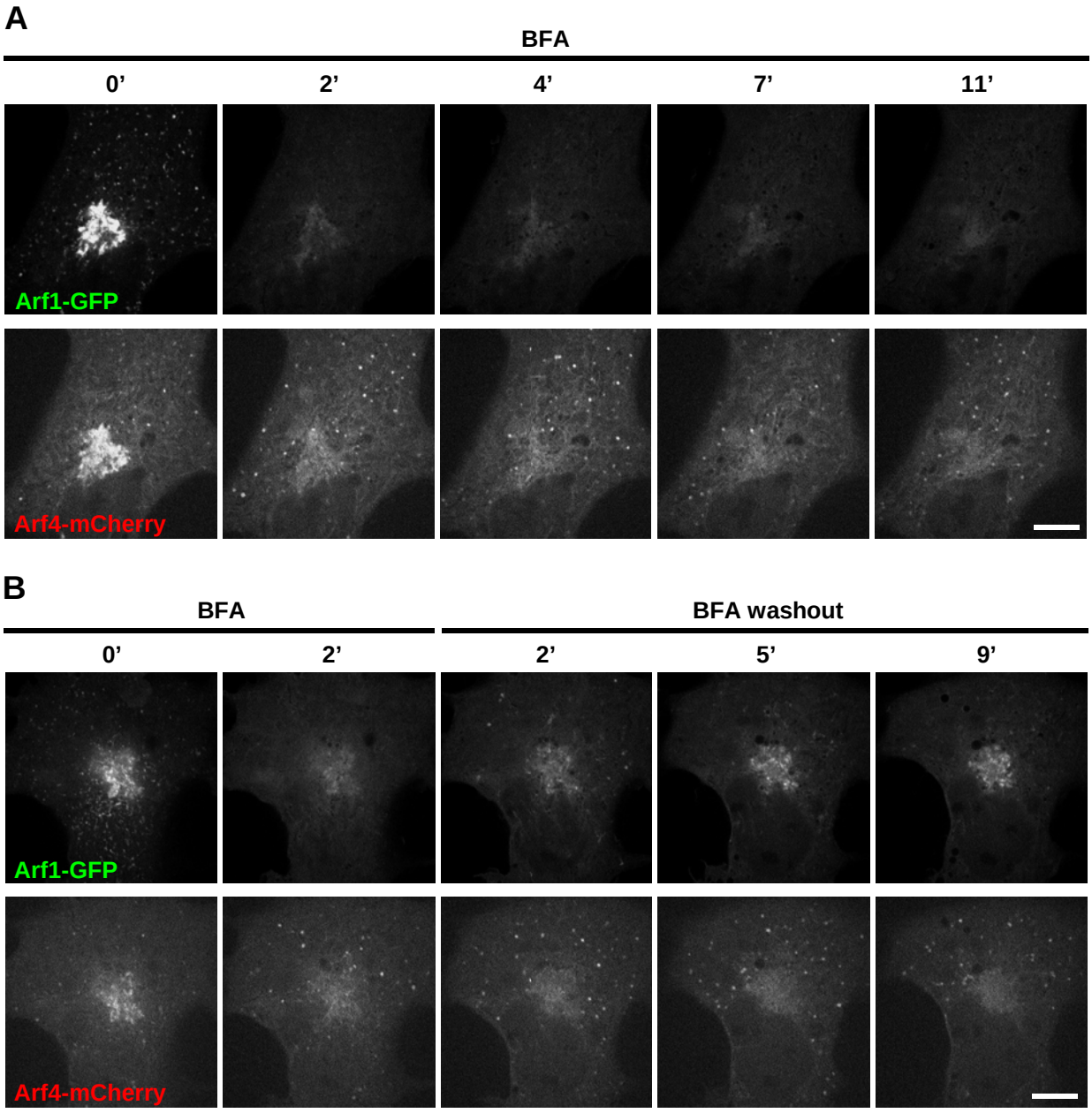

Figure 3.7 Arf4-mCherry, but not Arf1-GFP, remains associated with the ERGIC after BFA treatment in COS1 cells.

A) COS1 cells co-transfected with plasmids encoding Arf1-GFP and Arf4-mCherry were imaged continuously for 11 min following BFA addition. Panels show single channel images at the indicated time points. Representative of at least 3 experiments. Bar, 10 µm.

B) COS1 cells co-transfected with plasmids encoding Arf1-GFP and Arf4-mCherry were imaged continuously for 2 min following BFA addition and an additional 9 min after BFA washout as described in Chapter 2 section 2.8.3. Panels show single channel images at the indicated time points. Representative of at least 3 experiments. Bar, 10 µm.

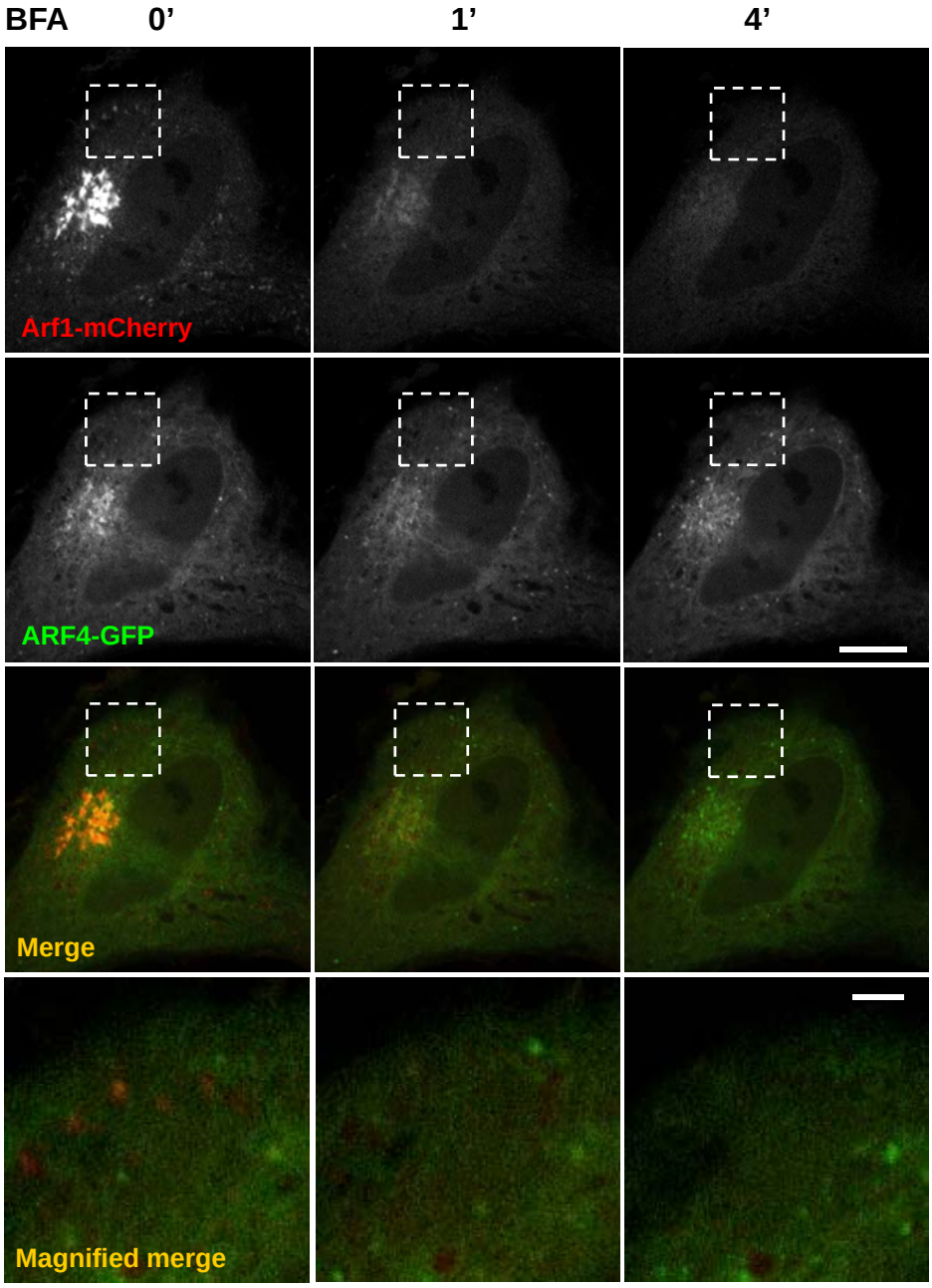

Figure 3.8 Arf4-GFP, but not Arf1-mCherry, remains associated with the ERGIC after BFA treatment in HeLa cells.
HeLa cells co-transfected with plasmids encoding Arf4-GFP and Arf1-mCherry were imaged continuously for 4 min following BFA addition. Panels show single channel and merged images at the indicated time points. Representative of at least 3 experiments. Bar, 10 µm for full image and 1 µm for magnified images.

at 2 min after BFA addition on peripheral puncta in COS1 and HeLa cells (Figure 3.7A and Figure 3.8). This signal continued to be present at about the same level for the duration of the experiment. To determine if Arf1 dissociated from the peripheral puncta following BFA treatment was able to repopulate peripheral ERGIC, we performed a BFA washout experiment. When COS1 cells were treated with BFA for 2 min, Arf1-GFP was undetectable at peripheral puncta as expected (Figure 3.7B). Arf1-GFP returned to both the Golgi complex and peripheral puncta within at least 2 min post-BFA washout (Figure 3.7B). At 2 min post-BFA washout, Arf1-GFP signal was strong at peripheral puncta and weak at the Golgi complex. Over time, the signal at the Golgi complex became more intense (Figure 3.7B). The signal for Arf4-mCherry at peripheral puncta remained strong following BFA treatment and washout (Figure 3.7B). Our results suggest that BFA-induced Arf dissociation from Golgi and ERGIC membranes can be reversed. Furthermore, repopulation of Arf1 to the Golgi and peripheral puncta following BFA washout appears to localize to puncta that were not positive for Arf4.

3.3 Class II Arfs can associate with the ERGIC independently of GBF1

The retention of class II Arfs at peripheral puncta after BFA treatment appears consistent with the predicted formation of membrane-bound Arf-GBF1 complex. However, two additional observations established that retention of class II Arfs on membranes does not involve GBF1. Firstly, many puncta retained Arf4-mCherry and Arf5-mCherry signal even after GFP-GBF1 had redistributed

to the ER at later time points (Figure 3.6A). Our second test took advantage of the fact that nocodazole (NOZ), a microtubule depolymerizing agent, prevents redistribution of GBF1 to the ER (Zhao *et al.*, 2006). We reasoned that retention of GBF1 at punctate structures in absence of microtubules would better test whether Arfs form a membrane-bound complex with GBF1 following BFA treatment. NRK-GFP-GBF1 cells were treated with NOZ and then imaged following BFA addition (NOZ/BFA; Figure 3.9B). NOZ treatment prolonged the presence of GFP-GBF1 on the Golgi complex and peripheral ERGIC (Figure 3.9B) as previously observed in absence of NOZ (Figure 3.6). As expected, the class II Arfs remained associated with peripheral puncta (Figure 3.9B, C). However, whereas Arf4/5-positive puncta co-localized with GBF1 shortly after BFA addition, most of the GBF1 redistributed to slightly larger structures that gradually separated from the puncta containing class II Arfs (Figure 3.9B). We suspect that class II Arfs remained on peripheral ERGIC structures while membrane-bound GBF1 redistributed to a distinct membrane structure since BFA treatment causes GBF1 to relocalize to the ER when microtubules are present (Zhao *et al.*, 2006).

To confirm that the class II Arf-positive structures observed following extended treatment with NOZ/BFA correspond to peripheral ERGIC, we repeated this experiment with cells co-transfected with a plasmid encoding p58-GFP. As shown in Figure 3.9C, most of the structures onto which class II Arfs persisted after 10 min treatment with NOZ/BFA were positive for p58-GFP. Quantitative analysis established that the vast majority of the Arf4 (91 ± 5%) and Arf5 (89 ±

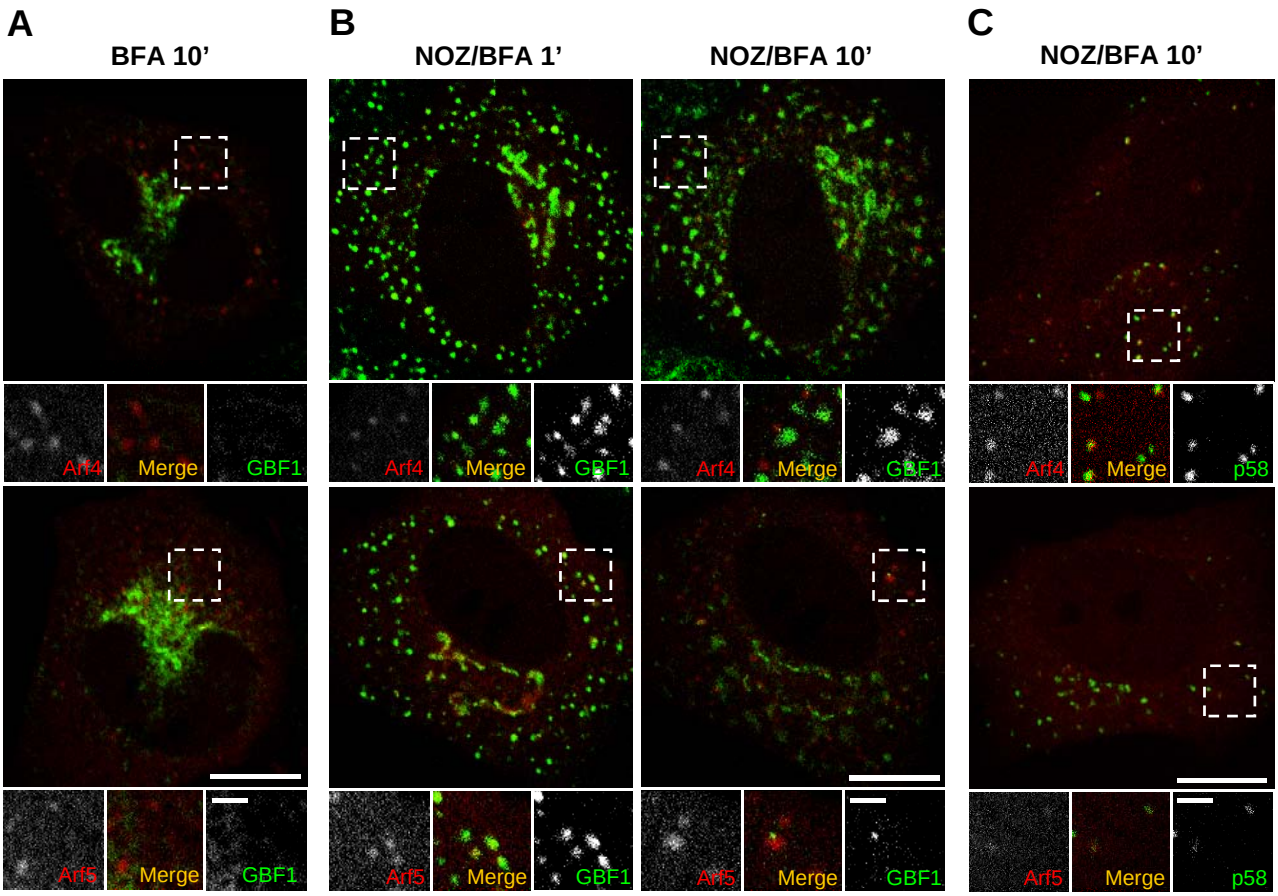

Figure 3.9 Stable association of class II Arfs with the ERGIC in the presence of BFA does not require GBF1.

A) Images correspond to the 10 min time points from the Arf4 and Arf5 movies shown in Figure 3A. Bottom panels show single and merged images acquired in the boxed area from the mCherry and GFP channels. Representative of at least 3 experiments in NRK-GFP-GBF1 cells. Bars, 10 µm for the full images and 2 µm for insets.

B) NRK-GFP-GBF1 cells transfected with either Arf4-mCherry (upper row) or Arf5-mCherry (lower row) were incubated on ice for 2 min followed by treatment with 20 µg NOZ/ml medium for 15 min on ice. Several min (5-10 min) after transfer to a heated stage, cells were treated with BFA and imaged every 5 s for 10 min. Images correspond to frames captured at the indicated time points. Bottom panels show single and merged images acquired in the boxed area from the mCherry and GFP channels. Images representative of at least 4 experiments in NRK-GFP-GBF1 cells. Bars, 10 µm for the full images and 2 µm for insets.

C) NRK cells were co-transfected with plasmids encoding p58-GFP, and either Arf4-mCherry (upper) or Arf5-mCherry (lower) and then treated and imaged as in panel B. Arf4/5-mCherry-positive structures after treatment with NOZ and BFA contain p58-GFP and correspond to the ERGIC. Images representative of at least 2 experiments in NRK cells. Bar, 10 µm.

6%) positive puncta also contained p58-GFP, confirming that they correspond to the ERGIC. These results demonstrate that class II Arfs can localize to specific membranes independently of GBF1 and suggest the presence of separate receptors for class II Arfs and GBF1.

3.4 Stimulation of Arf-GTP hydrolysis by Exo1 causes GBF1 to transiently concentrate on Golgi and ERGIC membranes

Our inability to detect BFA-dependent accumulation of stable 1:1 stoichiometric Arf-GBF1 complexes prompted us to consider an alternative explanation for the membrane recruitment of GBF1 caused by BFA treatment and expression of the Arf1(T31N) and GBF1(E794K) mutants. We hypothesized that loss of Arf-GTP, rather than formation of an abortive complex, traps GBF1 on membranes. To test this alternate mechanism, we turned to Exo1, a cell-permeable methylanthranilate analog that rapidly releases Arf1 from Golgi membranes. Exo1 does not affect Arf-GEFs and has been suggested to modify Golgi Arf1 activity by increasing the rate of GTP hydrolysis through an Arf-GAP dependent step (Feng *et al.*, 2003). We reasoned that if GBF1 accumulation on Golgi and ERGIC membranes were linked to loss of Arf-GTP, Exo1 should cause membrane accumulation of GBF1 similar to that observed with BFA.

As shown in Figure 3.10, treatment with Exo1 led to rapid but transient recruitment of both endogenous and GFP-GBF1 at the Golgi complex and the ERGIC. Examination of NRK cells by standard IF using anti-GBF1 antibodies first established that Exo1 causes membrane accumulation of endogenous

Figure 3.10 Exo1 causes GFP-GBF1 to concentrate on the Golgi complex and the ERGIC.
A) NRK cells were treated with carrier DMSO or 100 µM Exo1 for 90 sec, fixed and processed for IF using anti-GBF1 monoclonal antibody. Images were acquired and processed identically. Bar, 10 µm.

B) NRK-GFP-GBF1 cells were treated with carrier DMSO or 100 µM Exo1 and imaged for 10 min. Images correspond to single frames at the indicated time points. Images representative of at least 4 experiments in NRK cells. Bar, 10 µm.

C) Quantification of GFP-GBF1 relative signal intensities (percent of initial value) at the Golgi and peripheral puncta membranes after 1 min of treatment with Exo1. Values correspond to averages with standard error obtained from a minimum of 25 cells from at least 4 different sets of experiments.

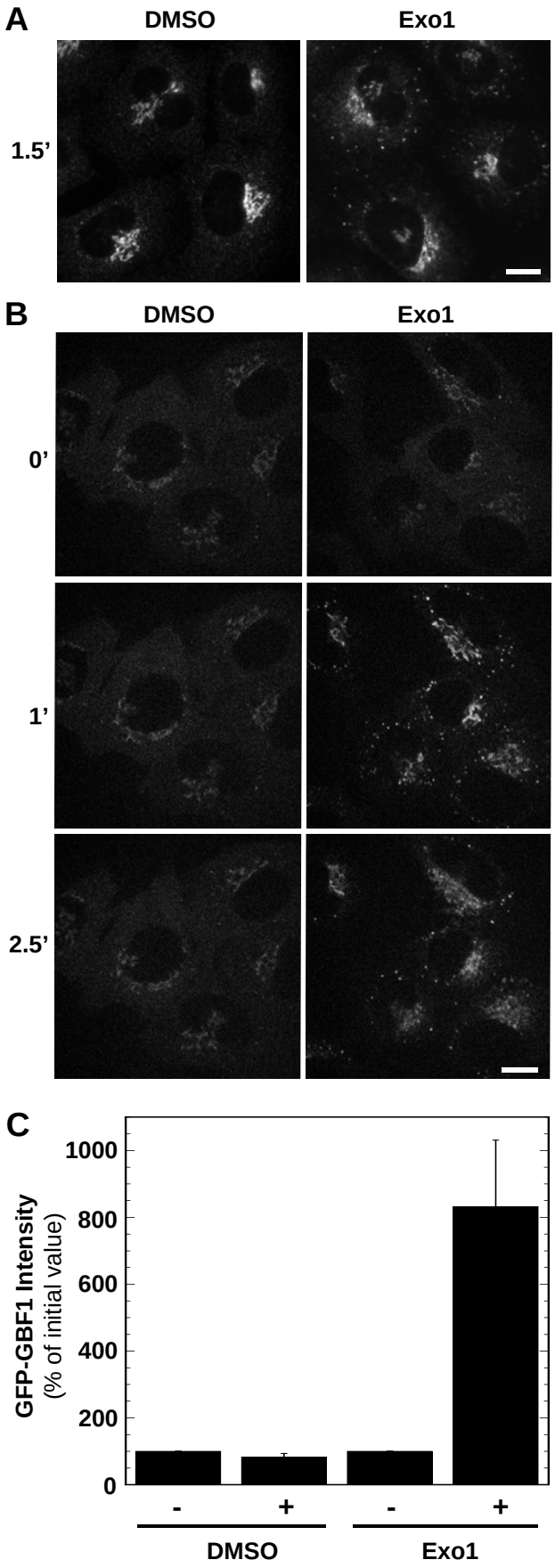

Figure 3.10 Exo1 causes GFP-GBF1 to concentrate on the Golgi complex and the ERGIC.

untagged GBF1, most conspicuously at peripheral puncta (Figure 3.10A). This effect was specific to GBF1, since as previously reported for BFA (Zhao *et al.*, 2006), Exo1 did not cause accumulation of BIG1 on peripheral puncta in NRK cells; similar effects were observed in HeLa and COS1 cells (Figure 3.11). As observed with BFA, GFP-GBF1 accumulated rapidly on membranes, reaching a maximum around one min after Exo1 addition and decreasing thereafter (Figure 3.10B). Quantification of several experiments similar to that shown in Figure 3.10B revealed an approximately 8-fold increase in membrane-associated GFP-GBF1 signal one min after Exo1 treatment (Figure 3.10C). These striking results demonstrate that GBF1 accumulation on Golgi and ERGIC membranes can result from loss of Arf-GTP and does not require formation of a stable, abortive complex. More importantly, they suggest a potentially novel regulatory mechanism for GBF1 recruitment.

3.5 Class II Arfs and GBF1 accumulate at the ERGIC following extended treatment with Exo1

The dramatic effects of Exo1 on GBF1 recruitment led us to investigate its impact on the class I and class II Arfs. As previously reported for Arf1 (Feng *et al.* 2003), Exo1 caused rapid release of all tested Arfs from the Golgi complex, suggesting that Exo1 promotes GTP hydrolysis on all Golgi-localized Arfs (Figure 3.12). Interestingly, as observed with BFA (Figure 3.2), class II Arfs but not class I Arfs remained on puncta shortly after Exo1 addition. Consistent with results presented in Figure 3.10, GBF1 accumulated on structures positive for

Figure 3.11 Exo1 causes rapid accumulation of endogenous GBF1 but not BIG1 onto ERGIC membranes.
NRK, HeLa and COS1 cells were treated with carrier DMSO, 5 µg BFA/ml medium or 100 µM Exo1 for 90 sec, fixed and processed for IF using a mixture of anti-GBF1 monoclonal antibody (green channel) and anti-BIG1 polyclonal antibody (red channel). All images were acquired and processed identically. Bar, 20 µm.

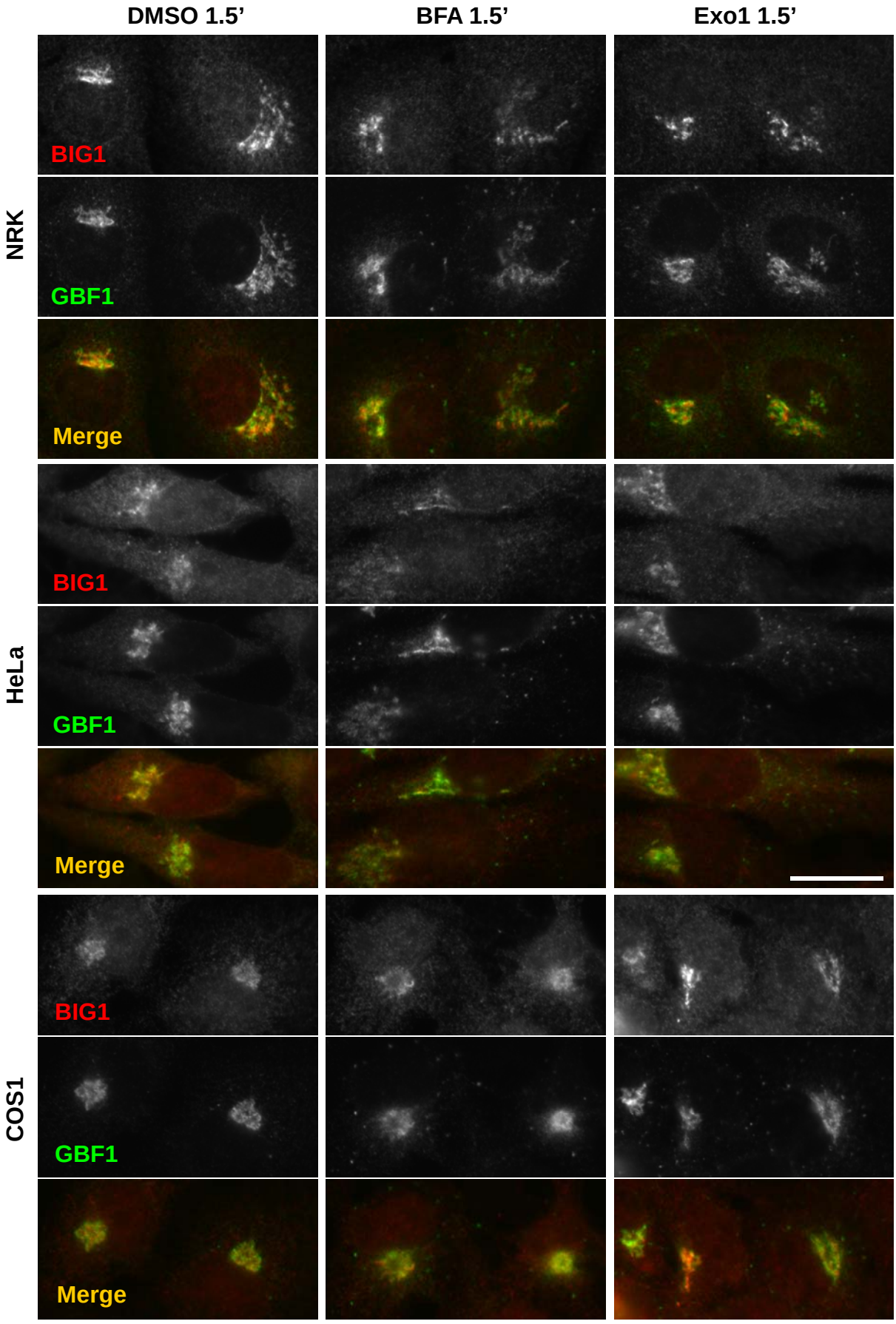

Figure 3.11 Exo1 causes rapid accumulation of endogenous GBF1 but not BIG1 onto ERGIC membranes.

class II Arfs (Figure 3.12). However, unlike what was observed with BFA (Figure 3.2), class II Arfs did not persist but rather redistributed with GBF1 2-3 min after Exo1 addition (Figure 3.12). The most striking difference between the two drugs was observed at later times when class II Arfs and GBF1-positive punctate structures reappeared (Figure 3.12 arrowheads). Puncta containing both Arf4 and GBF1 signal started to appear at about 7 min and grew progressively brighter for up to 20 min. Similar results were obtained in fixed NRK cells expressing Arf4-GFP (Figure 3.13A). These observations confirm that class I and class II Arfs behave differently and reveal that BFA and Exo1 impact ERGIC dynamics differently.

To determine whether the reappearing punctate structures correspond to the ERGIC or fragmented Golgi mini-stacks, we repeated our analysis with a wider range of markers in fixed cells. We chose to examine marker distribution 20 min after Exo1 addition, since this treatment yielded maximum signal in live cells. Images shown in Figure 3.13A (panels e, f) suggests that Arf4 accumulates in puncta positive for an ERGIC marker. Further labeling of Arf4-GFP transfectants for COPI or the Golgi marker Man II confirmed complete dispersal of both markers following treatment with Exo1 (Figure 3.13A, panels g, h). Live imaging of NRK cells cotransfected with Arf4-mCherry and galactosyltransferase-GFP (GalT-GFP) further confirmed the absence of Golgi markers in Arf4-positive puncta (Figure 3.13B). These observations demonstrate that Arf4-positive puncta do not correspond to Golgi fragments or mini-stacks that reformed near peripheral ERES and the ERGIC. The absence of COPI from

Figure 3.12 Exo1 causes rapid loss of Arfs from Golgi membranes but leads to eventual concentration of GFP-GBF1 and class II Arfs at the ERGIC.
NRK-GFP-GBF1 cells transfected with plasmids encoding Arfs tagged with mCherry were treated with carrier DMSO or 100 μM Exo1 and imaged for 20 min. Images correspond to single frames captured at the indicated time points. Arrowheads indicate some peripheral puncta positive for Arf4-mCherry or Arf5-mCherry and GFP-GBF1. Bars, 10 μm.

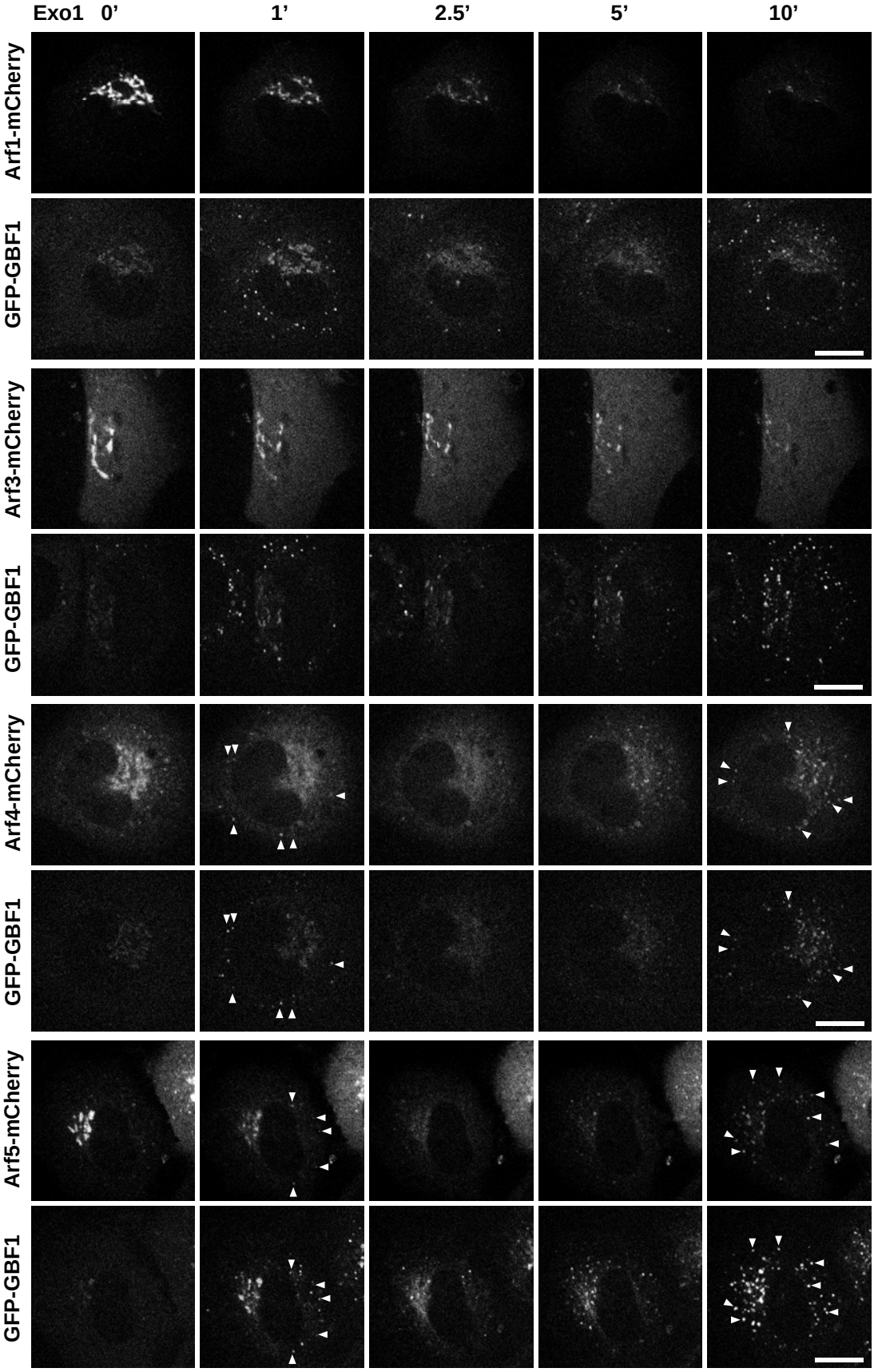

Figure 3.12 Exo1 causes rapid loss of Arfs from Golgi membranes but leads to eventual concentration of GFP-GBF1 and class II Arfs at the ERGIC.

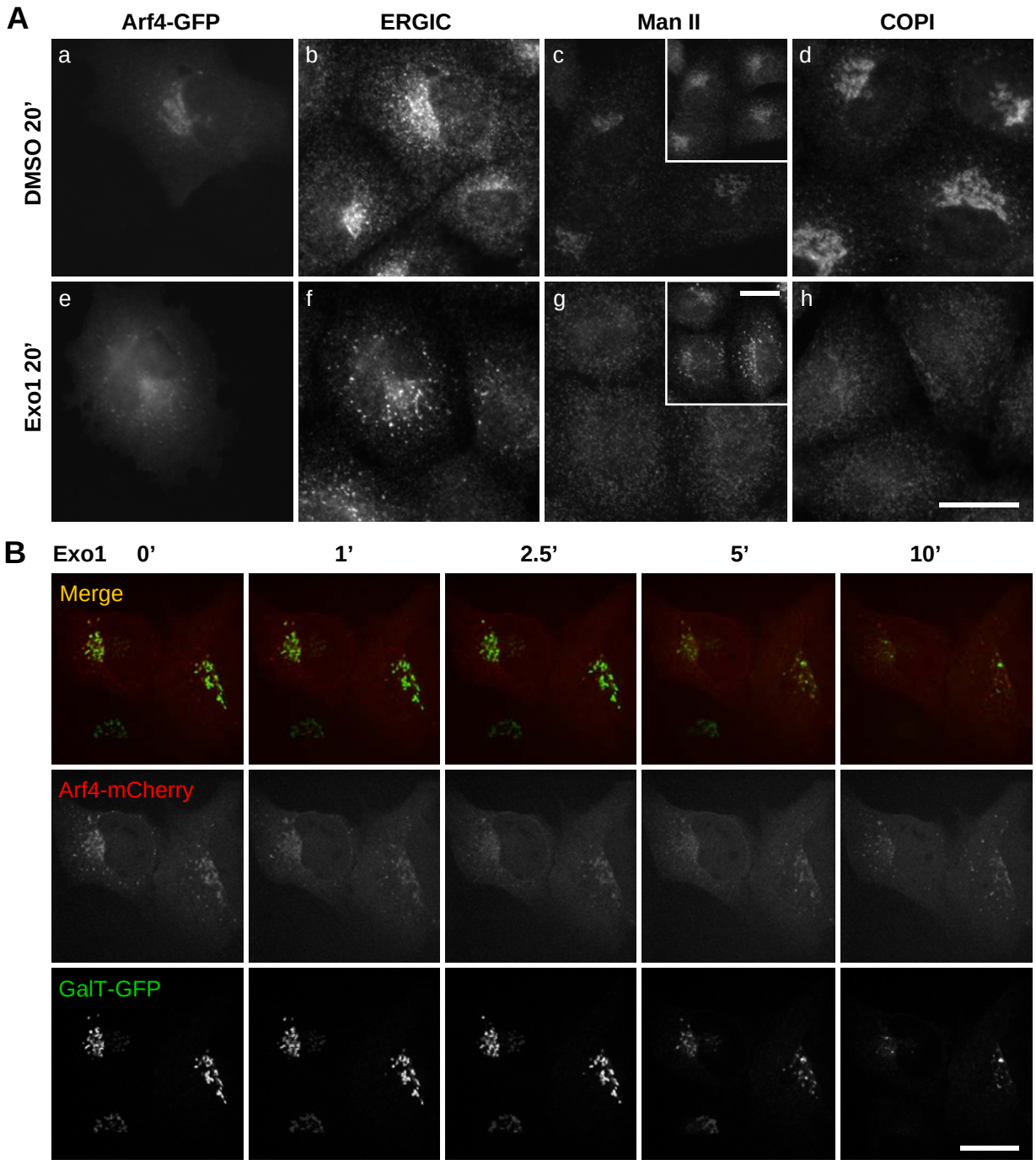

Figure 3.13 Treatment with Exo1 causes breakdown of the Golgi complex but maintains the ERGIC.

A) NRK cells were treated with DMSO (a-d) or 100 µM Exo1 (e-h) for 20 min and then processed for double-label IF using antibodies to the indicated markers. Paired panels a/b and e/f display green/red channels from the same area of cells transfected with plasmids encoding Arf4-GFP. Insets in panels c and g display images obtained with antibody to the ERGIC marker Molly 6. GBF1 and Arf4-GFP concentrate on ERGIC structures devoid of COPI and the Golgi marker Man II. Images representative of 4 experiments. Bars, 20 µm.

B) NRK cells co-transfected with plasmids encoding Arf4-mCherry and galactosyltransferase-GFP (GalT-GFP) were treated with 100 µM Exo1 and imaged for 10 min. Images correspond to single frames of single channels and merged images captured from live cells at the indicated time points. Bar, 10 µm.

Exo1-induced puncta further demonstrated effective loss of activated Arfs. The association of class II Arfs with the ERGIC in presence of either BFA or Exo1 suggests the presence of an organelle specific receptor with affinity for the inactive GDP-bound form of these Arfs.

3.6 Class II Arfs concentrate on peripheral puncta in their inactive, GDP-bound form

To confirm that the inactive GDP-bound form of Arf4 can associate specifically with ERGIC membranes, we examined the localization of a variant of Arf4-GFP containing the T31N mutation, previously shown in Arf1 to prevent stable GTP binding (Dascher and Balch, 1994). Overexpression of Arf1(T31N) interferes with the recruitment of COPI to Golgi membranes and causes disassembly of the Golgi complex (Dascher and Balch, 1994; Zhang *et al.*, 1994; Garcia-Mata *et al.*, 2003). Live NRK cells expressing similar levels of both wild type Arf4-mCherry and Arf4(T31N)-GFP were imaged in the absence and presence of Exo1. As predicted from the impact of BFA on the distribution of Arf4, Arf4(T31N)-GFP localized primarily to peripheral puncta and only weakly to the Golgi complex labeled with wild type Arf4 (Figure 3.14A). Treatment with Exo1 caused loss of wild type Arf4 from the Golgi region and accumulation of Arf4(T31N) on peripheral puncta positive for wild type Arf4. To confirm that the Arf4(T31N)-GFP puncta correspond to the ERGIC, we repeated this analysis in fixed cells labeled with an antibody to the ERGIC. As shown in Figure 3.14B, Arf4(T31N)-GFP associated weakly with puncta in mock-treated cells, and these

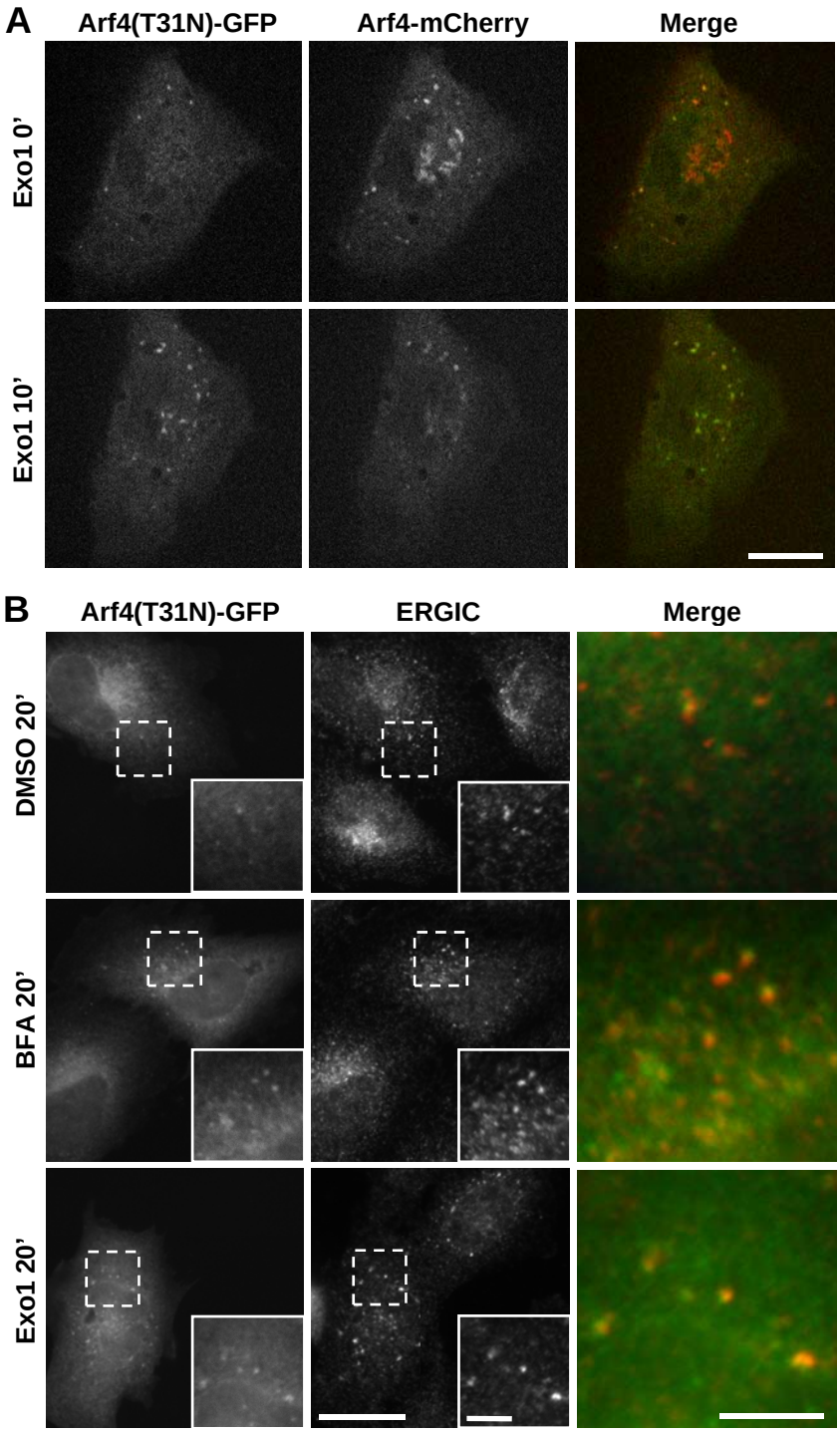

Figure 3.14 Inactive Arf4-GDP localizes to the ERGIC.

A) NRK cells were co-transfected with plasmids encoding wild-type Arf4-mCherry and the GDP-arrested mutant (T31N) of Arf4-GFP. Transfectants were imaged both before and after addition of 100 µM Exo1. Images correspond to single frames obtained immediately prior (t = 0') or 10 min after Exo1 addition. Wild-type (WT), but not the T31N mutant of Arf4-GFP, localizes to the Golgi complex; staining patterns for mutant and WT Arf4 become identical following Exo1 treatment. Bar, 10 µm.

B) NRK cells were transfected with plasmids encoding Arf4(T31N)-GFP. Following treatment with carrier DMSO, 5 µg BFA/ml medium or 100 µM Exo1, cells were fixed and processed for IF as before. Insets show enlargement of boxed area. Right panels show merged signal from the enlarged area. Bars, 20 µm.

structures were labeled with the ERGIC antibody. Treatment with either BFA or Exo1 caused further accumulation of Arf4(T31N)-GFP at the ERGIC (Figure 3.14B). These results demonstrate that the Arf4-GFP is bound to the ERGIC membranes in the GDP-bound form and indicates the presence of a receptor for Arf4 that localizes to peripheral ERGIC.

3.7 Discussion

GBF1, the only known Arf-GEF localized to the ERGIC and *cis*-Golgi complex (Claude *et al.*, 1999; Kawamoto *et al.*, 2002; Zhao *et al.*, 2002; Garcia-Mata *et al.*, 2003) plays a critical role in cargo transport from the ER to the Golgi complex (Zhao *et al.*, 2006; Szul *et al.*, 2007; Manolea *et al.*, 2008). However, until now, the preferred Arf substrates for GBF1 at the ERGIC remained unknown. In this study, we discovered that both class I and class II Arfs localize to peripheral structures. Surprisingly, whereas only about 50% of Arf1-positive puncta colocalize with the ERGIC marker p58, the vast majority of Arf4- and Arf5-positive punctate structures correspond to the ERGIC. Attempts to use BFA to trap GBF1 in abortive complexes with its preferred Arf substrates failed to detect co-recruitment of any Arf with GBF1. However, these experiments revealed that class II Arfs remain on peripheral ERGIC membranes, even after BFA treatment and subsequent redistribution of GBF1 to other compartments. Further experiments confirmed that Arf4 in its GDP-bound form associates selectively with ERGIC membranes. Our observations demonstrate the presence

of receptors specific for class II Arfs on the ERGIC and suggest potential regulatory functions for these Arfs in ER to Golgi traffic.

3.7.1 Class II Arfs localize to the Golgi complex and the ERGIC

We present the first direct evidence for the localization of both class I and class II Arfs at the ERGIC. Despite the clear expectation that Arfs participate in COPI recruitment at the ERGIC, no studies had yet reported the presence of either Arf classes on these structures. Imaging of fixed cells over-expressing untagged or HA-tagged forms of Arf1 and Arf5 readily detected Arfs at the Golgi complex, but only a fraction of the transfectants displayed clear Arf-positive peripheral puncta. Two serendipitous observations enabled the study reported here. First, we observed more GBF1 and Arfs localized to the ERGIC in cells kept at temperatures below 37ºC. In addition, Arfs tagged with fluorescent proteins were observed at puncta in live cells in nearly all transfectants examined when only a fraction of fixed transfectants showed this distribution. For these reasons, we examined Arfs in live cell experiments on a heated stage set at 37^{o}C where temperature at the point of imaging was closer to 25ºC. Almost all live cells expressing class I and II Arfs tagged with fluorescent proteins displayed Arf-positive peripheral puncta over a wide range of Arf expression. Nearly all of these puncta containing Arf4 and Arf5 corresponded to the ERGIC, since they were also positive for the ERGIC marker p58-GFP. Interestingly, a consistently smaller fraction of class I Arf-positive puncta contained p58-GFP. These observations suggest a potentially unique function for class II Arfs at the ERGIC.

3.7.2 GBF1 concentrates on Golgi and ERGIC membranes without forming a stable abortive complex with Arfs

To examine if class II Arfs were activated preferentially by GBF1 at peripheral ERGIC, we subjected live cells to specific treatments intended to promote the formation of a complex between GBF1 and its Arf substrates. As described in more detail in Results, previous work predicted that treatment with BFA would trap one or more Arfs on membranes commensurate with GBF1 recruitment and formation of a putative abortive Arf-GDP-BFA-GBF1 complex (Cherfils and Melançon, 2005; Niu *et al.*, 2005; Szul *et al.*, 2005; Zhao *et al.*, 2006). Contrary to expectation, our data demonstrate that BFA treatment does not promote association of class I or class II Arfs with GBF1. Analysis of live imaging experiments in Figure 3.6 revealed no concomitant increase of Arf-mCherry signal as GFP-GBF1 accumulated on Golgi and ERGIC membranes shortly following BFA treatment. Class II Arfs remained on punctate structures, but several experiments established that class II Arfs associated with membranes independently of GBF1. Additional experiments performed with interchanged fluorescent tags (Arf-GFP and mCherry-GBF1) in several other cell types yielded similar results. Even overexpression of GBF1 did not lead to BFA-dependent accumulation of tagged Arfs on membranes. Complementary sub-cellular fractionation studies confirmed that while BFA treatment caused dramatic recruitment of GBF1 from cytosol to membranes, we observed no concomitant Arf recruitment. Our observations may at first appear inconsistent with a previous report that treatment of cells overexpressing YFP-GBF1 with low (1 µg

BFA/ml medium) BFA concentration did not cause complete disassociation of Arf1-CFP [Figure 6 of (Niu *et al.*, 2005)]. However, retention of active Arf-GTP on Golgi membranes is exactly what one should expect from use of insufficient levels of drug in cells made partially BFA resistant by GBF1 overexpression (Claude *et al.*, 1999; Niu *et al.*, 2005).

Our results remain consistent with the well characterized mechanism of action of BFA. The demonstration that BFA is an uncompetitive inhibitor that can form ternary complexes with Arf and isolated Sec7 domains is incontrovertible (Mansour *et al.*, 1999; Peyroche *et al.*, 1999; Robineau *et al.*, 2000; Mossessova *et al.*, 2003; Renault *et al.*, 2003). However, our results suggest that such complexes must be transient and do not accumulate *in vivo*. Rapid inhibition of GBF1 activity may lead instead to modification of either GBF1 or its receptor that traps GBF1 on its receptor and decrease GBF1 activity towards Arfs (Figure 3.15). Formation of a transient abortive Arf-GDP-BFA-GBF1 complex is likely what allowed Jackson and colleagues to detect BFA-dependent interaction between GBF1 and Arf1 in their bimolecular fluorescence complementation assay (Niu *et al.*, 2005). It may be important to note that reconstitution of the split YFP is largely irreversible (Kerppola, 2006) and likely traps a transient intermediate rather than reveal a stable Arf-GEF complex. Finally, we cannot exclude the possibility that GBF1 forms undetectable but stable complexes with endogenous Arfs that could exclude tagged-Arfs. This possibility could explain association of Arf1 and Arf4 with GBF1 reported by Sztul and colleagues (Szul *et al.*, 2007), but could not be unambiguously tested since methods to efficiently detect complexes

Figure 3.15 "Arf-GTP loss" model for the effect of BFA and Exo1 on GBF1 association with membranes.
GBF1 and Arf-GDP are recruited to specific membranes through interaction with distinct receptors.
BFA or Exo1 absent (top). In the presence of a regulatory Arf-GTP (blue), membrane-bound GBF1 acquires an active conformation that can interact with membrane-bound substrate Arf-GDP (red) and promote release of GDP. GTP loading causes the release of a new Arf-GTP (red) and frees up active GBF1 for another cycle of nucleotide exchange. GBF1 dissociates rapidly from its receptor under these conditions but can activate multiple Arf substrates per binding cycle.

BFA present (middle). BFA forms an abortive Arf-GDP-BFA-GBF1 complex with membrane-bound GBF1 and blocks nucleotide exchange. Arf-GAP activity leads to rapid loss of regulatory Arf-GTP from the membrane, which induces a conformational change in GBF1. In the absence of Arf-GTP, membrane-bound GBF1 interacts poorly with Arf-GDP and dissociates slowly from its receptor. Some Arf-GDP remains associated with their receptors.

Exo1 present (bottom). Exo1 stimulates Arf-GAP activity leading to rapid loss of regulatory Arf-GTP from the membrane. Rapid loss of Arf-GTP from membranes induces a conformational change in GBF1. In the absence of Arf-GTP, membrane-bound GBF1 interacts poorly with Arf-GDP and dissociates slowly from its receptor. However, unlike the situation with BFA present, GBF1 will eventually dissociate and rebind to the membrane in its highly active form.

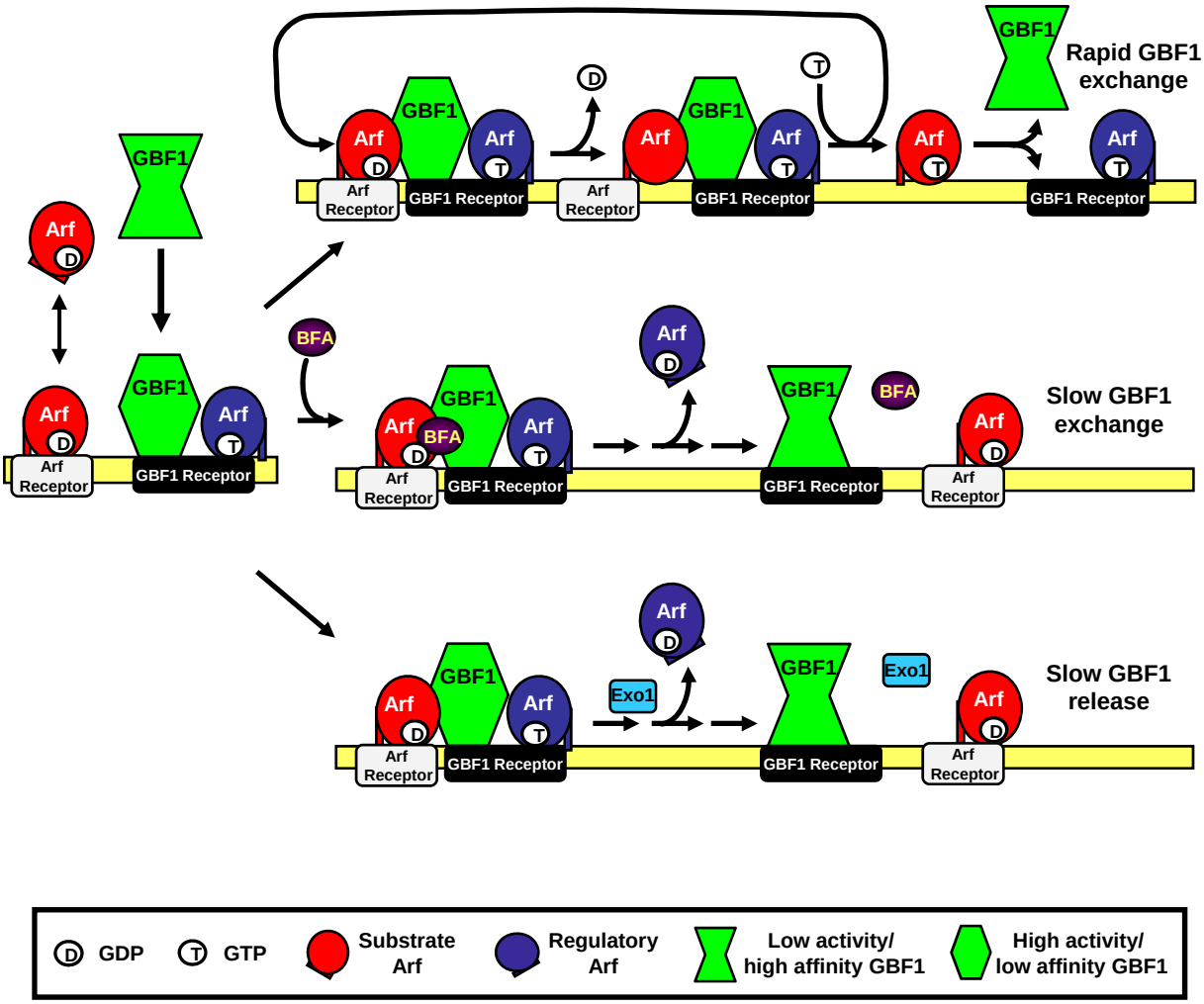

Figure 3.15 "Arf-GTP loss" model for the effect of BFA and Exo1 on GBF1 association with membranes.

containing endogenous Arfs have not been established. Instead, we demonstrated that accumulation of GBF1 on membranes in response to BFA treatment can result from loss of Arf-GTP from membranes and need not depend on formation of a stable abortive complex with BFA (Figure 3.15). Our "Arf-GTP loss" model was tested directly using Exo1, a drug that causes rapid release of Arf1 from membranes by promoting GTP hydrolysis on Arf rather than blocking the guanine nucleotide exchange of known GEFs (Feng *et al.*, 2003). As predicted by our model, Exo1 promoted release of Arfs and caused dramatic recruitment of both endogenous and GFP-GBF1 on Golgi and ERGIC membranes (Figures 3.11, 3.12 and 3.13). These results established that GBF1 can accumulate on ERGIC and Golgi membranes independently of a physical interaction with an Arf. Our "Arf-GTP loss" model is consistent with previous studies with GBF1(E794K) and Arf1(T31N) that cause similar loss of Arf-GTP and lead to accumulation of GBF1 at the membrane (Garcia-Mata *et al.*, 2003; Szul *et al.*, 2005).

Our "Arf-GTP loss" model eliminates troubling inconsistencies between the previous "abortive complex" model and the reported properties of Arf-Sec7d complexes. First, the "abortive complex" model proposes formation of stable abortive complexes between Arf and the charge reversal mutant GBF1(E794K) when such complexes should assemble only under non-physiological conditions containing very low Mg^{2+} concentrations (Beraud-Dufour *et al.*, 1998). Secondly, in the "abortive complex" model, GBF1 dissociation occurs simultaneously with Arf activation (Niu *et al.*, 2005; Szul *et al.*, 2005) and therefore limits the rate of Arf activation to that of GBF1 membrane dissociation [$t_{1/2}$ of 10-15 s; (Niu *et al.*,

2005; Szul *et al.*, 2005; Zhao *et al.*, 2006)]. In contrast, analysis of the kinetics of Arf1 activation by Sec7d yielded kcat values >10 s^{-1} and therefore predict that each membrane-bound GBF1 should activate a very large number of Arf molecules per binding cycle (Beraud-Dufour *et al.*, 1998). Revising this model to allow GBF1 to engage another Arf-GDP upon nucleotide exchange would permit multiple rounds of Arf activation per GBF1 binding cycle and thus eliminate this inconsistency. However, even a "revised abortive complex" model remains invalid, since our results clearly established that BFA does not cause accumulation of a significant level of abortive GBF1-Arf complexes *in vivo*.

As proposed in our "Arf-GTP loss" model, reduction in Arf-GTP levels caused by either BFA or Exo1 leads to a conformational change in GBF1 or its receptor that ultimately slows down dissociation of GBF1 from membranes. Arf-GTP could effect this change either directly as illustrated in Figure 3.15 or indirectly through another effector or lipid remodeling. The absence of Arf-GDP-BFA-GBF1 complexes suggests that membrane-trapped GBF1 displays low activity and no longer interacts productively with Arfs. However, we cannot rule out that membrane-bound GBF1 remains fully active but forms only weak Arf-GDP-BFA-GBF1 complexes. The expectation of a tight abortive complex arose from previous studies performed primarily with the isolated Sec7d of ARNO mutants rendered sensitive to BFA (Peyroche *et al.*, 1999; Mossessova *et al.*, 2003; Renault *et al.*, 2003). However, these studies did not allow any prediction as to the stability of complexes formed with full-length GBF1. For example, analysis with the isolated Sec7d of Gea2 revealed a dissociation rate of BFA from

the Arf-Gea2 complex that was 20-fold faster than that observed for the ARNO-complex (Robineau *et al.,* 2000). Such variations could explain why full-length GBF1 may form weak Arf-GDP-BFA-GEF complexes that cannot accumulate under *in vivo* conditions.

3.7.3 BFA traps GBF1 and class II Arfs on separate receptors

Another unexpected result of our study was the clear separation of GFP-GBF1 from Arf4-mCherry and Arf5-mCherry following treatment with BFA. This clear spatial separation between class II Arfs and GBF1 was best illustrated in cells lacking microtubules; in response to BFA, class II Arfs again remained localized to the ERGIC, but over time GBF1 redistributed to more diffuse, uncharacterized globular structures. The appearance of Arf4- and 5-positive puncta containing p58-GFP but devoid of GFP-GBF1 suggests the presence of specific binding sites for class II Arfs at the ERGIC. We hypothesized that these binding sites act as receptors for class II Arfs in their GDP-bound form, since they are retained on ERGIC membranes following treatment with either BFA or Exo1. This hypothesis was tested by examining the distribution of Arf4(T31N), a mutant expected to accumulate in the GDP form. As predicted, Arf4(T31N) localized to punctate structures that overlapped with p58, even when cells were treated with BFA or Exo1 to eliminate Arf-GTP.

Several lines of evidence support the idea that separate receptors exist for GBF1 and Arf-GDP. Although a membrane receptor for GBF1 has yet to be identified, hGmh1 (Chantalat *et al.*, 2003), p115 (Garcia-Mata and Sztul, 2003) and Rab1 (Monetta *et al.,* 2007) have been identified as interacting partners that

may contribute to membrane recruitment of GBF1. In contrast, several candidate receptors for Arf1-GDP have been reported. Arf1-GDP can associate with membranes by interacting with p23, a member of the p24 family of *trans*-membrane proteins (Gommel *et al.*, 2001). Donaldson and colleagues provided similar evidence that membrin (a SNARE) functions to recruit Arf1-GDP to early Golgi compartments (Honda *et al.*, 2005). Although the nature of the putative class II Arf receptors remains unknown, we expect their properties to be distinct from those reported for the Arf1-GDP receptors. Indeed, in contrast to the Golgi-localized p23 and membrin, the putative Arf4-GDP receptor should localize primarily at the ERGIC. Furthermore, the affinity and/or abundance of class II Arf receptors must be greater at the ERGIC, since much of Arf4 remains at the ERGIC following BFA or Exo1 treatment while significantly less Arf1 signal is retained on the Golgi complex.

Previous reports suggested that the Arf1-GDP receptors membrin and p23 function to concentrate Arf1 on membranes in order to facilitate its activation by membrane-associated GEFs (Rein *et al.*, 2002; Honda *et al.*, 2005). Distinct Arf-GDP receptors for different Arfs may similarly facilitate activation of distinct subsets of Arfs on specific compartments. The presence of separate receptors for the different classes of Arfs agrees with the observed co-requirement for both Arf1 and Arf4 in ER to Golgi traffic (Volpicelli-Daley *et al.*, 2005). For example, one possible role for class II Arf-GDP receptors at the ERGIC might be to concentrate Arf4 at the ERGIC. Subsequently, Arf4-GTP would regulate GBF1 recruitment/activation to facilitate sequential activation of Arf1. Unlike what was

reported for ARNO recruitment by Arf6-GTP for subsequent Arf1 activation (Cohen *et al.*, 2007), Arf4 cannot function as a receptor for GBF1 since they can be spatially separated. Proper testing of the interdependent activities of class I and II Arfs in ER to Golgi traffic will require future identification of receptors for both GBF1 and Arfs.

CHAPTER FOUR: CHARACTERIZATION OF GBF1 AND COPI AT MITOTIC GOLGI CLUSTERS

Overview

While examining GFP-GBF1 in live NRK cells, we serendipitously noticed mitotic Golgi clusters persisting throughout mitosis. Our observation contradicts recent work suggesting that mitotic Golgi fragments are inactive and are constantly communicating with the ER (ER-dependent model). Instead, our results are consistent with the autonomous model derived from many studies showing mitotic clusters to persist throughout mitosis in NRK, CHO and PtK cells. In support of Golgi fragments representing autonomous structures, our study provides evidence that the mitotic Golgi structures not only contain active COPI throughout mitosis, but also contain binding sites for GBF1. Using BFA and Exo1, we demonstrate that GBF1 can be trapped and concentrated on these mitotic Golgi cluster membranes. Interestingly, mitosis progresses with no obvious delay even when COPI is inactivated and GBF1 is trapped on the mitotic Golgi clusters. Further characterization established that mitotic Golgi clusters retain the *cis*-to-*trans* subcompartmental Golgi polarization characteristic of interphase cells indicating that COPI is active at the mitotic Golgi clusters. Our work demonstrates for the first time that distinct COPI-positive Golgi clusters persist throughout mitosis, suggesting a potential function for these structures during mitosis.

4.1 Live cell imaging reveals GBF1 localization to mitotic Golgi clusters

During our study of Arfs and GBF1 in live NRK cells, we became interested in studying GBF1 in mitotic cells following an unexpected and intriguing observation. According to the ER-dependent model, we expected the Golgi complex to be fragmented into a haze of barely visible structures that eventually redistribute to the ER (Altan-Bonnet *et al.*, 2004). In contrast to the predictions of the ER-dependent model for Golgi fragmentation, we consistently observed visible mitotic clusters positive for GBF1. Our results indicated that GBF1 localized to both sides of separated chromosomes during mitosis. In live cells, GFP-GBF1 maintained both cytosolic and membrane-bound populations throughout mitosis and could be readily observed at mitotic Golgi fragments during metaphase and anaphase (Figure 4.1). These results suggested a potentially important role for GBF1 on mitotic Golgi fragments, and we decided to further examine the function of GBF1 at the Golgi complex during mitosis.

4.2 Golgi enzymes remain at mitotic Golgi clusters at every stage of the cell cycle

The current models for Golgi partitioning during mitosis agree that the Golgi complex undergoes fragmentation and vesiculation at the onset of mitosis and then re-emerges as a ribbon-like juxtanuclear structure containing Golgi enzymes at the end of mitosis (Colanzi and Corda, 2007). However, several studies previously reported that Golgi proteins remain on mitotic Golgi structures supporting an autonomous role for the Golgi complex during mitosis. Proteins

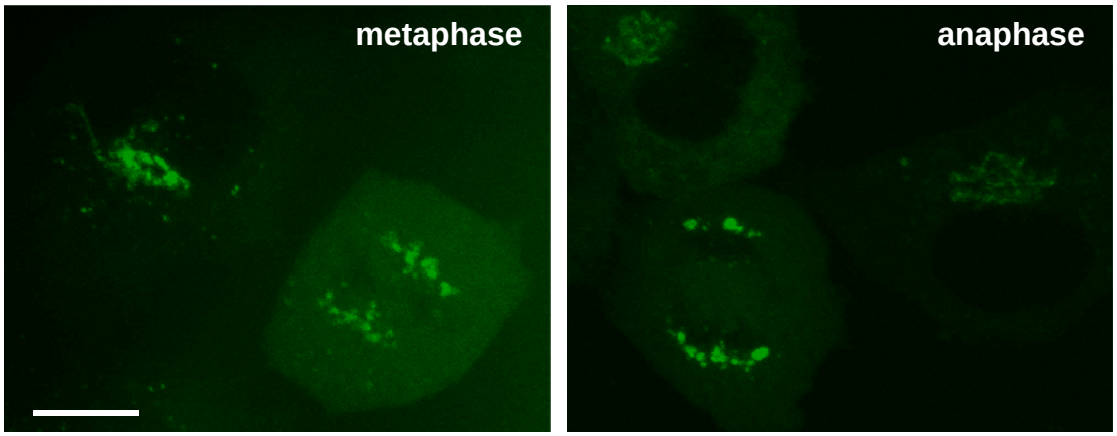

Figure 4.1 GFP-GBF1 localizes to clusters adjacent to the chromosomes in mitotic NRK-GFP-GBF1 cells.

Live mitotic NRK-GFP-GBF1 cells were imaged on a temperature controlled, heated stage set at 37^{o}C with a Zeiss Axiovert 200M spinning disk microscope. The images represent stills of projected Z-stacks of 6 slices, each 1 µm thick. Bar, 10 µm.

analyzed include a chimera containing the N-terminal retention signal of N-acetylglucosaminyltransferase I tagged with GFP in HeLa and NRK cells (Shima *et al.*, 1997; Jokitalo *et al.*, 2001), GM130 in PtK1 and NRK cells (Shima *et al.*, 1998; Seemann *et al.*, 2002), and sialyltransferase in NRK cells (Jokitalo *et al.*, 2001). In contrast, the observation that the Golgi enzyme galactosyltransferase (GalT) and Arf1 completely redistribute during mitosis (Altan-Bonnet *et al.*, 2003; Altan-Bonnet *et al.*, 2006) indicated a role for the ER during mitosis.

To resolve this apparent discrepancy, we examined in more detail the relative distribution of GBF1 and several well characterized Golgi markers in NRK cells at various stages of mitosis (Figure 4.2). This analysis first confirmed that endogenous GBF1 localizes to mitotic Golgi structures in NRK cells at every stage of mitosis (Figure 4.2a), in a spindle-concentrated pattern identical to that reported by Warren's group (Shima *et al.*, 1998). Further indirect IF of endogenous proteins confirmed that in addition to GBF1, resident Golgi enzymes such as giantin and Man II could also be detected at the mitotic Golgi clusters in NRK cells (Figure 4.2b, d). These results suggest that the GBF1-positive structures likely correspond to Golgi fragments, rather than ERGIC structures.

GBF1 selectively localizes to the *cis*-Golgi complex and the ERGIC to regulate COPI recruitment in interphase cells (Kawamoto *et al.*, 2002; Zhao *et al.*, 2002; 2006). We were therefore interested in determining if GBF1 remained functional on these mitotic structures and promoted recruitment of the COPI coat. Consistent with our hypothesis that GBF1 remained active, COPI was detected in almost all of the mitotic cells examined (Figure 4.2c: see below for quantitative

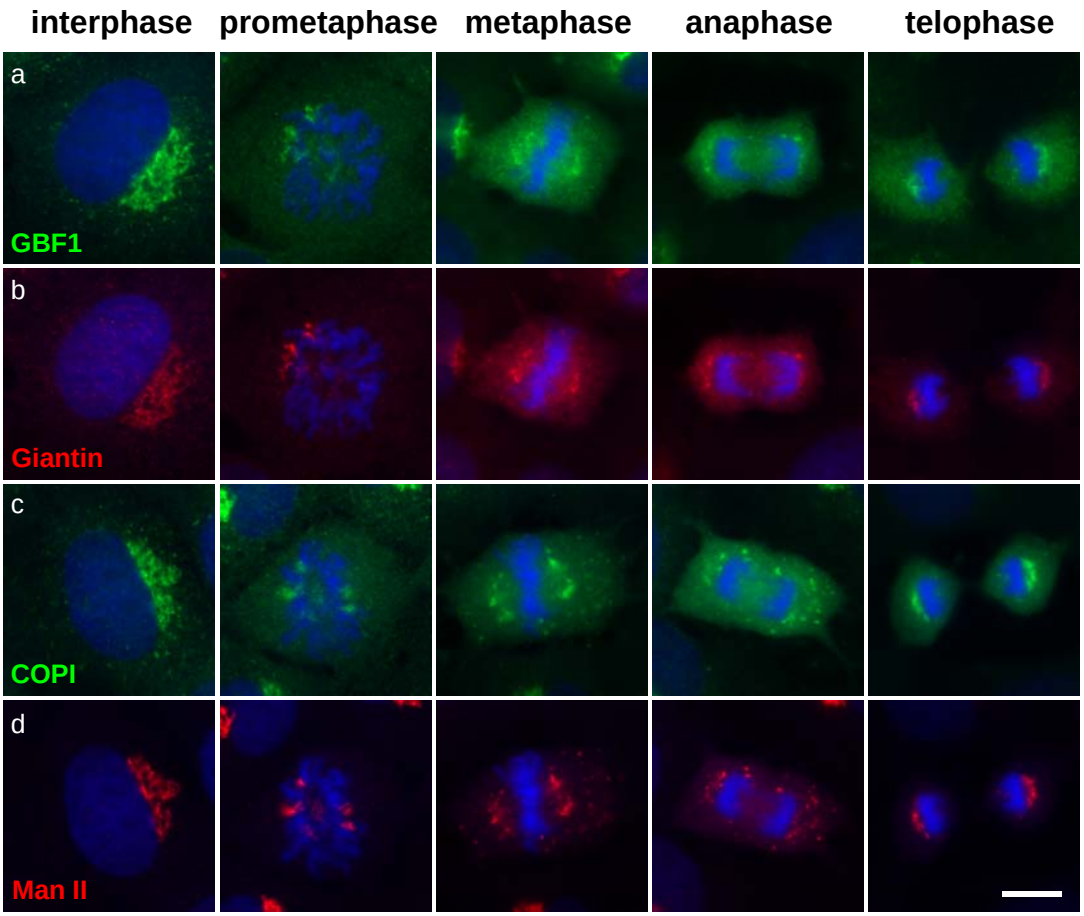

Figure 4.2 Mitotic Golgi clusters, positive for Golgi-localized proteins including GBF1 and COPI, are present at every stage of the cell cycle.
NRK cells were fixed with 3% PFA and then processed for triple-labelled indirect immunofluorescence with antibodies directed against endogenous GBF1, giantin, COPI or Man II in the presence of DAPI (blue). Mitotic cells at each stage of the cell cycle, representative of at least 3 different experiments, are shown. Paired panels a/b and c/d display green/red channels from the same cells. Bar, 10 µm.

analysis). These results suggest that the mitotic Golgi clusters are active structures that retain the activity of the interphase Golgi complex.

4.3 Treatment with BFA causes dissociation of COPI and concentration of GBF1 on the mitotic Golgi clusters but does not cause redistribution of the mitotic Golgi structures to the ER

The presence of COPI on mitotic Golgi membranes could represent either a trapped population or a population that remains dynamic and functional during mitosis. We reasoned that treating cells with BFA would cause dynamic COPI to dissociate from mitotic Golgi membranes in a manner similar to that observed on interphase Golgi membranes. In interphase cells, BFA has been well characterized to cause the rapid dissociation of both COPI (Donaldson *et al.*, 1990) and Arf1 (Donaldson *et al.*, 1992; Helms and Rothman, 1992). As discussed in Chapter 3, this results from inhibition of GBF1, which is accompanied by initial concentration of the GEF on Golgi and ERGIC membranes, followed by its redistribution to the ER (Zhao *et al.*, 2006). As expected for dynamic populations of COPI, BFA caused COPI to dissociate from both the interphase Golgi complex and mitotic Golgi clusters (Figure 4.3A). Quantification of mitotic cells for membrane-associated COPI at mitotic structures during prometaphase, metaphase and anaphase showed 100% (n = 82), 98 ± 2% (n = 135), and 97 ± 3% (n = 173), respectively, that were positive for COPI following DMSO treatment cells. In contrast, 0% (n = 97) of prometaphase, 2 ± 2% (n = 146) of metaphase, and 3 ± 3% (n = 150) of anaphase

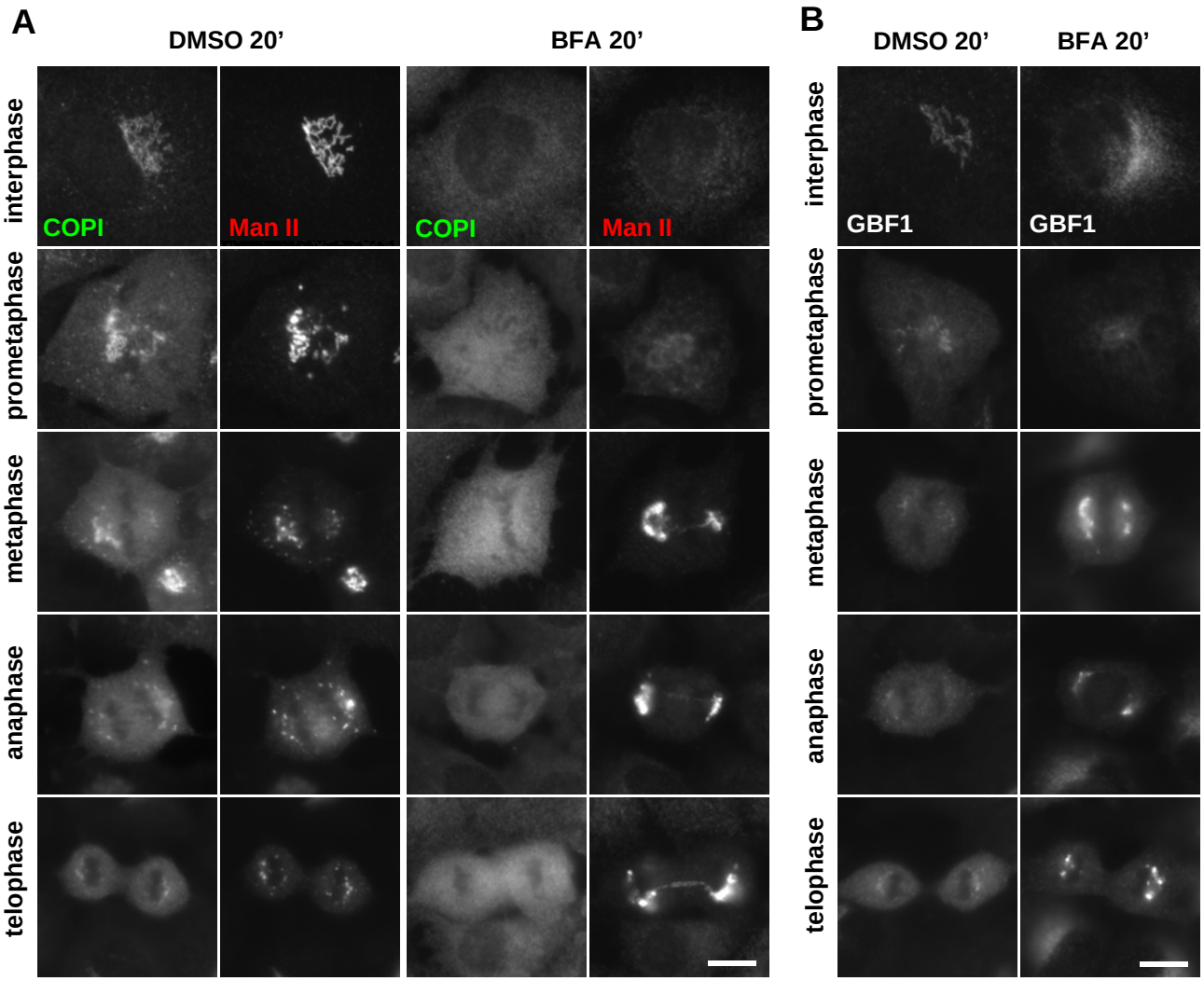

Figure 4.3 COPI dissociates and GBF1 concentrates on the mitotic Golgi clusters in NRK cells treated with BFA.

NRK cells were treated with 5 µg BFA/ml medium for 20 min, fixed and then processed for indirect IF with antibodies directed against COPI with Man II or GBF1. Images for cells representative of the different stages of the cell cycle and representative of at least three different experiments are shown.

Quantification of membrane-associated COPI in cells in prophase, metaphase and anaphase showed 100% (n = 82), 98.4% (n = 135), and 96.7% (n = 173), respectively, of mitotic cells containing Golgi clusters positive for COPI for the DMSO control and 0% (n = 97), 2.2% (n = 146), and 2.5% (n = 150) after BFA treatment. Bar, 10 µm.

cells displayed COPI-positive Golgi clusters after BFA treatment. These observations established that COPI recruitment remains dynamic on mitotic Golgi membranes and that ongoing Arf activation by GBF1 is required for its presence on mitotic Golgi clusters.

During interphase, prolonged treatment of cells with BFA has been shown to redistribute Golgi enzymes to the ER. Several studies have established that GBF1 and most Golgi resident enzymes eventually redistribute to the ER in a microtubule-dependent manner after prolonged treatment of cells with BFA (Lippincott-Schwartz *et al.*, 1989; Zhao *et al.*, 2002; 2006). Based on our observation that COPI was present at mitotic Golgi clusters, we expected that mitotic Golgi clusters behave like the interphase Golgi complex and redistribute Golgi enzymes to the ER following treatment with BFA. Surprisingly, in contrast to cells in interphase and prometaphase, even after 20 min treatment with BFA, Man II (Figure 4.3A) and GBF1 (Figure 4.3B) remained associated with discrete mitotic Golgi structures during metaphase, anaphase and telophase. The inability of Man II to redistribute to a diffuse ER pattern following BFA treatment suggests that the long tubular processes that normally extend out from the Golgi complex to ER (Klausner *et al.*, 1992) do not form during mitosis. These results are not completely unexpected, since the Golgi-derived tubules extend along microtubules that are probably absent during mitosis. Also, Jokitalo *et al.* has demonstrated previously that the Golgi matrix protein GM130 remains separate from the ER marker Bap31 during metaphase (Jokitalo *et al.*, 2001). Taken together, our results demonstrate that the Golgi fragments retain Golgi-localized

proteins during mitosis, do not redistribute to a diffuse pattern and appear to remain separate from the ER during mitosis.

4.4 GBF1 dynamics at the mitotic Golgi clusters and at the interphase Golgi complex are very similar

To compare the dynamic behavior of GBF1 at mitotic Golgi clusters to that of interphase cells, we turned to live cell imaging. We imaged NRK-GFP-GBF1 cells using Z-stack projections in order to capture all the GBF1-positive structures within the mitotic cell. Cells treated with DMSO showed the expected progression through mitosis (Figure 4.4). After approximately 20 to 25 min, the mitotic cells underwent cell division indicating that the imaging protocol had no adverse effect during mitosis. Also, as expected, the DMSO-treated cells showed no appreciable increase in GFP-GBF1 signal (Figure 4.4). In contrast, treatment of mitotic cells with BFA at metaphase caused GFP-GBF1 to rapidly concentrate at Golgi clusters. As expected, BFA caused GFP-GBF1 to rapidly concentrate at the ERGIC and Golgi complex in neighboring interphase cells. Also, consistent with the results obtained with fixed cells (Figure 4.3), GFP-GBF1 eventually redistributed to a diffuse ER pattern in the interphase cells but remained tightly associated with the mitotic Golgi clusters after BFA treatment.

To further confirm that GBF1 membrane association at mitotic Golgi clusters and the interphase Golgi complex is similar, we treated a population of mixed mitotic cells and interphase cells with Exo1. We previously established

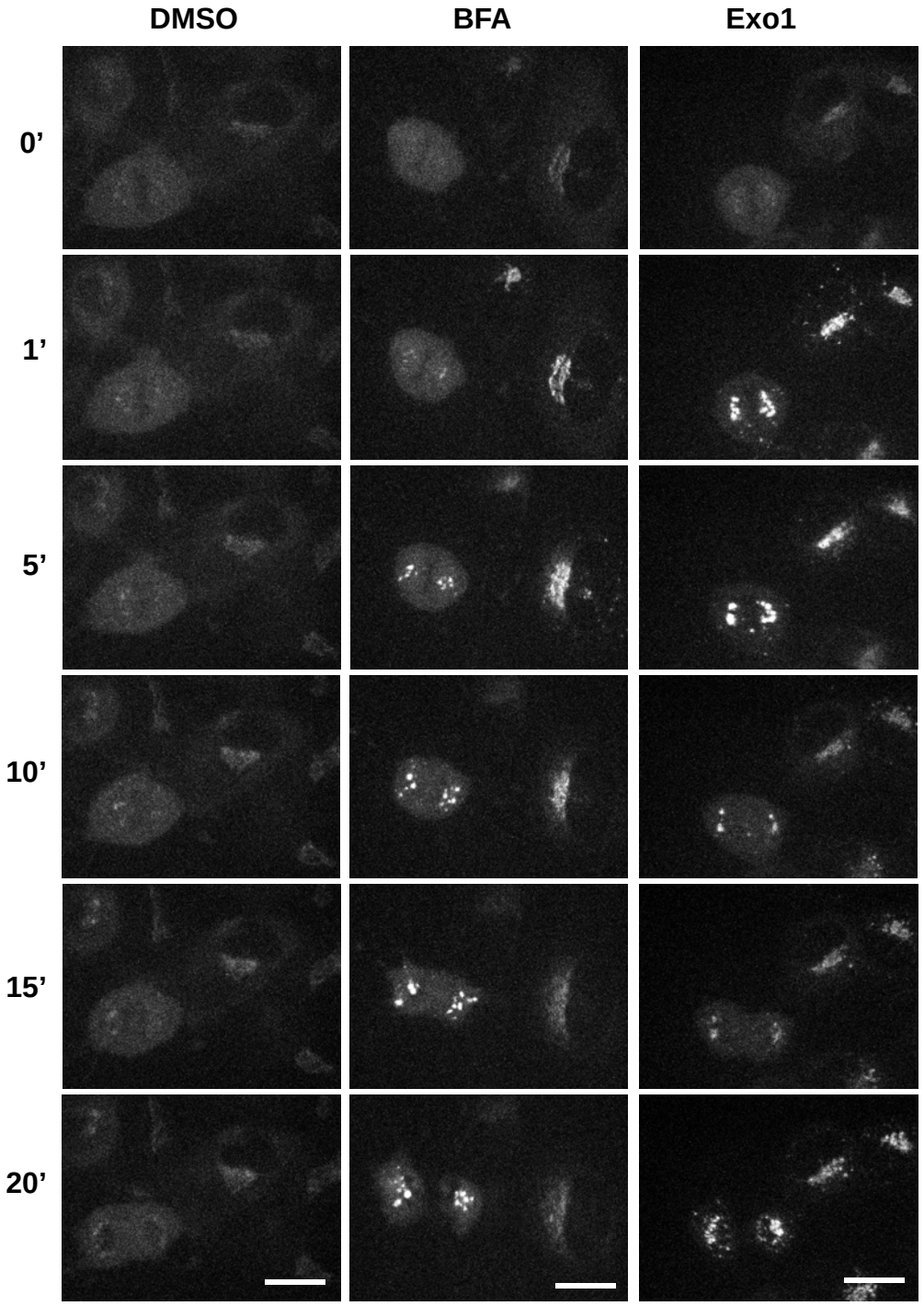

Figure 4.4 GBF1 concentrates to and remains associated with mitotic Golgi clusters after treatment with BFA or Exo1.

Live NRK cells were imaged using a spinning disk confocal microscope following treatment with DMSO (control), 5 µg BFA/ml medium, or 100 µM Exo1 as described in Chapter 2 section 2.8.3. Each panel represents a Z-stack of 13 to 19 slices, each 0.5 µm thick, at the indicated time points after drug addition. Stills show the progression of a mitotic cell beginning in metaphase following drug treatment. Representative of at least 3 experiments. Bars, 10 µm.

that Exo1 alters the recruitment of GBF1 to the Golgi complex and the ERGIC (Chapter 3). We expected that if the behavior of GBF1 is the same during mitosis and interphase, then GFP-GBF1 should initially concentrate, then disappear, and finally reaccumulate on the mitotic Golgi clusters following Exo1 treatment as shown for the interphase Golgi complex (Figure 3.13). Indeed, as shown in Figure 4.4, GFP-GBF1 concentrated on the mitotic Golgi clusters approximately 3 min after Exo1 addition (compared to 1 min in interphase cells), diminished in signal between 8 to 9 min (2-3 min for interphase cells), and then reaccumulated after 15 min (7-8 min for interphase cells). These results indicate that the recruitment, dissociation and re-accumulation of GFP-GBF1 in mitotic cells in response to Exo1 are similar to that observed during interphase but delayed by approximately 2- to 3-fold compared to interphase cells (Figure 4.4). Interestingly, even after treatment with BFA or Exo1 at metaphase, the mitotic cells (n = 3) were able to progress through mitosis and undergo cytokinesis without any obvious delay. These results suggest that GBF1 and COPI are active at the mitotic Golgi clusters, but their activity is not required for cell cycle progression.

To further examine the dynamics of GBF1, we performed fluorescence recovery after photobleaching (FRAP) of GFP-GBF1 at mitotic Golgi clusters. Specifically, we wished to determine if GBF1 exchanged rapidly between a soluble and membrane-bound pools and if this exchange was dramatically reduced in the presence of BFA. First we compared, side-by-side, the recovery of GFP-GBF1 at mitotic Golgi clusters and the Golgi complex of an interphase cell

(Figure 4.5). In untreated cells, GFP-GBF1 signal recovered on mitotic Golgi clusters at a rate comparable to interphase cells (Figure 4.5A). Much of the GFP-GBF1 signal appeared to recover within 30 s after bleaching. Next, treatment of NRK-GFP-GBF1 cells with BFA resulted in the concentration of GFP-GBF1 on the membranes of both mitotic and interphase cells as expected and observed previously (Figure 4.5B). When regions of the mitotic Golgi clusters and the interphase Golgi complex were bleached in these cells (Figure 4.5C; areas outlined in red) and assessed for recovery after BFA treatment, the recovery of GFP-GBF1 signal at both the mitotic Golgi clusters and interphase Golgi complex appeared to be significantly delayed compared to that observed in untreated cells (Figure 4.5C). To accurately compare and quantitate the FRAP of GFP-GBF1 at the Golgi complex and mitotic Golgi clusters, we modified the protocol to subject cells only once to photobleaching following treatment with DMSO or BFA. NRK cells were treated with DMSO or 5μg BFA/ml medium for 2 min and then assessed for GFP-GBF1 signal recovery after photobleaching. In untreated cells, GFP-GBF1 signal recovered on mitotic Golgi clusters to near initial levels within 15-30 s (Figure 4.6A). This recovery in signal appeared to be comparable but reproducibly faster than the membrane dynamics for GFP-GBF1 observed with interphase Golgi ($t_{1/2}$ of 16-17 s) (Szul *et al.*, 2005; Zhao *et al.*, 2006). More importantly, when mitotic cells were treated with BFA and assessed for FRAP, the recovery of GFP-GBF1 signal was significantly delayed compared to that observed in untreated cells (Figure 4.6A). As observed in the DMSO treated mitotic cells, the recovery of GFP-GBF1 signal at mitotic Golgi fragments

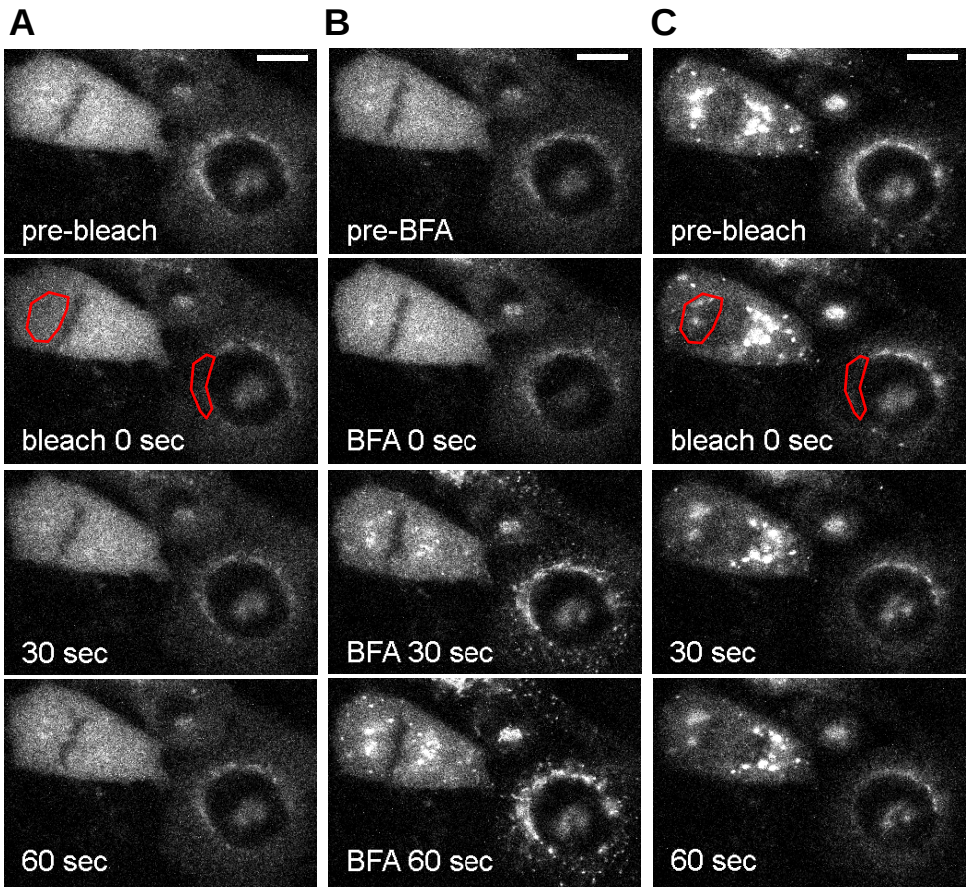

Figure 4.5 Fluorescence recovery after photobleaching (FRAP) of GFP-GBF1 reveals similar recovery of GFP-GBF1 at both the interphase Golgi complex and the mitotic Golgi clusters in NRK cells. A) Untreated NRK cells stably expressing low levels of GFP-GBF1 (NRK-GFP-GBF1) were bleached in the areas outlined in red and observed for GFP-GBF1 fluorescence recovery as described in Chapter 2 section 2.9. Each still shows representative metaphase (left) and interphase (right) cells.

B) Approximately 2 min after bleaching, the same cells from panel A were treated with 5 µg BFA/ml medium for 1.5 min.

C) Approximately 2 min after treatment with BFA, the areas outlined in red (identical to the regions bleached in A) were bleached and monitored again for GFP-GBF1 fluorescence recovery. Representative of at least 3 experiments. Bar, 10 µm.

in mitotic cells treated with BFA was slightly faster than recovery at the interphase Golgi complex after treatment with BFA for 2 min. We hypothesized that cells with BFA traps GFP-GBF1 on mitotic Golgi cluster membranes resulting in a larger proportion of the membrane being occupied by GBF1. Indeed in cells treated with BFA the proportion of membrane-bound GBF1 was greater following treatment with BFA (Figure 4.6B). Our results for FRAP dynamics of GFP-GBF1 at the interphase Golgi complex are in agreement with previous studies reporting the kinetics of GFP-GBF1 recovery to be slower in the presence of BFA (Niu *et al.*, 2005; Szul *et al.*, 2005; Zhao *et al.*, 2006). Taken together, these results further confirm that the characteristics of GBF1 dynamics at the mitotic Golgi clusters are similar to those of the interphase Golgi complex in both the absence and presence of BFA.

4.5 Mitotic Golgi clusters maintain characteristic *cis/trans*-Golgi polarization

Mitotic Golgi fragments are often described as inactive structures that are further fragmented into the smallest possible units to facilitate the equal partitioning of the Golgi complex during mitosis (Jokitalo *et al.*, 2001). We reasoned that since the mitotic Golgi clusters dynamically recruit both GBF1 and COPI, the COPI machinery may be active to facilitate cargo sorting and ongoing cisternal maturation required to maintain polarization of Golgi structures. If so, Golgi proteins such as GBF1 would localize to the *cis*-Golgi cisterna, mannosidase II to the *medial*-Golgi cisterna, and BIG1 to the *trans*- Golgi network. Consistent with polarization observed in the mitotic Golgi fragments

Figure 4.6 FRAP of GFP-GBF1 in mitotic cells is similar to that of interphase cells in both the presence and absence of BFA.

A) Quantification of FRAP performed on interphase NRK-GFP-GBF1 cells or mitotic cells treated with DMSO or BFA prior to bleaching the Golgi complex or mitotic Golgi fragments. Fresh NRK-GFP-GBF1 cells that were not subjected to photobleaching were treated with DMSO or 5 µg BFA/ml medium for 2 min prior to bleaching. Each curve represent the ratio of relative Golgi (or mitotic Golgi fragments)/total cell fluorescence against treatment length. Interphase cells treated 2 min with DMSO (open circle) or with 5 µg BFA/ml medium (filled circle). Mitotic cells were treated with 2 min with DMSO (open square) or with 5 µg BFA/ml medium (filled square). Each curve is an average of 3 experiments.

B) Quantification of GFP-GBF1 signal on membranes relative to total cell fluorescence in live interphase NRK-GFP-GBF1 cells or mitotic cells treated with DMSO or BFA. NRK-GFP-GBF1 cells were treated DMSO or 5 µg BFA/ml medium for 2 min. Quantification of membranes includes relative Golgi and puncta (or mitotic Golgi fragments)/total cell fluoresence ratio against treatment length. Each treatment is an average of at least 3 experiments.

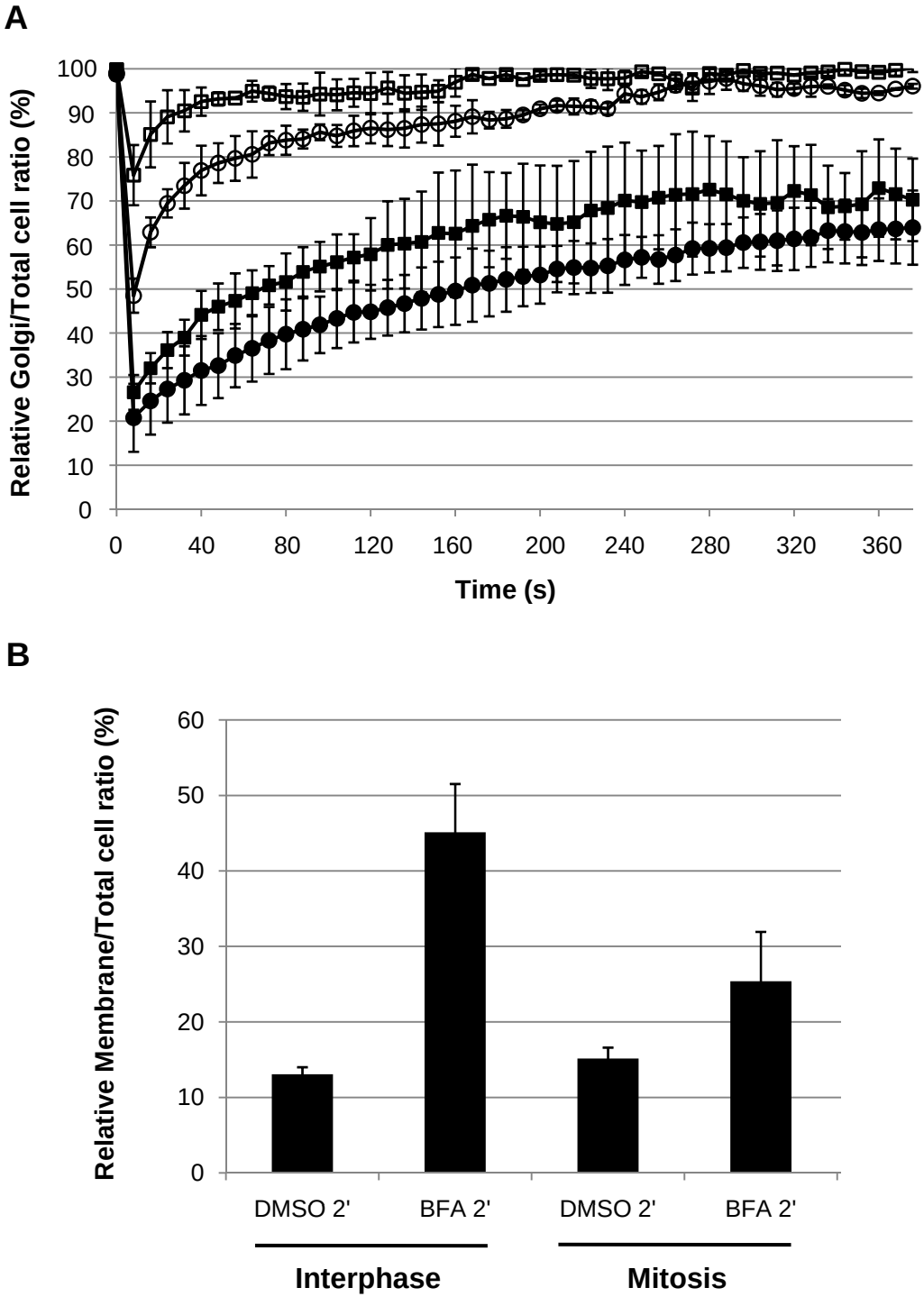

Figure 4.6 FRAP of GFP-GBF1 in mitotic cells is similar to that of interphase cells in both the presence and absence of BFA.

of HeLa cells (Shima *et al.*, 1997), we found very good separation between GBF1 and BIG1 and significant overlap of GBF1 and Man II in all mitotic Golgi clusters examined (Figure 4.7A, B). Quantification of GBF1 overlap with the medial marker Man II showed 82 ± 10% colocalization in metaphase cells and 70 ± 11% in anaphase cells. In contrast, the colocalization of GBF1 with BIG1 in metaphase and anaphase cells was only 32 ± 16% and 22 ± 9%, respectively (Figure 4.7C). Our results demonstrate that the Golgi markers examined at the mitotic Golgi structures have an organization similar to that of the interphase Golgi complex. This polarization of the mitotic Golgi structures demonstrates ongoing sorting by COPI and strongly suggests that the dynamically recruited GBF1 and COPI remain functional on mitotic Golgi clusters.

4.6 Examination of GBF1 in different cell lines reveals the existence of Golgi fragments with different patterns

Many studies have used different cell lines interchangeably to study Golgi fragmentation during mitosis. However, while some cell lines such as NRK, CHO and PtK1 cells display mitotic Golgi clusters organized near a developing half-spindle (Shima *et al.*, 1998; Jokitalo *et al.*, 2001; Seemann *et al.*, 2002), other cell lines such as HeLa cells display a more dispersed, evenly distributed pattern of Golgi fragments (Shima *et al.*, 1998; Zaal *et al.*, 1999). We attempted to characterize the differences in patterns for the Golgi fragments by briefly treating different cell lines with BFA and staining for GBF1. We reasoned that a brief (1.5 min) treatment would be sufficient to reveal GBF1-positive Golgi fragments

Figure 4.7 Mitotic Golgi clusters maintain the *cis/trans*-Golgi separation in NRK cells.

A) NRK cells were briefly treated with 5 µg BFA/ml medium for 1.5 min, fixed and then processed for indirect IF. Cells were dual-labelled with antibodies directed against GBF1 and either Man II (medial-Golgi) or BIG1 (trans-Golgi network). Images for cells representative of the different stages of the cell cycle and representative of at least three different experiments are shown. Bars, 10 µm.

B) Enlarged insets from boxed regions of the merged images of metaphase and anaphase cells shown in panel A stained with Man II (a, b) and BIG1 (c, d). Bars, 2 µm.

C) Quantification of GBF1 overlap with Man II and BIG1 using cells similar to those shown in panel A for metaphase (M) and anaphase (A) cells as described in Materials and Methods. Metaphase: n = 12 for Man II and n = 10 for BIG1. Anaphase: n = 6 for Man II and n = 13 for BIG1.

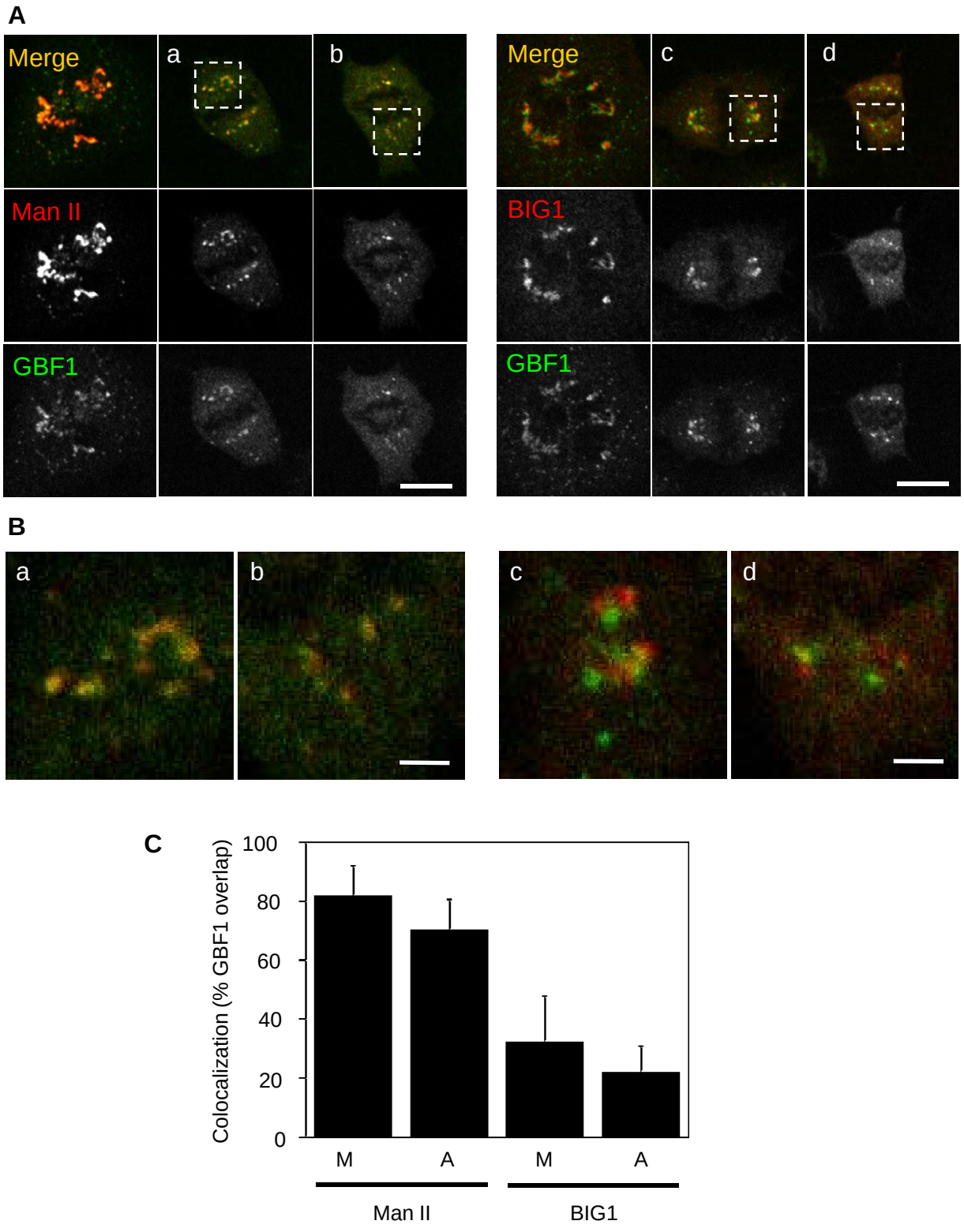

Figure 4.7 Mitotic Golgi clusters maintain the *cis/trans*-Golgi separation in NRK cells.

without interfering with any other mitotic activities. Also, we made the assumption that GBF1 would concentrate only to membranes of Golgi origin. In all cell lines tested, BFA treatment caused membrane recruitment of GBF1, resulting in readily visible GBF1-positive Golgi elements (Figure 4.8). Quantitative analysis confirmed that nearly all cells examined displayed GBF1-positive fragments (Figure 4.8B). BFA treatment revealed Golgi fragments even in 50% of mitotic HeLa cells previously assumed to completely disperse their Golgi markers. Interestingly, our results demonstrate that while NRK, CHO, and Vero cells showed a concentrated localization of GBF1 close to the spindle poles after BFA treatment (Figure 4.8), HeLa, A549 and COS1 cells appeared to have a more dispersed pattern of Golgi fragments. These results show for the first time by light microscopy that the mechanism of Golgi partitioning during mitosis may differ in details between different cell lines but involves in all cases maintenance of distinct Golgi-derived fragments.

4.7 Discussion

GBF1 has been characterized as a *cis*-Golgi localized Arf-GEF regulating the recruitment of COPI to membranes in the early secretory pathway during interphase (Szul *et al.*, 2005; Niu *et al.*, 2005 Zhao *et al.*, 2006). However, recent biochemical studies demonstrating a role for Arf1 and COPI during mitosis (Xiang *et al.*, 2007; Tang *et al.*, 2008) and our observation of GBF1 localizing to mitotic Golgi clusters (Figure 4.2) led us to investigate GBF1 recruitment to mitotic Golgi membranes. Since GBF1 is the only GEF that is required for COPI

Figure 4.8 Brief treatment of different cell lines with BFA concentrates GBF1 on mitotic Golgi fragments that differ in pattern.
A) HeLa, A549, COS1, Vero, CHO and NRK cells were treated with DMSO or 5 µg BFA/ml medium for 1.5 min, fixed with 3% PFA and stained with antibodies directed against GBF1 (mGBF1). Representative of at least 3 experiments for each cell line tested. Bars, 10 µm.

B) Quantification of mitotic Golgi fragments positive for GBF1 at metaphase (M) or anaphase (A) after treatment with 5 µg BFA/ml medium for 1.5 min. Values are a percentage of the total number of cells counted that had cells with GBF1-positive mitotic Golgi fragments.
HeLa: metaphase 52%, anaphase 45%
A549: metaphase 96%, anaphase 97%
COS1: metaphase 90%, anaphase 83%
Vero: metaphase 97%, anaphase 100%
CHO: metaphase 96%, anaphase 88%
NRK: metaphase 100%, anaphase 100%

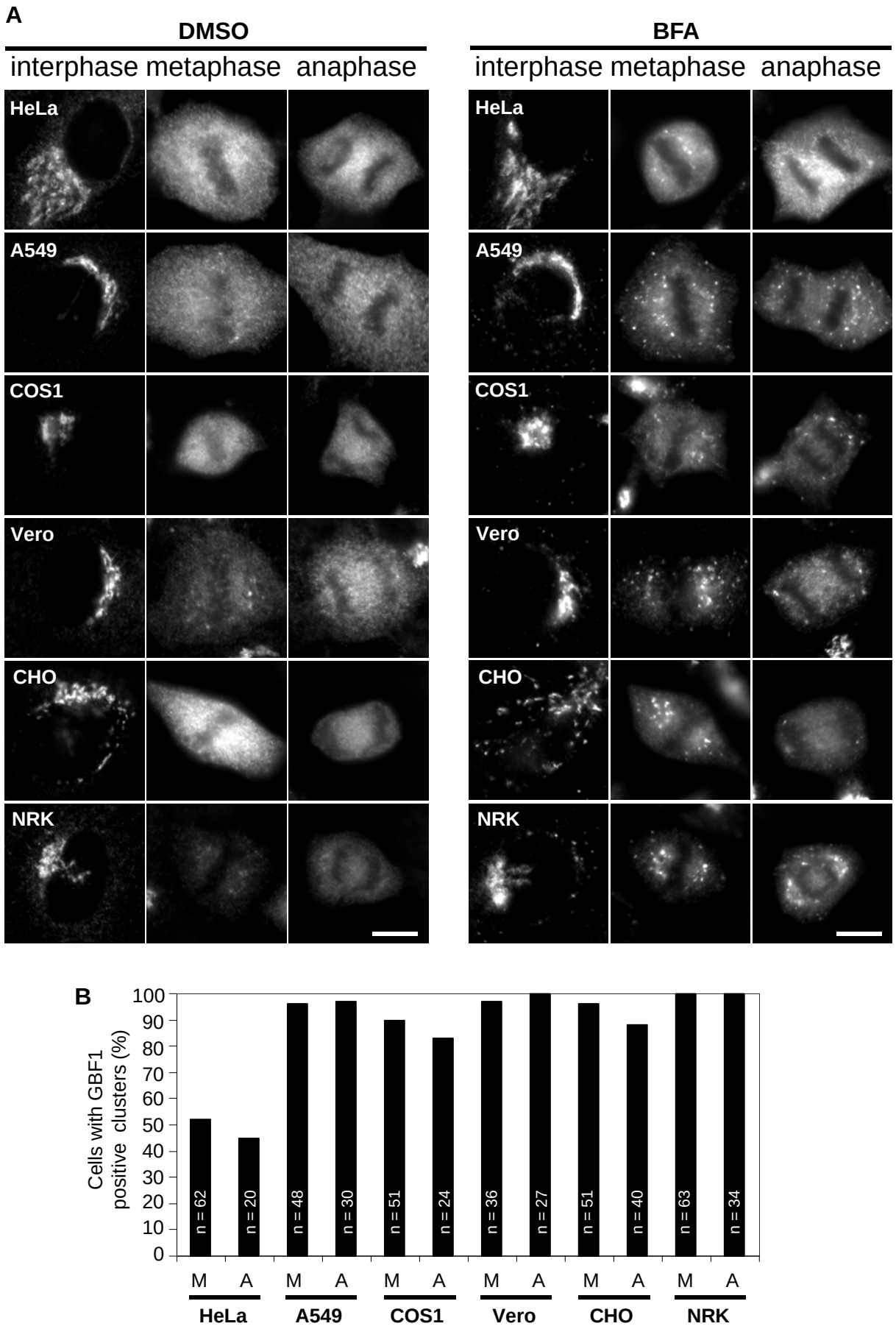

Figure 4.8 Brief treatment of different cell lines with BFA concentrates GBF1 on mitotic Golgi fragments that differ in pattern.

function (Manolea *et al.*, 2008), we hypothesized that COPI activity at mitotic Golgi fragments would be regulated by GBF1. The presence of COPI and various Golgi enzymes suggested that the mitotic Golgi fragments remain active during mitosis. Furthermore, our results established that association of GBF1 onto the mitotic Golgi clusters remain dynamic, since FRAP kinetics onto Golgi fragments closely resembled that observed on interphase Golgi membranes. Even the FRAP kinetics on mitotic Golgi clusters after BFA treatment were greatly reduced, analogous to that of the recovery previously reported in interphase cells. Lastly, the characteristic polarization of the Golgi complex as observed by colocalization analysis of the *cis*- and *trans*-Golgi markers, further indicates that the mitotic Golgi fragments are functioning in a manner very similar to the interphase Golgi complex. These results strongly suggest that COPI has an active role at the mitotic Golgi clusters in establishing and maintaining polarization. Taken together, our results indicate that the mitotic Golgi clusters are *bona fide* Golgi membranes with a functional COPI machinery.

4.7.1 Mitotic Golgi clusters are *bona fide* Golgi structures

The fate of the Golgi complex during mitosis has been long debated. The inability to readily detect Golgi proteins such as fluorescently tagged GalT and Arf1 at mitotic Golgi fragments has been used as evidence for Golgi protein redistributing to the ER during mitosis (Zaal *et al.*, 1999; Altan-Bonnet *et al.*, 2003). The suspected redistribution of Golgi proteins to the ER during mitosis has been compared to the BFA-induced perturbation of ER-Golgi trafficking pathways in interphase that cause Golgi enzymes to redistribute to the ER

(Lippincott-Schwartz *et al.*, 1989; Zaal *et al.*, 1999). Although there is a possibility that certain Golgi enzymes or subpopulations of certain Golgi enzymes redistribute to the ER, the Golgi enzymes reported in this study (GBF1, COPI, Man II, giantin, BIG1) can be clearly observed at the mitotic Golgi structures in NRK cells. Future studies will require a detailed analysis of the fraction of each Golgi marker localized at mitotic Golgi fragments. In addition, several other groups have noted other Golgi enzymes including GalT (Lucocq *et al.*, 1987), the GFP-tagged N-terminal retention signal of N-acetylglucosaminyltransferase I (NAGFP), GM130, and TGN46 at mitotic Golgi clusters in HeLa, PtK1, CHO and NRK cells (Lucocq *et al.*, 1987; Shima *et al.*, 1997; Shima *et al.*, 1998; Jokitalo *et al.*, 2001; Seemann *et al.*, 2002). Although Lippincott-Schwartz and colleagues suggest that fluorescently labeled GalT and Arf1 distribute to the ER during mitosis (Altan-Bonnet *et al.*, 2003; Altan-Bonnet *et al.*, 2006), it is actually clear from their own results that some GalT and Arf1 can be detected on mitotic fragments [E.g., see Altan-Bonnet *et al.* (2006), Figure 5C]. The decrease of Arf1-CFP during mitosis in the study by Altan-Bonnet *et al.* was likely due to the decreased size of the mitotic Golgi fragments rather than a decrease in Arf1 activity since COPI is active at these structures.

Our IF data in Figures 4.2 and 4.3 demonstrated a clear localization of endogenous COPI to mitotic Golgi structures in NRK cells. Also, by live cell imaging, we demonstrated that GBF1, initially detected weakly on mitotic Golgi clusters, concentrated on membranes upon treatment with BFA and Exo1 (Figure 4.4). The ability to concentrate GBF1 on mitotic Golgi clusters provides the first

direct evidence that mitotic Golgi structures behave as interphase Golgi independently of the ER. In addition, while Golgi proteins may continuously traffic between the Golgi and ER (Cole *et al.*, 1998; Storrie *et al.*, 1998; Miles *et al.*, 2001; Ward *et al.*, 2001), the connections between the ER and Golgi appeared to be severed sometime during prometaphase and reappear only after telophase. Persistence of ER-Golgi connections may explain why Man II and GBF1 can sometimes redistribute to the ER during prometaphase as characterized by Altan-Bonnet *et al.* (2006) but not during metaphase or anaphase following treatment with BFA (Figure 4.3).

Our work did not address the ability of the ER to communicate with mitotic Golgi fragments as suggested by Lippincott-Schwartz and colleagues (Altan-Bonnet *et al.*, 2006). According to Altan-Bonnet *et al*. (2006), there may be constant communication between the ER and the mitotic Golgi fragments. With regards to mitotic cells treated with BFA, it is possible that certain Golgi enzymes and a population of GBF1 may be distributing to the ER, but our results clearly show that much of the GBF1 does not leave the mitotic Golgi clusters. However, it may be possible that the GBF1 concentrated on the mitotic Golgi fragments may take much longer to redistribute to the ER compared to GBF1 redistribution during interphase. Nevertheless, since brief treatment with BFA was able to rapidly recruit GBF1 to membranes, we can conclude that the mitotic fragments are pre-existing structures with the characteristics of the interphase Golgi complex.

4.7.2 Membrane recruitment of GFP-GBF1 to mitotic Golgi clusters and interphase Golgi complex is dependent on the levels of membrane-associated GBF1

Our FRAP analysis of GFP-GBF1 in mitotic cells revealed GBF1 dynamics at mitotic Golgi clusters similar, but not identical, to that of interphase Golgi. Comparison of recovery of GBF1 signal in interphase cells with mitotic cells revealed a more rapid recovery of GBF1 signal in mitotic cells treated with DMSO or BFA for 2 min compared to interphase cells (Figure 4.6A). Several possibilities exist for the difference in FRAP kinetics at mitotic Golgi clusters compared to interphase Golgi complex. First, the ratio of GBF1 present in the cytoplasm relative to the membrane associated GBF1 may determine how quickly GBF1 associates with membranes. We would predict that increased levels of GBF1 present in the cytoplasm relative to both the Golgi or mitotic Golgi cluster membranes would result in faster fluorescence recovery of GFP-GBF1 following photobleaching. This is consistent with our result demonstrating that treatment of mitotic cells with BFA resulted in slower recovery kinetics as a result of more membrane-associated GBF1. However, this possibility cannot be distinguished from a second scenario in which the off rate of GBF1 that is membrane-associated controls the rate for GBF1 association. If more GBF1 molecules occupy binding sites, then fewer GBF1 molecules can associate with the membrane leading to slower reassociation of GBF1 onto both interphase and mitotic Golgi cluster membranes. Lastly, we cannot exclude that the receptor for GBF1 or GBF1 itself may be altered in the presence of BFA and/or during mitosis. For example, if

there is a modification of GBF1 or its receptor that affects their binding kinetics following BFA treatment or during mitosis, membrane recruitment can be significantly altered. Although the mechanism regulating GBF1 membrane association remains unclear, our results demonstrate that mitotic cells can be used to investigate GBF1 membrane dynamics over extended periods of time follow treatment with BFA. Since mitotic Golgi clusters do not redistribute to the ER after BFA treatment, future studies can precisely characterize the relationship between membrane-associated GBF1 and the rate of GBF1 membrane association.

4.7.3 Discrepancies in Golgi fragmentation between cell types

Although the fate of the Golgi complex during mitosis has been hotly debated, how the Golgi is fragmented in mammalian cells appears to be cell type dependent and more variable than previously thought. For example, very early work using electron microscopy demonstrated that the Golgi complex disappears during metaphase and reappears in telophase for HeLa cells (Robbins and Gonatas, 1964). Similarly, in human melanoma cells, the Golgi complex was observed to undergo extensive fragmentation, and the Golgi elements were not frequently seen during anaphase (Maul and Brinkley, 1970). In contrast, and consistent with our results, Golgi elements persisted throughout mitosis in rat hepatic cells (Dougherty, 1964) and transplantable rat hepatomas (Chang and Gibley, 1968). Since all cell lines tested in our study clearly displayed distinct Golgi structures, Golgi structures persisting throughout mitosis may be the rule rather than the exception. In our study, mitotic Golgi structures were especially

revealed by examining GBF1 after treatment with BFA. Following treatment with BFA, we observed that while NRK, PtK1, CHO and Vero cells showed a large degree of mitotic Golgi fragments localizing to the spindle pole regions in metaphase, HeLa, A549, and COS1 cells displayed Golgi fragments that were more dispersed (Figure 4.8). Is it possible that the mechanism by which the Golgi complex is partitioned is different in higher mammals such as humans compared to the rodents and marsupials? This would be a very intriguing avenue to pursue since it would reveal mechanistic differences in the way the Golgi complex is divided. Such differences in mechanism may explain differences in the length of the cell cycle and the extent to which the Golgi fragments.

4.7.4 Potential roles for GBF1 and COPI at the mitotic Golgi clusters

Our results are consistent with the biochemical studies by Wang's group that demonstrated the importance of Arf1 and COPI in facilitating the fragmentation/vesiculation of the Golgi complex during mitosis (Xiang *et al.*, 2007; Tang *et al.*, 2008). Our experiments using BFA demonstrated that without GBF1/COPI activity, the mitotic Golgi clusters cluster into inactive structures. It appears that inhibiting the COPI machinery either prevents vesiculation of the Golgi fragments (autonomous model) or halts communication of the mitotic Golgi fragments with the ER (ER-dependent model). Inconsistent with our results is the observation that H89 or Arf1(Q71L) also prevented Golgi fragmentation (Altan-Bonnet *et al.*, 2003). These effects may have resulted from constitutively activating Arf1 prior to cell entry into mitosis, since Wang and colleagues found that Arf1(Q71L) microinjected into mitotic cells had no impact on Golgi

fragmentation or cell cycle progression through mitosis (Xiang *et al.*, 2007). Interestingly, our results show that vesiculation of the mitotic fragments was not compulsory for progression through mitosis, since treatment with BFA or Exo1 prevented Golgi vesiculation but not cell division. Constant vesiculation of the mitotic Golgi fragments may be important for appropriately allocating Golgi elements to each daughter cell. Vesicles may be transported from one daughter cell to the other depending on which requires the vesicles. Hence the focus for future characterization of the mitotic Golgi clusters will not be to address whether or not Golgi enzymes redistribute to the ER, but to examine the active role for the mitotic Golgi fragments.

CHAPTER FIVE: GENERAL DISCUSSION AND FUTURE PERSPECTIVES

5.1 Synopsis

The work presented in this thesis attempted to characterize the roles of GBF1 and Arfs and their regulation of COPI using live imaging. First, our characterization of Arfs at the ERGIC revealed striking differences between the recruitment of class I and class II Arfs at the ERGIC. Using pharmacological agents and GDP-arrested Arf mutants, we established that class II Arfs associate with ERGIC in their GDP-bound by a class II Arf-specific receptor. GBF1, on the other hand, is independently recruited to the Golgi and ERGIC membranes by a separate receptor. Furthermore, our observations suggest for the first time that GBF1 recruitment and concentration to Golgi and ERGIC membranes following BFA treatment is due to loss of Arf-GTP rather than the formation of an abortive complex with an Arf. In addition, throughout the course of my work, the nature of the ERGIC has been reassessed. The stable population of the ERGIC is positive for both GBF1 and class II Arfs indicating that they are structures with potential sorting functions. Finally, our investigation of GBF1 and COPI at mitotic Golgi clusters established that the COPI machinery is active throughout mitosis. We not only established that mitotic Golgi clusters persist as ER-independent structures, but these structures maintain their characteristic *cis-to-trans* subcompartmental polarization. The work presented in this thesis has uncovered many potential directions for future research. Thus, for the discussion below, I will emphasize the significance of our findings and propose potential directions that may be pursued to extend the work presented in this thesis.

5.2 Testing our "Arf-GTP loss" model

The "Arf-GTP loss" model we proposed in Chapter 3 (Figure 3.15) and our manuscript (Chun *et al.*, 2008) is provocative and requires thorough examination. The "Arf-GTP loss" model is based mainly on the surprising effect on GBF1 in cells treated to either prevent Arf nucleotide exchange using BFA or stimulation of Arf-GTP hydrolysis by Exo1. Interestingly, brief treatment of cells with either drugs caused GBF1 to accumulate on the ERGIC and Golgi membranes. In contrast to the widely held belief that BFA traps an abortive complex with GBF1 and Arfs at the membrane, our model is better able to explain the results obtained from our drug studies. GBF1 accumulation on membranes following treatments that either inactivate Arfs or stimulate GAP activity can be explained by attributing the effects to Arf-GTP dissociation from membranes. Furthermore, our "Arf-GTP loss" model would be interesting to test since it reveals an unexpected regulatory mechanism for GBF1.

To obtain stronger evidence for our "Arf-GTP loss" model, approaches such as live cell imaging in combination with pharmacological agents and hydrolysis-deficient Arf mutants that accumulate in the GTP-bound form can be used. Currently, Nathan Summerfeldt, a new graduate student in the Melançon laboratory, is testing our "Arf-GTP loss" model by challenging with BFA cells expressing hydrolysis-deficient Arf mutants tagged with GFP. Our hypothesis is that expression of Arf1(Q71I)-GFP alone or in combination with Arf4(Q71L)-GFP will mitigate or even prevent the BFA-induced recruitment of GBF1 at the Golgi complex and/or the ERGIC. Interestingly, preliminary data obtained in

fixed cells transfected with either Arf1(Q71I)-GFP or Arf4(Q71L)-GFP alone show no prevention of GBF1 recruitment after brief treatment with BFA. However, any redundant or compensatory function of Arf3/5 or the loss of endogenous GTP-bound Arfs may interfere with the interpretation. Therefore, attempting to prevent the recruitment of GBF1 to membranes in response to BFA will need to take into account the effect of endogenous Arf proteins or require knocking down endogenous Arf prior to treatment with BFA. The best approach will likely be comparing Arf1/4-GFP(WT) with the GTP-arrested mutant in live cells. Live cell imaging may reveal differences between the wild type and GTP-arrested mutants that may be difficult to observe in fixed cells. Furthermore, a careful examination of GBF1 binding kinetics in cells overexpressing a range of different levels of Arf1/4(Q71L) may be required.

In addition, future studies can further examine our model by testing the response of GBF1 to other pharmacological agents such as LM11 and AG1478. The small molecule inhibitor LM11 was identified by structure-based screening of molecules that inhibit the catalytic activity of both BFA-sensitive and BFA-insensitive GEFs (Viaud *et al.*, 2007). Similar to BFA, LM11 prevents conformational changes required for nucleotide exchange by binding to a pocket near the Arf/Sec7 interface. However, unlike the uncompetitive mechanism utilized by BFA to form an inactive Arf-GEF complex, LM11 is a non-competitive inhibitor that does not compete with nucleotides and has a binding site that is remote from the site that binds BFA (Viaud *et al.*, 2007). Since our "Arf-GTP loss" model predicts that Arf-GTP loss from Golgi and ERGIC

membranes will result in GBF1 accumulation, we expect to see similar or identical results using LM11.

Very recently, Pan *et al.* identified AG1478, a small molecule previously known to inhibit epidermal growth factor receptor, to have an activity in inducing the disassembly of the Golgi complex in human cells (Pan *et al.*, 2008). Interestingly, AG1478 causes disassembly of the Golgi complex in the human cell lines tested but not in rodent, PtK1 or MDCK cells. Also, unlike the non-specific effect of BFA on the secretory pathway, AG1478 appears to be more specific to the *cis*-Golgi. Although the authors propose that AG1478 inhibits the catalytic activity of GBF1 by forming a complex with Arf1-GDP based on the similarities to BFA, future studies may reveal mechanistic differences. With the availability of LM11 and AG1478, our "Arf-GTP loss" model can be rigorously tested by using these drugs in parallel with BFA.

5.3 The ERGIC: transport carriers or a stable sorting organelle?

Our live imaging studies on the regulatory roles of GBF1 and Arfs at the ERGIC have opened up other avenues of research. Many of our observations are unexpected and challenge us to reassess the nature of the ERGIC. For example, our results demonstrating class II Arfs remaining at the ERGIC independently of GBF1 following BFA treatment suggest that separate receptors exist for GBF1 and class II Arf receptors. Also, class II Arfs may function cooperatively with each other or other mediators at the ERGIC. Lastly, the possibility of a network

interconnecting stable ERGIC structures with fast-moving transport ERGIC carriers may redefine the function of the ERGIC.

5.3.1 Identifying GBF1 and Arf receptors localized to the ERGIC

If indeed the ERGIC is a stable sorting station, the exact roles of GBF1, Arfs and their respective putative receptors must be re-evaluated. The unique localization of class II Arfs at the ERGIC suggests ERGIC-localized class II Arf receptors. Evidence for a distinct role of class II Arfs at the ERGIC comes from the correlation between the number of Arf classes expressed and the presence or absence of an ERGIC. Interestingly, while multicellular organisms appear to have at least one member of each class of Arf, class II Arfs are absent in *S. cerevisiae*, an organism that does not have the ERGIC (Donaldson *et al.*, 2005). Also, why GBF1 redistributes to the ER while the class II Arfs remain at the ERGIC in the presence of BFA remains unclear. To examine the independent activities of these proteins, the identification of the receptors specific for each protein will be crucial. Identification of the GBF1 receptor will likely involve crosslinking of the putative GBF1 receptor to GBF1 enriched on membranes. Several attempts have been made by our laboratory to enrich GBF1 on membranes by brief treatment with BFA without much success. One major difficulty with experiments using BFA is the fact that the majority of GBF1 redistributes to the ER following treatment of cells with BFA (Zhao *et al.*, 2002). Receptor-bound GBF1 can be retrieved by immunoprecipitation from microsomes following subcellular fractionation. Future studies for identifying the GBF1 receptor may benefit from the knowledge we obtained from our analysis of GBF1

during mitosis. Since mitotic Golgi clusters do not redistribute to the ER when mitotic cells are treated BFA, GBF1 immunoprecipitated from cells synchronized in mitosis and treated with BFA may yield enough GBF1 bound to its receptor.

Our results demonstrated that Arf4 remains at the ERGIC following treatment with either BFA or Exo1. Since Arf4 and Arf5 can localize to the ERGIC independently of BFA, the identification of a class II Arf receptor may be easier to achieve than the GBF1 receptor. Isolation and identification of the receptor for class II Arfs at the ERGIC may be possible by purification of ERGIC membranes using subcellular fractionation and mass spectrometry methods described by Hauri's group (Breuza *et al.*, 2004).

5.3.2 Interaction of Arfs with ERGIC-localized proteins

Examining exactly how GBF1 and Arfs function at the ERGIC may give clues as to how the morphology of the stable ERGIC is maintained and what gives rise to transport carriers. To investigate GBF1 or Arf interaction with ERGIC-localized proteins, future studies could use dual label live cell imaging to track GBF1 or Arfs with p58. Such experiments may provide insight into how specific proteins are involved at each population of the ERGIC. Also, particle tracking of class I Arfs with class II Arfs may reveal cooperative, sequential activities of the Arfs and reveal ERGIC-specific functions. In addition, cargo receptors such as the p24 proteins should be considered since they appear to be essential for maintaining ERGIC architecture by regulating COPI recruitment (Mitrovic *et al.*, 2008). Future studies will need to address how the Arfs interact with cargo

receptors at the ERGIC and if this interaction is important for COPI coat recruitment.

5.3.3 The ERGIC network

The identity and function of the ERGIC has been evolving from a set of transient transport carriers to a more dynamic network consisting of both a stable population and a fast-moving population within a reticular network (Ben-Tekaya *et al.*, 2005). In addition, there is now evidence that the ERGIC constitutes a stable tubular network that maintains its dynamics in the presence of BFA (Marie *et al.*, 2008). This visible reticular network interconnecting elements of the ERGIC appears to be separate from the ER. One proposed function for this ERGIC reticular network would be the bidirectional transport of cargo to the plasma membrane without the need to visit the Golgi complex. Akin to the ER, the ERGIC network may allow cargo transport within a preformed structure. For example, rather than the ERGIC elements acting as vesicular structures transporting cargo, some cargo may be transported in tubes directly connecting one ERGIC "station" to another. The tubes interconnecting each station may form a reticular network to facilitate movement of certain proteins from station to station without necessarily passing through the Golgi complex. The stations would probably function in cargo sorting and redirecting cargoes to their appropriate destination within the cell. Since our work demonstrates unique localization of Arf4 to the ERGIC stations in a GDP-bound manner, we expect that Arf4 will be a key regulator at these structures. Whether the transport of

protein within this network requires specific signals or microtubule-dependent motors will require further investigation.

5.4 Regulation of GBF1 by phosphorylation

Our FRAP results suggest that GBF1 membrane exchange at mitotic Golgi occurs at a slightly faster rate compared to exchange in interphase Golgi membranes. One possibility is that GBF1 is regulated by phosphorylation during interphase and mitosis by different kinases. Examining how GBF1 is regulated by phosphorylation may help to understand its function in coordinating the activities of Arfs. Eleven phosphorylated residues in GBF1 have been identified by the combined efforts several groups (Ballif *et al.*, 2004; Beausoleil *et al.*, 2004; Nousiainen *et al.*, 2006; Olsen *et al.*, 2006). Future studies could attempt to obtain better coverage of GBF1 phosphopeptides by mass spectrometry for immunoprecipitated GBF1 samples obtained from sufficient amounts of cell lysate.

To thoroughly examine the importance of GBF1 phosphorylation, an analysis to identify potential kinases as well as determining the role of site-specific phosphorylation events will be required. Analysis of GBF1 from cells properly arrested in mitosis may reveal a specific role for GBF1 phosphorylation by mitotic kinases. To analyze differences in GBF1 phosphorylation state during interphase compared to mitosis, synchronization and arrest of the cells would be required to compare the phosphopeptides of GBF1 immunoprecipitated from interphase and mitotic cells. Although the double thymidine block of HeLa cells

is readily used, future experiments would benefit from using NRK cells synchronized with aphidicolin (Sutterlin *et al.*, 2002; Altan-Bonnet *et al.*, 2003; Hidalgo Carcedo *et al.*, 2004), since our results using NRK cells show GBF1 localization to mitotic Golgi fragments.

There is now evidence that phosphorylation of GBF1 may play a critical role in the disassembly of the Golgi complex induced under conditions of stress that decrease the intracellular concentration of ATP (Miyamoto *et al.*, 2008). Miyamoto and colleagues characterized AMP-activated protein kinase as a kinase that is thought to attenuate GBF1 activity by phosphorylating Thr1337 of GBF1. This study not only provides a physiological role for GBF1, but also indicates that phosphorylation of a specific residue results in a physiological consequence. It may be possible phosphorylation of some residues attenuate the function of GBF1, as is the case for Thr1337 by AMPK, while that of other sites may regulate cytosol-membrane cycling or cell cycle-specific activities. Future studies will be required to elucidate the mechanism by which phosphorylation of GBF1 by AMPK causes Golgi disassembly and to determine the physiological relevance for each phosphorylation site identified in GBF1 thus far.

AMPK is the first kinase identified that has been characterized to act on GBF1, but we expect other kinases to contribute to GBF1 regulation since many putative phosphorylation sites have been identified. Also, Thr1337, the site identified by Miyamoto *et al.* (2008), can also be potentially phosphorylated by PKA, which has a phosphorylation consensus sequence RXXpS/T. The use of H89 to study ER-to-Golgi trafficking will require some caution, since H89 is not

as selective for PKA as once thought and is known to inhibit other kinases. For example, H89 is a potent inhibitor of PKD, which is a resident kinase of the Golgi complex (Johannes *et al.*, 1995; Prestle *et al.*, 1996). H89 block of IQ and Gβγ-mediated Golgi fragmentation was shown to be due to its inhibition of PKD but not PKA (Jamora *et al.*, 1999). However, while it is now established that PKD regulates fission at the TGN of transport carriers to deliver cargo to the plasma membrane (Liljedahl *et al.*, 2001; Yeaman *et al.*, 2004; Diaz Anel and Malhotra, 2005), it is also known that PKA is required in the formation of vesicles from the TGN (Muniz *et al.*, 1997). To complicate matters, block of ER-to-Golgi trafficking is thought to be due primarily to H89-mediated block of COPII and not COPI (Lee and Linstedt, 2000). Therefore, future studies using H89 may reveal the involvement of multiple kinases and steps of the secretory pathway, which may also include a role for GBF1 phosphorylation.

5.5 Regulation of class II Arfs by phosphorylation

Our work studying class I and II Arfs at the ERGIC established for the first time that class I and class II Arfs behave differently in response to BFA and Exo1 treatment. Although very little is known about the class II Arfs, most studies to date have assumed class II Arfs to be similar to class I Arfs, since they have a high degree of sequence identity. However, when the sequences of Arf4 and Arf5 are compared to Arf1 and Arf3, the most obvious differences are the number of potentially phosphorylatable residues present in the class II Arfs throughout the protein. Most striking, Arf4 and Arf5 have at many more

potentially phosphorylatable residues than Arf3 or Arf1, most notably within a short distance of the N-terminus (Table 5.1).

Table 5.1 Alignment of the first 15 N-terminal residues of the human Arf family members

Arf	Protein Sequence
1	MGNIFANLFKGLFGK
3	MGNIFGNLLK**S**LIGK
4	MGL**T**I**SS**LF**S**RLFGK
5	MGL**T**V**S**ALF**S**RIFGK
6	MG----KVL**S**KIFGN

Potentially phosphorylatable residues indicated in boldface

In addition to the surprisingly large number of phosphorylatable residues in the protein sequence of the class II Arfs, examining the regulation of the large GTPase, dynamin related protein 1 (Drp1), may provide insight as to how the class II Arfs may be regulated by phosphorylation. Drp1 has an important function in mitochondrial morphology that is highly regulated by phosphorylation. Three phosphorylation sites in Drp1 have been identified, each regulating the protein differently (Jahani-Asl and Slack, 2007). First, PKA-mediated phosphorylation of Drp1 at Ser656 promotes mitochondrial elongation and attenuates its GTPase activity, while dephosphorylation of the serine residue by calcineurin induces mitochondrial fragmentation (Cribbs and Strack, 2007). Next, phosphorylation of Drp1 by PKA within the GTPase effector domain at Ser637 has been shown to inhibit Drp1 GTPase activity (Chang and Blackstone, 2007). Lastly, a cyclin-dependent kinase (Cdk) site at Ser585 in Drp1 has been

proposed to be phosphorylated, leading to a transient breakdown of the mitochondrial reticulum during mitosis (Taguchi *et al.*, 2007). Phosphorylation of Drp1 at specific amino acids by different kinases illustrates how phosphorylation can produce distinct consequences. Although the class II Arfs are much smaller than Drp1, we predict that phosphorylation of specific serine or threonine residues in the class II Arfs may contribute to distinct physiological effects.

Although there is no published evidence demonstrating phosphorylation of Arfs, previous analyses of Arfs by mass spectrometry were not designed to detect Arf phosphorylation. For example, biochemical characterization of Arfs performed in our laboratory detected post-translational modifications such as acylation and mono-glutathionation of Arfs, but not phosphorylation (Berger *et al.*, 1995; 1998). However, no conclusion can be made with regards to Arf phosphorylation, since no phosphatase inhibitors were used during the preparation and isolation of the Arfs. Therefore, future studies would require IP of tagged Arfs in the presence of phosphatase inhibitors in cells metabolically labeled with [^{32}P]orthophosphate. Alternatively, Arfs purified in the presence of phosphatase inhibitors can be analyzed by mass spectrometry to identify phosphorylated residues. Next, since the potential phosphorylation sites in the class II Arfs are localized to the N- and C- termini, site-directed mutagenesis using PCR may be able to determine if the phosphorylated residues are important physiologically. Finally, the role for Arf4/5 phosphorylation can be studied using live cell imaging experiments by examining membrane localization or behavior of the Arfs in

response to pharmacological agents. Furthermore, future studies can substitute the N-terminus of the class I Arfs with the N-terminus of the class II Arfs to study localization to the ERGIC and response to BFA. We hypothesize that phosphorylation of the class II Arfs may regulate specific targeting of these Arfs to the ERGIC or contribute to Arf4/5-GDP binding to the ERGIC even after prolonged treatment with BFA. Future studies may establish a role for phosphorylation of class II Arfs for specific localization and function at the ERGIC.

5.6 Examining the function of COPI at mitotic Golgi fragments

Our examination of mitotic cells revealed the localization of both GBF1 and COPI at mitotic Golgi fragments that was especially obvious in NRK cells. Why the Golgi fragments to varying extents in different cell types and what role COPI plays in the fragmentation process are interesting avenues of research. Although purely speculative, we consider likely the notion that the extent of Golgi fragmentation during mitosis may be species-specific. The fragmentation pattern of the Golgi complex during mitosis in the primate cell lines tested (Figure 4.8) appears to be more complete resulting in a mitotic haze. Rat, hamster, and rat kangaroo cells appear to preserve larger Golgi fragments. Interestingly, AG1478, a small molecule that inhibits the activity of GBF1, has recently been shown to disrupt the Golgi complex in human cell lines but not multiple rodent cell lines tested (Pan *et al.*, 2008). These results suggest that there may be regulators or structural components that differ between primates and rodents. Future work may

be able to identify novel proteins that differ between species at the Golgi complex.

Further examination of COPI activity during mitosis may reveal surprising regulatory roles for COPI during mitosis. Shortly after entry into mitosis, COPI specifically interacts with the nucleoporins Nup153 and Nup358 to facilitate nuclear envelope breakdown in *Xenopus* egg extracts (Liu *et al.*, 2003; Prunuske *et al.*, 2006). It appears that COPI function at mitosis differs from its role during interphase, since COPI normally acts at the ERGIC and *cis*-Golgi complex. Similarly, during later stages of mitosis, one may envision specific proteins such as Nup153 or Nup358 that also play a role in directing COPI to the mitotic Golgi fragments. To further probe the connection between the population of COPI that localizes to the mitotic Golgi fragments, we may be able to examine the activities of the different Arfs or modifications to GBF1 activity. Is it possible that specific classes of Arfs have a predominant role during mitosis at the mitotic Golgi fragments? Does the phosphorylation state of GBF1 or its receptor differ during mitosis? Future experiments would need to closely examine the different Arfs during mitosis and to better assess differences in phosphorylation state of GBF1 during interphase compared to mitosis.

5.7 Concluding remarks

Technological advances such as live cell microscopy using fluorescently tagged proteins have had a dramatic impact on our ability to examine fine cellular structures. Using live cell microscopy, we were able to reveal unanticipated roles

for class II Arfs and GBF1 at the ERGIC and at mitotic Golgi clusters. Surprisingly, much of the work presented in this thesis was based on serendipitous findings that have progressed to new models for Arf regulation, ERGIC function, and Golgi partitioning during mitosis.

Our work is just the beginning for our understanding of Arf function at the ERGIC and mitotic Golgi clusters. We believe that our work is a starting point for many new avenues of research that will ultimately lead to a better understanding of Arf function, establishing the role of the ERGIC and reassessment of mitotic Golgi structures of mammalian cells.

CHAPTER SIX: REFERENCES

Acharya, U., Mallabiabarrena, A., Acharya, J.K., and Malhotra, V. (1998). Signaling via mitogen-activated protein kinase kinase (MEK1) is required for Golgi fragmentation during mitosis. Cell *92*, 183-192.

Axelsson, M.A., and Warren, G. (2004). Rapid, endoplasmic reticulum-independent diffusion of the mitotic Golgi haze. Mol Biol Cell *15*, 1843-1852.

Allan, V.J., and Kreis, T.E. (1986). A microtubule-binding protein associated with membranes of the Golgi apparatus. J Cell Biol, 2229-2239.

Altan-Bonnet, N., Phair, R.D., Polishchuk, R.S., Weigert, R., and Lippincott-Schwartz, J. (2003). A role for Arf1 in mitotic Golgi disassembly, chromosome segregation, and cytokinesis. Proc Natl Acad Sci U S A *100*, 13314-13319.

Altan-Bonnet, N., Sougrat, R., and Lippincott-Schwartz, J. (2004). Molecular basis for Golgi maintenance and biogenesis. Curr Opin Cell Biol *16*, 364-372.

Altan-Bonnet, N., Sougrat, R., Liu, W., Snapp, E.L., Ward, T., and Lippincott-Schwartz, J. (2006). Golgi inheritance in mammalian cells is mediated through endoplasmic reticulum export activities. Mol Biol Cell *17*, 990-1005.

Antonny, B., Beraud-Dufour, S., Chardin, P., and Chabre, M. (1997). N-terminal hydrophobic residues of the G-protein ADP-ribosylation factor-1 insert into membrane phospholipids upon GDP to GTP exchange. Biochemistry *36*, 4675-4684.

Antonny, B., Madden, D., Hamamoto, S., Orci, L., and Schekman, R. (2001). Dynamics of the COPII coat with GTP and stable analogues. Nat Cell Biol *3*, 531-537.

Appenzeller, C., Andersson, H., Kappeler, F., and Hauri, H.P. (1999). The lectin ERGIC-53 is a cargo transport receptor for glycoproteins. Nat Cell Biol *1*, 330-334.

Appenzeller-Herzog, C., and Hauri, H.P. (2006). The ER-Golgi intermediate compartment (ERGIC): in search of its identity and function. J Cell Sci *119*, 2173-2183.

Balch, W.E., Kahn, R.A., and Schwaninger, R. (1992). ADP-ribosylation factor is required for vesicular trafficking between the endoplasmic reticulum and the *cis*-Golgi compartment. J Biol Chem *267*, 13053-13061.

Ballif, B.A., Villen, J., Beausoleil, S.A., Schwartz, D., and Gygi, S.P. (2004). Phosphoproteomic analysis of the developing mouse brain. Mol Cell Proteomics *3*, 1093-1101.

Banfield, D.K., Lewis, M.J., Rabouille, C., Warren, G., and Pelham, H.R. (1994). Localization of Sed5, a putative vesicle targeting molecule, to the *cis*-Golgi network involves both its transmembrane and cytoplasmic domains. J Cell Biol *127*, 357-371.

Bannykh, S.I., and Balch, W.E. (1997). Membrane dynamics at the endoplasmic reticulum-Golgi interface. J Cell Biol *138*, 1-4.

Bannykh, S.I., Nishimura, N., and Balch, W.E. (1998). Getting into the Golgi. Trends Cell Biol *8*, 21-25.

Bannykh, S.I., Rowe, T., and Balch, W.E. (1996). The organization of endoplasmic reticulum export complexes. J Cell Biol *135*, 19-35.

Barlowe, C. (2003). Signals for COPII-dependent export from the ER: what's the ticket out? Trends Cell Biol *13*, 295-300.

Barlowe, C., Orci, L., Yeung, T., Hosobuchi, M., Hamamoto, S., Salama, N., Rexach, M.F., Ravazzola, M., Amherdt, M., and Schekman, R. (1994). COPII: a membrane coat formed by sec proteins that drive vesicle budding from the endoplasmic reticulum. Cell *77*, 895-907.

Beausoleil, S.A., Jedrychowski, M., Schwartz, D., Elias, J.E., Villen, J., Li, J., Cohn, M.A., Cantley, L.C., and Gygi, S.P. (2004). Large-scale characterization of HeLa cell nuclear phosphoproteins. Proc Natl Acad Sci U S A *101*, 12130-12135.

Belov, G.A., Altan-Bonnet, N., Kovtunovych, G., Jackson, C.L., Lippincott-Schwartz, J., and Ehrenfeld, E. (2007). Hijacking components of the cellular secretory pathway for replication of poliovirus RNA. J Virol *81*, 558-567.

Ben-Tekaya, H., Miura, K., Pepperkok, R., and Hauri, H.P. (2005). Live imaging of bidirectional traffic from the ERGIC. J Cell Sci *118*, 357-367.

Beraud-Dufour, S., and Balch, W. (2002). A journey through the exocytic pathway. J Cell Sci *115*, 1779-1780.

Beraud-Dufour, S., Paris, S., Chabre, M., and Antonny, B. (1999). Dual interaction of ADP ribosylation factor 1 with Sec7 domain and with lipid membranes during catalysis of guanine nucleotide exchange. J Biol Chem *274*, 37629-37636.

Beraud-Dufour, S., Robineau, S., Chardin, P., Paris, S., Chabre, M., Cherfils, J., and Antonny, B. (1998). A glutamic finger in the guanine nucleotide exchange

factor ARNO displaces Mg^{2+} and the β-phosphate to destabilize GDP on ARF1. EMBO J *17*, 3651-3659.

Berger, J., Hauber, J., Hauber, R., Geiger, R., and Cullen, B.R. (1988). Secreted placental alkaline phosphatase: a powerful new quantitative indicator of gene expression in eukaryotic cells. Gene *66*, 1-10.

Berger, S.J., Claude, A.C., and Melançon, P. (1998). Analysis of recombinant human ADP-ribosylation factors by reversed-phase high-performance liquid chromatography and electrospray mass spectrometry. Anal Biochem *264*, 53-65.

Berger, S.J., Resing, K.A., Taylor, T.C., and Melançon, P. (1995). Mass-spectrometric analysis of ADP-ribosylation factors from bovine brain: identification and evidence for homogeneous acylation with the C14:0 fatty acid (myristate). Biochem J *311*, 125-132.

Bethune, J., Kol, M., Hoffmann, J., Reckmann, I., Brugger, B., and Wieland, F. (2006a). Coatomer, the coat protein of COPI transport vesicles, discriminates endoplasmic reticulum residents from p24 proteins. Mol Cell Biol *26*, 8011-8021.

Bethune, J., Wieland, F., and Moelleken, J. (2006b). COPI-mediated transport. The J Memb Biol *211*, 65-79.

Bi, X., Corpina, R.A., and Goldberg, J. (2002). Structure of the Sec23/24-Sar1 pre-budding complex of the COPII vesicle coat. Nature *419*, 271-277.

Bigay, J., Casella, J.F., Drin, G., Mesmin, B., and Antonny, B. (2005). ArfGAP1 responds to membrane curvature through the folding of a lipid packing sensor motif. EMBO J *24*, 2244-2253.

Bigay, J., Gounon, P., Robineau, S., and Antonny, B. (2003). Lipid packing sensed by ArfGAP1 couples COPI coat disassembly to membrane bilayer curvature. Nature *426*, 563-566.

Boman, A.L., Taylor, T.C., Melançon, P., and Wilson, K.L. (1992). A role for ADP-ribosylation factor in nuclear vesicle dynamics. Nature *358*, 512-514.

Bonfanti, L., Mironov, A.A., Jr., Martinez-Menarguez, J.A., Martella, O., Fusella, A., Baldassarre, M., Buccione, R., Geuze, H.J., Mironov, A.A., and Luini, A. (1998). Procollagen traverses the Golgi stack without leaving the lumen of cisternae: evidence for cisternal maturation. Cell *95*, 993-1003.

Bonifacino, J.S., and Glick, B.S. (2004). The mechanisms of vesicle budding and fusion. Cell *116*, 153-166.

Breuza, L., Halbeisen, R., Jeno, P., Otte, S., Barlowe, C., Hong, W., and Hauri, H.P. (2004). Proteomics of endoplasmic reticulum-Golgi intermediate compartment (ERGIC) membranes from brefeldin A-treated HepG2 cells identifies ERGIC-32, a new cycling protein that interacts with human Erv46. J Biol Chem *279*, 47242-47253.

Burke, B., Griffiths, G., Reggio, H., Louvard, D., and Warren, G. (1982). A monoclonal antibody against a 135-K Golgi membrane protein. EMBO J *1*, 1621-1628.

Cavenagh, M.M., Whitney, J.A., Carroll, K., Zhang, C., Boman, A.L., Rosenwald, A.G., Mellman, I., and Kahn, R.A. (1996). Intracellular distribution of Arf proteins in mammalian cells. Arf6 is uniquely localized to the plasma membrane. J Biol Chem *271*, 21767-21774.

Chang, C.R., and Blackstone, C. (2007). Cyclic AMP-dependent protein kinase phosphorylation of Drp1 regulates its GTPase activity and mitochondrial morphology. J Biol Chem *282*, 21583-21587.

Chang, J.P., and Gibley, C.W., Jr. (1968). Ultrastructure of tumor cells during mitosis. Cancer Res *28*, 521-534.

Chantalat, S., Courbeyrette, R., Senic-Matuglia, F., Jackson, C.L., Goud, B., and Peyroche, A. (2003). A novel Golgi membrane protein is a partner of the ARF exchange factors Gea1p and Gea2p. Mol Biol Cell *14*, 2357-2371.

Chun, J., Shapovalova, Z., Dejgaard, S.Y., Presley, J.F., and Melançon, P. (2008). Characterization of class I and II ADP-ribosylation factors (Arfs) in live cells: GDP-bound class II Arfs associate with the ER-Golgi intermediate compartment independently of GBF1. Mol Biol Cell *19*, 3488-3500.

Citterio, C., Vichi, A., Pacheco-Rodriguez, G., Aponte, A.M., Moss, J., and Vaughan, M. (2008). Unfolded protein response and cell death after depletion of brefeldin A-inhibited guanine nucleotide-exchange protein GBF1. Proc Natl Acad Sci U S A *105*, 2877-2882.

Claude, A., Zhao, B.P., Kuziemsky, C.E., Dahan, S., Berger, S.J., Yan, J.P., Armold, A.D., Sullivan, E.M., and Melançon, P. (1999). GBF1: A novel Golgi-associated BFA-resistant guanine nucleotide exchange factor that displays specificity for ADP-ribosylation factor 5. J Cell Biol *146*, 71-84.

Cohen, L.A., Honda, A., Varnai, P., Brown, F.D., Balla, T., and Donaldson, J.G. (2007). Active Arf6 recruits ARNO/cytohesin GEFs to the PM by binding their PH domains. Mol Biol Cell *18*, 2244-2253.

Colanzi, A., Suetterlin, C., and Malhotra, V. (2003). Cell-cycle-specific Golgi fragmentation: how and why? Curr Opin Cell Biol *15*, 462-467.

Colanzi, A., and Corda, D. (2007). Mitosis controls the Golgi and the Golgi controls mitosis. Curr Opin Cell Biol *19*, 386-393.

Cole, N.B., Ellenberg, J., Song, J., DiEuliis, D., and Lippincott-Schwartz, J. (1998). Retrograde transport of Golgi-localized proteins to the ER. J Cell Biol *140*, 1-15.

Connerly, P.L., Esaki, M., Montegna, E.A., Strongin, D.E., Levi, S., Soderholm, J., and Glick, B.S. (2005). Sec16 is a determinant of transitional ER organization. Curr Biol *15*, 1439-1447.

Cosson, P., and Letourneur, F. (1994). Coatomer interaction with dilysine endoplasmic reticulum retention motifs. Science *263*, 1629-1631.

Cox, R., Mason-Gamer, R.J., Jackson, C.L., and Segev, N. (2004). Phylogenetic analysis of Sec7-domain-containing Arf nucleotide exchangers. Mol Biol Cell *15*, 1487-1505.

Cribbs, J.T., and Strack, S. (2007). Reversible phosphorylation of Drp1 by cyclic AMP-dependent protein kinase and calcineurin regulates mitochondrial fission and cell death. EMBO Rep *8*, 939-944.

D'Souza-Schorey, C., and Chavrier, P. (2006). ARF proteins: roles in membrane traffic and beyond. Nat Rev Mol Cell Biol *7*, 347-358.

D'Souza-Schorey, C., Li, G., Colombo, M.I., and Stahl, P.D. (1995). A regulatory role for ARF6 in receptor-mediated endocytosis. Science *267*, 1175-1178.

Dascher, C., and Balch, W.E. (1994). Dominant inhibitory mutants of ARF1 block endoplasmic reticulum to Golgi transport and trigger disassembly of the Golgi apparatus. J Biol Chem *269*, 1437-1448.

Deretic, D., Williams, A.H., Ransom, N., Morel, V., Hargrave, P.A., and Arendt, A. (2005). Rhodopsin C terminus, the site of mutations causing retinal disease, regulates trafficking by binding to ADP-ribosylation factor 4 (ARF4). Proc Natl Acad Sci U S A *102*, 3301-3306.

Diaz Anel, A.M., and Malhotra, V. (2005). PKCη is required for beta1gamma2/beta3gamma2- and PKD-mediated transport to the cell surface and the organization of the Golgi apparatus. J Cell Biol *169*, 83-91.

Donaldson, J.G., Finazzi, D., and Klausner, R.D. (1992). Brefeldin A inhibits Golgi membrane-catalysed exchange of guanine nucleotide onto ARF protein. Nature *360*, 350-352.

Donaldson, J.G., Honda, A., and Weigert, R. (2005). Multiple activities for Arf1 at the Golgi complex. Biochim Biophys Acta *1744*, 364-373.

Donaldson, J.G., and Jackson, C.L. (2000). Regulators and effectors of the ARF GTPases. Curr Opin Cell Biol *12*, 475-482.

Donaldson, J.G., Lippincott, S.J., Bloom, G.S., Kreis, T.E., and Klausner, R.D. (1990). Dissociation of a 110-kD peripheral membrane protein from the Golgi apparatus is an early event in brefeldin A action. J Cell Biol *111*, 2295-2306.

Dougherty, W.J. (1964). Fate of the Golgi complex, lysosomes and microbodies during mitosis of rat hepatic cells. J Cell Biol *23*, 25A.

Duden, R., Griffiths, G., Frank, R., Argos, P., and Kreis, T.E. (1991). β-COP, a 110 kd protein associated with non-clathrin-coated vesicles and the Golgi complex, shows homology to β-adaptin. Cell *64*, 649-665.

Elsner, M., Hashimoto, H., Simpson, J.C., Cassel, D., Nilsson, T., and Weiss, M. (2003). Spatiotemporal dynamics of the COPI vesicle machinery. EMBO Rep *4*, 1000-1004.

Espenshade, P., Gimeno, R.E., Holzmacher, E., Teung, P., and Kaiser, C.A. (1995). Yeast *SEC16* gene encodes a multidomain vesicle coat protein that interacts with Sec23p. J Cell Biol *131*, 311-324.

Feng, Y., Yu, S., Lasell, T.K., Jadhav, A.P., Macia, E., Chardin, P., Melançon, P., Roth, M., Mitchison, T., and Kirchhausen, T. (2003). Exo1: a new chemical inhibitor of the exocytic pathway. Proc Natl Acad Sci U S A *100*, 6469-6474.

Franco, M., Chardin, P., Chabre, M., and Paris, S. (1993). Myristoylation is not required for GTP-dependent binding of ADP-ribosylation factor ARF1 to phospholipids. J Biol Chem *268*, 24531-24534.

Fromme, J.C., Orci, L., and Schekman, R. (2008). Coordination of COPII vesicle trafficking by Sec23. Trends Cell Biol *18*, 330-336.

Futai, E., Hamamoto, S., Orci, L., and Schekman, R. (2004). GTP/GDP exchange by Sec12p enables COPII vesicle bud formation on synthetic liposomes. EMBO J *23*, 4146-4155.

Garcia-Mata, R., and Sztul, E. (2003). The membrane-tethering protein p115 interacts with GBF1, an ARF guanine-nucleotide-exchange factor. EMBO Rep *4*, 320-325.

Garcia-Mata, R., Szul, T., Alvarez, C., and Sztul, E. (2003). ADP-ribosylation factor/COPI-dependent events at the endoplasmic reticulum-Golgi interface are regulated by the guanine nucleotide exchange factor GBF1. Mol Biol Cell *14*, 2250-2261.

Ghanekar, Y., and Lowe, M. (2005). Protein kinase D: activation for Golgi carrier formation. Trends Cell Biol *15*, 511-514.

Gilchrist, A., Au, C.E., Hiding, J., Bell, A.W., Fernandez-Rodriguez, J., Lesimple, S., Nagaya, H., Roy, L., Gosline, S.J., Hallett, M., Paiement, J., Kearney, R.E., Nilsson, T., and Bergeron, J.J. (2006). Quantitative proteomics analysis of the secretory pathway. Cell *127*, 1265-1281.

Gillingham, A.K., and Munro, S. (2007). The small G proteins of the Arf family and their regulators. Annu Rev Cell Dev Biol *23*, 579-611.

Gimeno, R.E., Espenshade, P., and Kaiser, C.A. (1996). COPII coat subunit interactions: Sec24p and Sec23p bind to adjacent regions of Sec16p. Mol Biol Cell *7*, 1815-1823.

Glick, B.S., and Malhotra, V. (1998). The curious status of the Golgi apparatus. Cell *95*, 883-889.

Goldberg, J. (1998). Structural basis for activation of ARF GTPase: mechanisms of guanine nucleotide exchange and GTP-myristoyl switching. Cell *95*, 237-248.

Hara-Kuge, S., Kuge, O., Orci, L., Amherdt, M., Ravazzola, M., Wieland, F.T., and Rothman, J.E. (1994). En bloc incorporation of coatomer subunits during the assembly of COP-coated vesicles. J Cell Biol *124*, 883-892.

Harlow, E., and Lane, D. (1988). Antibodies, A Laboratory Manual. Cold Spring Harbor Laboratory: Cold Spring Harbor, NY.

Hauri, H.P., and Schweizer, A. (1992). The endoplasmic reticulum-Golgi intermediate compartment. Curr Opin Cell Biol *4*, 600-608.

Hauri, H.P., Kappeler, F., Andersson, H., and Appenzeller, C. (2000). ERGIC-53 and traffic in the secretory pathway. J Cell Sci *113*, 587-596.

Helms, J.B., Palmer, D.J., and Rothman, J.E. (1993). Two distinct regulations of ARF bound to Golgi membranes. J Cell Biol *121*, 751-760.

Helms, J.B., and Rothman, J.E. (1992). Inhibition by brefeldin A of a Golgi membrane enzyme that catalyses exchange of guanine nucleotide bound to ARF. Nature *360*, 352-354.

Hidalgo Carcedo, C., Bonazzi, M., Spano, S., Turacchio, G., Colanzi, A., Luini, A., and Corda, D. (2004). Mitotic Golgi partitioning is driven by the membrane-fissioning protein CtBP3/BARS. Science *305*, 93-96.

Honda, A., Al-Awar, O.S., Hay, J.C., and Donaldson, J.G. (2005). Targeting of Arf-1 to the early Golgi by membrin, an ER-Golgi SNARE. J Cell Biol *168*, 1039-1051.

Honda, A., Nogami, M., Yokozeki, T., Yamazaki, M., Nakamura, H., Watanabe, H.,
Kawamoto, K., Nakayama, K., Morris, A.J., Frohman, M.A., and Kanaho, Y. (1999). Phosphatidylinositol 4-phosphate 5-kinase α is a downstream effector of the small G protein ARF6 in membrane ruffle formation. Cell *99*, 521-532.

Jahani-Asl, A., and Slack, R.S. (2007). The phosphorylation state of Drp1 determines cell fate. EMBO Rep *8*, 912-913.

Jamora, C., Yamanouye, N., van Lint, J., Laudenslager, J., Vandenheede, J.R., Faulkner, D.J., and Malhotra, V. (1999). Gβγ-mediated regulation of Golgi organization is through the direct activation of protein kinase D. Cell *98*, 59-68.

Jesch, S.A., and Linstedt, A.D. (1998). The Golgi and endoplasmic reticulum remain independent during mitosis in HeLa cells. Mol Biol Cell *9*, 623-635.

Johannes, F.J., Prestle, J., Dieterich, S., Oberhagemann, P., Link, G., and Pfizenmaier, K. (1995). Characterization of activators and inhibitors of protein kinase C μ. Eur J Biochem *227*, 303-307.

Jokitalo, E., Cabrera-Poch, N., Warren, G., and Shima, D.T. (2001). Golgi clusters and vesicles mediate mitotic inheritance independently of the endoplasmic reticulum. J Cell Biol *154*, 317-330.

Kahn, R.A., Cherfils, J., Elias, M., Lovering, R.C., Munro, S., and Schurmann, A. (2006). Nomenclature for the human Arf family of GTP-binding proteins: ARF, ARL, and SAR proteins. J Cell Biol *172*, 645-650.

Kahn, R.A., and Gilman, A.G. (1986). The protein cofactor necessary for ADP-ribosylation of Gs by cholera toxin is itself a GTP binding protein. J Biol Chem *261*, 7906-7911.

Kawamoto, K., Yoshida, Y., Tamaki, H., Torii, S., Shinotsuka, C., Yamashina, S., and Nakayama, K. (2002). GBF1, a guanine nucleotide exchange factor for ADP-ribosylation factors, is localized to the *cis*-Golgi and involved in membrane association of the COPI coat. Traffic *3*, 483-495.

Kerppola, T.K. (2006). Design and implementation of bimolecular fluorescence complementation (BiFC) assays for the visualization of protein interactions in living cells. Nature Protocols *1*, 1278-1286.

Klausner, R.D., Donaldson, J.G., and Lippincott, S.J. (1992). Brefeldin A: insights into the control of membrane traffic and organelle structure. J Cell Biol *116*, 1071-1080.

Klumperman, J., Schweizer, A., Clausen, H., Tang, B.L., Hong, W., Oorschot, V., and Hauri, H.P. (1998). The recycling pathway of protein ERGIC-53 and dynamics of the ER-Golgi intermediate compartment. J Cell Sci *111*, 3411-3425.

Lanoix, J., Ouwendijk, J., Lin, C.C., Stark, A., Love, H.D., Ostermann, J., and Nilsson, T. (1999). GTP hydrolysis by Arf-1 mediates sorting and concentration of Golgi resident enzymes into functional COP I vesicles. EMBO J *18*, 4935-4948.

Lahtinen, U., Dahllof, B., and Saraste, J. (1992). Characterization of a 58 kDa *cis*-Golgi protein in pancreatic exocrine cells. J Cell Sci *103*, 321-333.

Lee, M.C., Miller, E.A., Goldberg, J., Orci, L., and Schekman, R. (2004). Bi-directional protein transport between the ER and Golgi. Annu Rev Cell Dev Biol *20*, 87-123.

Lee, S.Y., Yang, J.S., Hong, W., Premont, R.T., and Hsu, V.W. (2005). ARFGAP1 plays a central role in coupling COPI cargo sorting with vesicle formation. J Cell Biol *168*, 281-290.

Lee, T.H., and Linstedt, A.D. (2000). Potential role for protein kinases in regulation of bidirectional endoplasmic reticulum-to-Golgi transport revealed by protein kinase inhibitor H89. Mol Biol Cell *11*, 2577-2590.

Lenhard, J.M., Kahn, R.A., and Stahl, P.D. (1992). Evidence for ADP-ribosylation factor (ARF) as a regulator of *in vitro* endosome-endosome fusion. J Biol Chem *267*, 13047-13052.

Letourneur, F., Gaynor, E.C., Hennecke, S., Demolliere, C., Duden, R., Emr, S.D., Riezman, H., and Cosson, P. (1994). Coatomer is essential for retrival of dilysine-tagged proteins to the endoplasmic reticulum. Cell *79*, 1199-1207.

Liang, J.O., and Kornfeld, S. (1997). Comparative activity of ADP-ribosylation factor family members in the early steps of coated vesicle formation on rat liver Golgi membranes [published erratum appears in J Biol Chem (1998) *273*, 2488]. J Biol Chem *272*, 4141-4148.

Liang, J.O., Sung, T.C., Morris, A.J., Frohman, M.A., and Kornfeld, S. (1997). Different domains of mammalian ADP-ribosylation factor 1 mediate interaction with selected target proteins. J Biol Chem *272*, 33001-33008.

Liljedahl, M., Maeda, Y., Colanzi, A., Ayala, I., Van Lint, J., and Malhotra, V. (2001). Protein kinase D regulates the fission of cell surface destined transport carriers from the *trans*-Golgi network. Cell *104*, 409-420.

Lippincott-Schwartz, J., Yuan, L.C., Bonifacino, J.S., and Klausner, R.D. (1989). Rapid redistribution of Golgi proteins into the ER in cells treated with brefeldin A: evidence for membrane cycling from Golgi to ER. Cell *56*, 801-813.

Lippincott-Schwartz, J., and Zaal, K.J. (2000). Cell cycle maintenance and biogenesis of the Golgi complex. Histochem Cell Biol *114*, 93-103.

Liu, J., Prunuske, A.J., Fager, A.M., and Ullman, K.S. (2003). The COPI complex functions in nuclear envelope breakdown and is recruited by the nucleoporin Nup153. Dev Cell *5*, 487-498.

Losev, E., Reinke, C.A., Jellen, J., Strongin, D.E., Bevis, B.J., and Glick, B.S. (2006). Golgi maturation visualized in living yeast. Nature *441*, 1002-1006.

Lowe, M., Rabouille, C., Nakamura, N., Watson, R., Jackman, M., Jamsa, E., Rahman, D., Pappin, D.J., and Warren, G. (1998). Cdc2 kinase directly phosphorylates the *cis*-Golgi matrix protein GM130 and is required for Golgi fragmentation in mitosis. Cell *94*, 783-793.

Lowe, S.L., Wong, S.H., and Hong, W. (1996). The mammalian ARF-like protein 1 (Arl1) is associated with the Golgi complex. J Cell Sci *109*, 209-220.

Lu, L., Horstmann, H., Ng, C., and Hong, W. (2001). Regulation of Golgi structure and function by ARF-like protein 1 (Arl1). J Cell Sci *114*, 4543-4555.

Lucocq, J.M., Pryde, J.G., Berger, E.G., and Warren, G. (1987). A mitotic form of the Golgi apparatus in HeLa cells. J Cell Biol *104*, 865-874.

Lucocq, J., Berger, E., and Hug, C. (1995). The pathway of Golgi cluster formation in okadaic acid-treated cells. J Struct Biol *115*, 318-330.

Macia, E., Luton, F., Partisani, M., Cherfils, J., Chardin, P., and Franco, M. (2004). The GDP-bound form of Arf6 is located at the plasma membrane. J Cell Sci *117*, 2389-2398.

Malsam, J., Gommel, D., Wieland, F.T., and Nickel, W. (1999). A role for ADP ribosylation factor in the control of cargo uptake during COPI-coated vesicle biogenesis. FEBS Lett *462*, 267-272.

Manolea, F., Claude, A., Chun, J., Rosas, J., and Melançon, P. (2008). Distinct functions for Arf guanine nucleotide exchange factors at the Golgi complex: GBF1 and BIGs are required for assembly and maintenance of the Golgi stack and *trans*-Golgi Network, respectively. Mol Biol Cell *19*, 523-535.

Marie, M., Sannerud, R., Avsnes Dale, H., and Saraste, J. (2008). Membrane traffic in the secretory pathway : Take the 'A' train: on fast tracks to the cell surface. Cell Mol Life Sci *65*, 2859-2874.

Marsh, B.J., Mastronarde, D.N., McIntosh, J.R., and Howell, K.E. (2001). Structural evidence for multiple transport mechanisms through the Golgi in the pancreatic β-cell line, HIT-T15. Biochem Soc Trans *29*, 461-467.

Martinez-Menarguez, J.A., Geuze, H.J., Slot, J.W., and Klumperman, J. (1999). Vesicular tubular clusters between the ER and Golgi mediate concentration of soluble secretory proteins by exclusion from COPI-coated vesicles. Cell *98*, 81-90.

Martinez-Menarguez, J.A., Prekeris, R., Oorschot, V.M., Scheller, R., Slot, J.W., Geuze, H.J., and Klumperman, J. (2001). Peri-Golgi vesicles contain retrograde but not anterograde proteins consistent with the cisternal progression model of intra-Golgi transport. J Cell Biol *155*, 1213-1224.

Matsuura-Tokita, K., Takeuchi, M., Ichihara, A., Mikuriya, K. and Nakano, A. (2006).
Live imaging of yeast Golgi cisternal maturation. *Nature* 441, 1007-1010.

Maul, G.G., and Brinkley, B.R. (1970). The Golgi apparatus during mitosis in human melanoma cells in vitro. Cancer Res *30*, 2326-2335.

Mellman, I., and Simons, K. (1992). The Golgi complex: in vitro veritas? Cell *68*, 829-840.

Miles, S., McManus, H., Forsten, K.E., and Storrie, B. (2001). Evidence that the entire Golgi apparatus cycles in interphase HeLa cells: sensitivity of Golgi matrix proteins to an ER exit block. J Cell Biol *155*, 543-555.

Mironov, A.A., Beznoussenko, G.V., Nicoziani, P., Martella, O., Trucco, A., Kweon, H.S., Di Giandomenico, D., Polishchuk, R.S., Fusella, A., Lupetti, P., Berger, E.G., Geerts, W.J., Koster, A.J., Burger, K.N., and Luini, A. (2001). Small cargo proteins and large aggregates can traverse the Golgi by a common mechanism without leaving the lumen of cisternae. J Cell Biol *155*, 1225-1238.

Mironov, A.A., Beznoussenko, G.V., Polishchuk, R.S., and Trucco, A. (2005). Intra-Golgi transport: a way to a new paradigm? Biochim Biophys Acta *1744*, 340-350.

Misteli, T., and Warren, G. (1995a). Mitotic disassembly of the Golgi apparatus *in vivo*. J Cell Sci *108*, 2715-2727.

Misteli, T., and Warren, G. (1995b). A role for tubular networks and a COP I-independent pathway in the mitotic fragmentation of Golgi stacks in a cell-free system. J Cell Biol *130*, 1027-1039.

Mitrovic, S., Ben-Tekaya, H., Koegler, E., Gruenberg, J., and Hauri, H.P. (2008). The cargo receptors Surf4, endoplasmic reticulum-Golgi intermediate compartment (ERGIC)-53, and p25 are required to maintain the architecture of ERGIC and Golgi. Mol Biol Cell *19*, 1976-1990.

Miyamoto, T., Oshiro, N., Yoshino, K., Nakashima, A., Eguchi, S., Takahashi, M., Ono, Y., Kikkawa, U., and Yonezawa, K. (2008). AMP-activated protein kinase phosphorylates Golgi-specific brefeldin A resistance factor 1 at Thr1337 to induce disassembly of Golgi apparatus. J Biol Chem *283*, 4430-4438.

Mogelsvang, S., Marsh, B.J., Ladinsky, M.S., and Howell, K.E. (2004). Predicting function from structure: 3D structure studies of the mammalian Golgi complex. Traffic *5*, 338-345.

Monetta, P., Slavin, I., Romero, N., and Alvarez, C. (2007). Rab1b interacts with GBF1 and modulates both ARF1 dynamics and COPI association. Mol Biol Cell *18*, 2400-2410.

Mossessova, E., Corpina, R.A., and Goldberg, J. (2003). Crystal structure of ARF1*Sec7 complexed with Brefeldin A and its implications for the guanine nucleotide exchange mechanism. Mol Cell *12*, 1403-1411.

Mouratou, B., Biou, V., Joubert, A., Cohen, J., Shields, D.J., Geldner, N., Jurgens, G., Melançon, P., and Cherfils, J. (2005). The domain architecture of large guanine nucleotide exchange factors for the small GTP-binding protein Arf. BMC Genomics *6*, 20.

Muniz, M., Martin, M.E., Hidalgo, J., and Velasco, A. (1997). Protein kinase A activity is required for the budding of constitutive transport vesicles from the *trans*-Golgi network. Proc Natl Acad Sci U S A *94*, 14461-14466.

Munro, S. (2005). The Arf-like GTPase Arl1 and its role in membrane traffic. Biochem Soc Trans *33*, 601-605.

Nelson, D.S., Alvarez, C., Gao, Y.S., Garcia-Mata, R., Fialkowski, E., and Sztul, E. (1998). The membrane transport factor TAP/p115 cycles between the Golgi and earlier secretory compartments and contains distinct domains required for its localization and function. J Cell Biol *143*, 319-331.

Nichols, W.C., Seligsohn, U., Zivelin, A., Terry, V.H., Hertel, C.E., Wheatley, M.A., Moussalli, M.J., Hauri, H.P., Ciavarella, N., Kaufman, R.J., and Ginsburg, D. (1998). Mutations in the ER-Golgi intermediate compartment protein ERGIC-53 cause combined deficiency of coagulation factors V and VIII. Cell *93*, 61-70.

Nickel, W., Malsam, J., Gorgas, K., Ravazzola, M., Jenne, N., Helms, J.B., and Wieland, F.T. (1998). Uptake by COPI-coated vesicles of both anterograde and retrograde cargo is inhibited by GTPγS *in vitro*. J Cell Sci *111*, 3081-3090.

Niu, T.K., Pfeifer, A.C., Lippincott-Schwartz, J., and Jackson, C.L. (2005). Dynamics of GBF1, a Brefeldin A-sensitive Arf1 exchange factor at the Golgi. Mol Biol Cell *16*, 1213-1222.

Nousiainen, M., Sillje, H.H., Sauer, G., Nigg, E.A., and Korner, R. (2006). Phosphoproteome analysis of the human mitotic spindle. Proc Natl Acad Sci U S A *103*, 5391-5396.

Nyfeler, B., Zhang, B., Ginsburg, D., Kaufman, R.J., and Hauri, H.P. (2006). Cargo selectivity of the ERGIC-53/MCFD2 transport receptor complex. Traffic *7*, 1473-1481.

Nyfeler, B., Reiterer, V., Wendeler, M.W., Stefan, E., Zhang, B., Michnick, S.W., and Hauri, H.P. (2008). Identification of ERGIC-53 as an intracellular transport receptor of alpha1-antitrypsin. J Cell Biol *180*, 705-712.

Olsen, J.V., Blagoev, B., Gnad, F., Macek, B., Kumar, C., Mortensen, P., and Mann, M. (2006). Global, in vivo, and site-specific phosphorylation dynamics in signaling networks. Cell *127*, 635-648.

Orci, L., Glick, B.S., and Rothman, J.E. (1986). A new type of coated vesicular carrier that appears not to contain clathrin: its possible role in protein transport within the Golgi stack. Cell *46*, 171-184.

Orci, L., Perrelet, A., and Rothman, J.E. (1998). Vesicles on strings: morphological evidence for processive transport within the Golgi stack. Proc Natl Acad Sci U S A *95*, 2279-2283.

Orci, L., Ravazzola, M., Volchuk, A., Engel, T., Gmachl, M., Amherdt, M., Perrelet, A., Sollner, T.H., and Rothman, J.E. (2000). Anterograde flow of cargo across the Golgi stack potentially mediated via bidirectional "percolating" COPI vesicles. Proc Natl Acad Sci U S A *97*, 10400-10405.

Palade, G. (1975). Intracellular aspects of the process of protein synthesis. Science *189*, 347-358.

Pan, H., Yu, J., Zhang, L., Carpenter, A., Zhu, H., Li, L., Ma, D., and Yuan, J. (2008). A novel small molecule regulator of guanine nucleotide exchange activity of ARF and Golgi membrane trafficking. J Biol Chem *283*, 31087-31096.

Panic, B., Whyte, J.R., and Munro, S. (2003). The ARF-like GTPases Arl1p and Arl3p act in a pathway that interacts with vesicle-tethering factors at the Golgi apparatus. Curr Biol *13*, 405-410.

Patterson, G.H., Hirschberg, K., Polishchuk, R.S., Gerlich, D., Phair, R.D., and Lippincott-Schwartz, J. (2008). Transport through the Golgi apparatus by rapid partitioning within a two-phase membrane system. Cell *133*, 1055-1067.

Pelham, H.R., and Rothman, J.E. (2000). The debate about transport in the Golgi--two sides of the same coin? Cell *102*, 713-719.

Pecot, M.Y., and Malhotra, V. (2004). Golgi membranes remain segregated from the endoplasmic reticulum during mitosis in mammalian cells. Cell *116*, 99-107.

Pepperkok, R., Whitney, J.A., Gomez, M., and Kreis, T.E. (2000). COPI vesicles accumulating in the presence of a GTP-restricted Arf1 mutant are depleted of anterograde and retrograde cargo. J Cell Sci *113*, 135-144.

Peters, P.J., Hsu, V.W., Ooi, C.E., Finazzi, D., Teal, S.B., Oorschot, V., Donaldson, J.G., and Klausner, R.D. (1995). Overexpression of wild-type and mutant ARF1 and ARF6: distinct perturbations of nonoverlapping membrane compartments. J Cell Biol *128*, 1003-1017.

Pfeffer, S.R. (2001). Constructing a Golgi complex. J Cell Biol *155*, 873-875.

Presley, J.F., Cole, N.B., Schroer, T.A., Hirschberg, K., Zaal, K.J., and Lippincott-Schwartz, J. (1997). ER-to-Golgi transport visualized in living cells. Nature *389*, 81-85.

Presley, J.F., Ward, T.H., Pfeifer, A.C., Siggia, E.D., Phair, R.D., and Lippincott-Schwartz, J. (2002). Dissection of COPI and Arf1 dynamics *in vivo* and role in Golgi membrane transport. Nature *417*, 187-193.

Prestle, J., Pfizenmaier, K., Brenner, J., and Johannes, F.J. (1996). Protein kinase C μ is located at the Golgi compartment. J Cell Biol *134*, 1401-1410.

Prunuske, A.J., Liu, J., Elgort, S., Joseph, J., Dasso, M., and Ullman, K.S. (2006). Nuclear envelope breakdown is coordinated by both Nup358/RanBP2 and Nup153, two nucleoporins with zinc finger modules. Mol Biol Cell *17*, 760-769.

Rein, U., Andag, U., Duden, R., Schmitt, H.D., and Spang, A. (2002). ARF-GAP-mediated interaction between the ER-Golgi v-SNAREs and the COPI coat. J Cell Biol *157*, 395-404.

Renault, L., Guibert, B., and Cherfils, J. (2003). Structural snapshots of the mechanism and inhibition of a guanine nucleotide exchange factor. Nature *426*, 525-530.

Robbins, E., and Gonatas, N.K. (1964). The ultrastructure of a mammalian cell during the mitotic cycle. J Cell Biol *21*, 429-463.

Robineau, S., Chabre, M., and Antonny, B. (2000). Binding site of brefeldin A at the interface between the small G protein ADP-ribosylation factor 1 (ARF1) and the nucleotide-exchange factor Sec7 domain. Proc Natl Acad Sci U S A *97*, 9913-9918.

Rojo, M., Pepperkok, R., Emery, G., Kellner, R., Stang, E., Parton, R.G., and Gruenberg, J. (1997). Involvement of the transmembrane protein p23 in biosynthetic protein transport. J Cell Biol *139*, 1119-1135.

Rothman, J.E., and Wieland, F.T. (1996). Protein sorting by transport vesicles. Science *272*, 227-234.

Saraste, J., and Kuismanen, E. (1992). Pathways of protein sorting and membrane traffic between the rough endoplasmic reticulum and the Golgi complex. Semin Cell Biol *3*, 343-355.

Saraste, J., Palade, G.E., and Farquhar, M.G. (1987). Antibodies to rat pancreas Golgi subfractions: identification of a 58- kD *cis*-Golgi protein. J Cell Biol *105*, 2021-2029.

Scales, S.J., Pepperkok, R., and Kreis, T.E. (1997). Visualization of ER-to-Golgi transport in living cells reveals a sequential mode of action for COPII and COPI. Cell *90*, 1137-1148.

Schindler, R., Itin, C., Zerial, M., Lottspeich, F., and Hauri, H.P. (1993). ERGIC-53, a membrane protein of the ER-Golgi intermediate compartment, carries an ER retention motif. Eur J Cell Biol *61*, 1-9.

Schweizer, A., Fransen, J.A., Bachi, T., Ginsel, L., and Hauri, H.P. (1988). Identification, by a monoclonal antibody, of a 53-kD protein associated with a tubulo-vesicular compartment at the *cis*-side of the Golgi apparatus. J Cell Biol *107*, 1643-1653.

Schweizer, A., Fransen, J.A., Matter, K., Kreis, T.E., Ginsel, L., and Hauri, H.P. (1990). Identification of an intermediate compartment involved in protein transport from endoplasmic reticulum to Golgi apparatus. Eur J Cell Biol *53*, 185-196.

Seemann, J., Pypaert, M., Taguchi, T., Malsam, J., and Warren, G. (2002). Partitioning of the matrix fraction of the Golgi apparatus during mitosis in animal cells. Science *295*, 848-851.

Setty, S.R., Shin, M.E., Yoshino, A., Marks, M.S., and Burd, C.G. (2003). Golgi recruitment of GRIP domain proteins by Arf-like GTPase 1 is regulated by Arf-like GTPase 3. Curr Biol *13*, 401-404.

Shaywitz, D.A., Espenshade, P.J., Gimeno, R.E., and Kaiser, C.A. (1997). COPII subunit interactions in the assembly of the vesicle coat. J Biol Chem *272*, 25413-25416.

Shima, D.T., Cabrera-Poch, N., Pepperkok, R., and Warren, G. (1998). An ordered inheritance strategy for the Golgi apparatus: visualization of mitotic disassembly reveals a role for the mitotic spindle. J Cell Biol *141*, 955-966.

Shima, D.T., Haldar, K., Pepperkok, R., Watson, R., and Warren, G. (1997). Partitioning of the Golgi apparatus during mitosis in living HeLa cells. J Cell Biol *137*, 1211-1228.

Shin, H.W., and Nakayama, K. (2004). Guanine nucleotide-exchange factors for Arf GTPases: their diverse functions in membrane traffic. J Biochem (Tokyo) *136*, 761-767.

Stagg, S.M., Gurkan, C., Fowler, D.M., LaPointe, P., Foss, T.R., Potter, C.S., Carragher, B., and Balch, W.E. (2006). Structure of the Sec13/31 COPII coat cage. Nature *439*, 234-238.

Stephens, D.J., and Pepperkok, R. (2001). Illuminating the secretory pathway: when do we need vesicles? J Cell Sci *114*, 1053-1059.

Storrie, B., White, J., Rottger, S., Stelzer, E.H., Suganuma, T., and Nilsson, T. (1998). Recycling of Golgi-resident glycosyltransferases through the ER reveals a novel pathway and provides an explanation for nocodazole-induced Golgi scattering. J Cell Biol *143*, 1505-1521.

Supek, F., Madden, D.T., Hamamoto, S., Orci, L., and Schekman, R. (2002). Sec16p potentiates the action of COPII proteins to bud transport vesicles. J Cell Biol *158*, 1029-1038.

Sutterlin, C., Hsu, P., Mallabiabarrena, A., and Malhotra, V. (2002). Fragmentation and dispersal of the pericentriolar Golgi complex is required for entry into mitosis in mammalian cells. Cell *109*, 359-369.

Sutterlin, C., Lin, C.Y., Feng, Y., Ferris, D.K., Erikson, R.L., and Malhotra, V. (2001). Polo-like kinase is required for the fragmentation of pericentriolar Golgi stacks during mitosis. Proc Natl Acad Sci U S A *98*, 9128-9132.

Szul, T., Garcia-Mata, R., Brandon, E., Shestopal, S., Alvarez, C., and Sztul, E. (2005). Dissection of membrane dynamics of the ARF-guanine nucleotide exchange factor GBF1. Traffic *6*, 374-385.

Szul, T., Grabski, R., Lyons, S., Morohashi, Y., Shestopal, S., Lowe, M., and Sztul, E. (2007). Dissecting the role of the ARF guanine nucleotide exchange factor GBF1 in Golgi biogenesis and protein trafficking. J Cell Sci *120*, 3929-3940.

Taguchi, N., Ishihara, N., Jofuku, A., Oka, T., and Mihara, K. (2007). Mitotic phosphorylation of dynamin-related GTPase Drp1 participates in mitochondrial fission. J Biol Chem *282*, 11521-11529.

Takatsu, H., Yoshino, K., Toda, K., and Nakayama, K. (2002). GGA proteins associate with Golgi membranes through interaction between their GGAH domains and ADP-ribosylation factors. Biochem J *365*, 369-378.

Takizawa, P.A., Yucel, J.K., Veit, B., Faulkner, D.J., Deerinck, T., Soto, G., Ellisman, M., and Malhotra, V. (1993). Complete vesiculation of Golgi membranes and inhibition of protein transport by a novel sea sponge metabolite, ilimaquinone. Cell *73*, 1079-1090.

Tang, B.L., Zhang, T., Low, D.Y., Wong, E.T., Horstmann, H., and Hong, W. (2000). Mammalian homologues of yeast Sec31p. An ubiquitously expressed form is localized to endoplasmic reticulum (ER) exit sites and is essential for ER-Golgi transport. J Biol Chem *275*, 13597-13604.

Tang, D., Mar, K., Warren, G., and Wang, Y. (2008). Molecular mechanism of mitotic Golgi disassembly and reassembly revealed by a defined reconstitution assay. J Biol Chem *283*, 6085-6094.

Tanigawa, G., Orci, L., Amhead, M., Ravazzola, M., Helms, J.B., and Rothman, J.E. (1993). Hydrolysis of bound GTP by ARF proteins triggers uncoating of Golgi-derived COP-coated vesicles. J. Cell Biol. *123*, 1365-1371.

Taylor, T.C., Kahn, R.A., and Melançon, P. (1992). Two distinct members of the ADP-ribosylation factor family of GTP- binding proteins regulate cell-free intra-Golgi transport. Cell *70*, 69-79.

Thingholm, T.E., Jorgensen, T.J., Jensen, O.N., and Larsen, M.R. (2006). Highly selective enrichment of phosphorylated peptides using titanium dioxide. Nature protocols *1*, 1929-1935.

Thyberg, J., and Moskalewski, S. (1992). Reorganization of the Golgi complex in association with mitosis: redistribution of mannosidase II to the endoplasmic reticulum and effects of brefeldin A. J Submicrosc Cytol Pathol *24*, 495-508.

Trucco, A., Polishchuk, R.S., Martella, O., Di Pentima, A., Fusella, A., Di Giandomenico, D., San Pietro, E., Beznoussenko, G.V., Polishchuk, E.V., Baldassarre, M., Buccione, R., Geerts, W.J., Koster, A.J., Burger, K.N., Mironov, A.A., and Luini, A. (2004). Secretory traffic triggers the formation of tubular continuities across Golgi sub-compartments. Nat Cell Biol *6*, 1071-1081.

Tsai, S.C., Adamik, R., Haun, R.S., Moss, J., and Vaughan, M. (1992). Differential interaction of ADP-ribosylation factors 1, 3, and 5 with rat brain Golgi membranes. Proc Natl Acad Sci U S A *89*, 9272-9276.

Vasudevan, C., Han, W., Tan, Y., Nie, Y., Li, D., Shome, K., Watkins, S., Levitan, E., and Romero, G. (1998). The distribution and translocation of the G protein ADP-ribosylation factor 1 in live cells is determined by its GTPase activity. J Cell Sci *111*, 1277-1285.

Velasco, A., Hendricks, L., Moremen, K.W., Tulsiani, D.R., Touster, O., and Farquhar, M.G. (1993). Cell type-dependent variations in the subcellular distribution of α-mannosidase I and II. J Cell Biol *122*, 39-51.

Viaud, J., Zeghouf, M., Barelli, H., Zeeh, J.C., Padilla, A., Guibert, B., Chardin, P., Royer, C.A., Cherfils, J., and Chavanieu, A. (2007). Structure-based discovery of an inhibitor of Arf activation by Sec7 domains through targeting of protein-protein complexes. Proc Natl Acad Sci U S A *104*, 10370-10375.

Vollenweider, F., Kappeler, F., Itin, C., and Hauri, H.P. (1998). Mistargeting of the lectin ERGIC-53 to the endoplasmic reticulum of HeLa cells impairs the secretion of a lysosomal enzyme. J Cell Biol *142*, 377-389.

Volpicelli-Daley, L.A., Li, Y., Zhang, C.J., and Kahn, R.A. (2005). Isoform-selective effects of the depletion of Arfs 1-5 on membrane traffic. Mol Biol Cell 16, 4495-4508.

Ward, T.H., Polishchuk, R.S., Caplan, S., Hirschberg, K., and Lippincott-Schwartz, J. (2001). Maintenance of Golgi structure and function depends on the integrity of ER export. J Cell Biol *155*, 557-570.

Wessels, E., Duijsings, D., Lanke, K.H., van Dooren, S.H., Jackson, C.L., Melchers, W.J., and van Kuppeveld, F.J. (2006a). Effects of picornavirus 3A proteins on protein transport and GBF1-dependent COPI recruitment. J Virol *80*, 11852-11860.

Wessels, E., Duijsings, D., Niu, T.K., Neumann, S., Oorschot, V.M., de Lange, F., Lanke, K.H., Klumperman, J., Henke, A., Jackson, C.L., Melchers, W.J., and van Kuppeveld, F.J. (2006b). A viral protein that blocks Arf1-mediated COP-I assembly by inhibiting the guanine nucleotide exchange factor GBF1. Dev Cell *11*, 191-201.

Whitfield, M.L., Zheng, L.X., Baldwin, A., Ohta, T., Hurt, M.M., and Marzluff, W.F. (2000). Stem-loop binding protein, the protein that binds the 3' end of histone mRNA, is cell cycle-regulated by both translational and posttranslational mechanisms. Mol Cell Biol *20*, 4188-4198.

Xiang, Y., Seemann, J., Bisel, B., Punthambaker, S., and Wang, Y. (2007). Active ADP-ribosylation factor-1 (ARF1) is required for mitotic Golgi fragmentation. J Biol Chem *282*, 21829-21837.

Yeaman, C., Ayala, M.I., Wright, J.R., Bard, F., Bossard, C., Ang, A., Maeda, Y., Seufferlein, T., Mellman, I., Nelson, W.J., and Malhotra, V. (2004). Protein kinase D regulates basolateral membrane protein exit from *trans*-Golgi network. Nat Cell Biol *6*, 106-112.

Yoshihisa, T., Barlowe, C., and Schekman, R. (1993). Requirement for a GTPase-activating protein in vesicle budding from the endoplasmic reticulum. Science *259*, 1466-1468.

Zaal, K.J., Smith, C.L., Polishchuk, R.S., Altan, N., Cole, N.B., Ellenberg, J., Hirschberg, K., Presley, J.F., Roberts, T.H., Siggia, E., Phair, R.D., and Lippincott-Schwartz, J. (1999). Golgi membranes are absorbed into and reemerge from the ER during mitosis. Cell *99*, 589-601.

Zeghouf, M., Guibert, B., Zeeh, J.C., and Cherfils, J. (2005). Arf, Sec7 and Brefeldin A: a model towards the therapeutic inhibition of guanine nucleotide-exchange factors. Biochem Soc Trans *33*, 1265-1268.

Zhang, C., Rosenwald, A.G., Willingham, M.C., Skuntz, S., Clark, J., and Kahn, R.A. (1994). Expression of a dominant allele of human ARF1 inhibits membrane traffic *in vivo*. J. Cell Biol. *124*, 289-300.

Zhang, B., Cunningham, M.A., Nichols, W.C., Bernat, J.A., Seligsohn, U., Pipe, S.W., McVey, J.H., Schulte-Overberg, U., de Bosch, N.B., Ruiz-Saez, A., White, G.C., Tuddenham, E.G., Kaufman, R.J., and Ginsburg, D. (2003). Bleeding due to disruption of a cargo-specific ER-to-Golgi transport complex. Nat Genet *34*, 220-225.

Zhao, X., Claude, A., Chun, J., Shields, D.J., Presley, J.F., and Melançon, P. (2006). GBF1, a *cis*-Golgi and VTCs-localized ARF-GEF, is implicated in ER-to-Golgi protein traffic. J Cell Sci *119*, 3743-3753.

Zhao, X., Lasell, T.K., and Melançon, P. (2002). Localization of large ADP-ribosylation factor-guanine nucleotide exchange factors to different Golgi compartments: evidence for distinct functions in protein traffic. Mol Biol Cell *13*, 119-133.

Zuber, C., Fan, J.Y., Guhl, B., Parodi, A., Fessler, J.H., Parker, C., and Roth, J. (2001). Immunolocalization of UDP-glucose:glycoprotein glucosyltransferase indicates involvement of pre-Golgi intermediates in protein quality control. Proc Natl Acad Sci U S A *98*, 10710-10715.

CHAPTER SEVEN: APPENDIX

This appendix contains several unpublished results that have been excluded from the previously presented Results chapters. Although the results presented in this appendix do not fit directly with the continuity of the Results sections of the previous chapters, they will be a useful resource for future members of the laboratory.

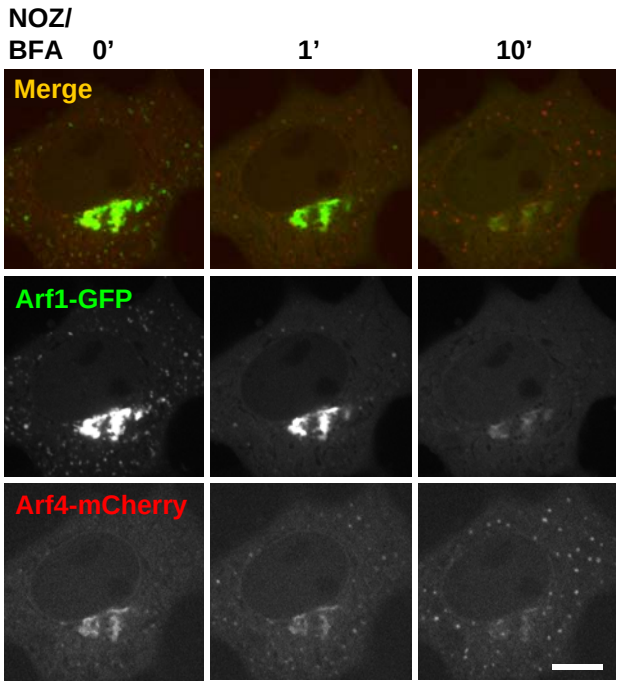

Figure 7.1 Arf4, but not Arf1, remains associated with the ERGIC after treatment with nocodazole and BFA.
COS1 cells co-transfected with plasmids encoding Arf1-GFP and Arf4-mCherry were incubated on ice for 2 min followed by treatment with 20 µg NOZ/ml medium for 15 min on ice. Several minutes (5-10 min) after transfer to a heated stage, cells were treated with BFA and imaged every five seconds for 10 min. Images correspond to frames captured at the indicated time points. Bottom panels show single and merged images acquired in the boxed area from the mCherry and GFP channels. Bar, 10 µm.

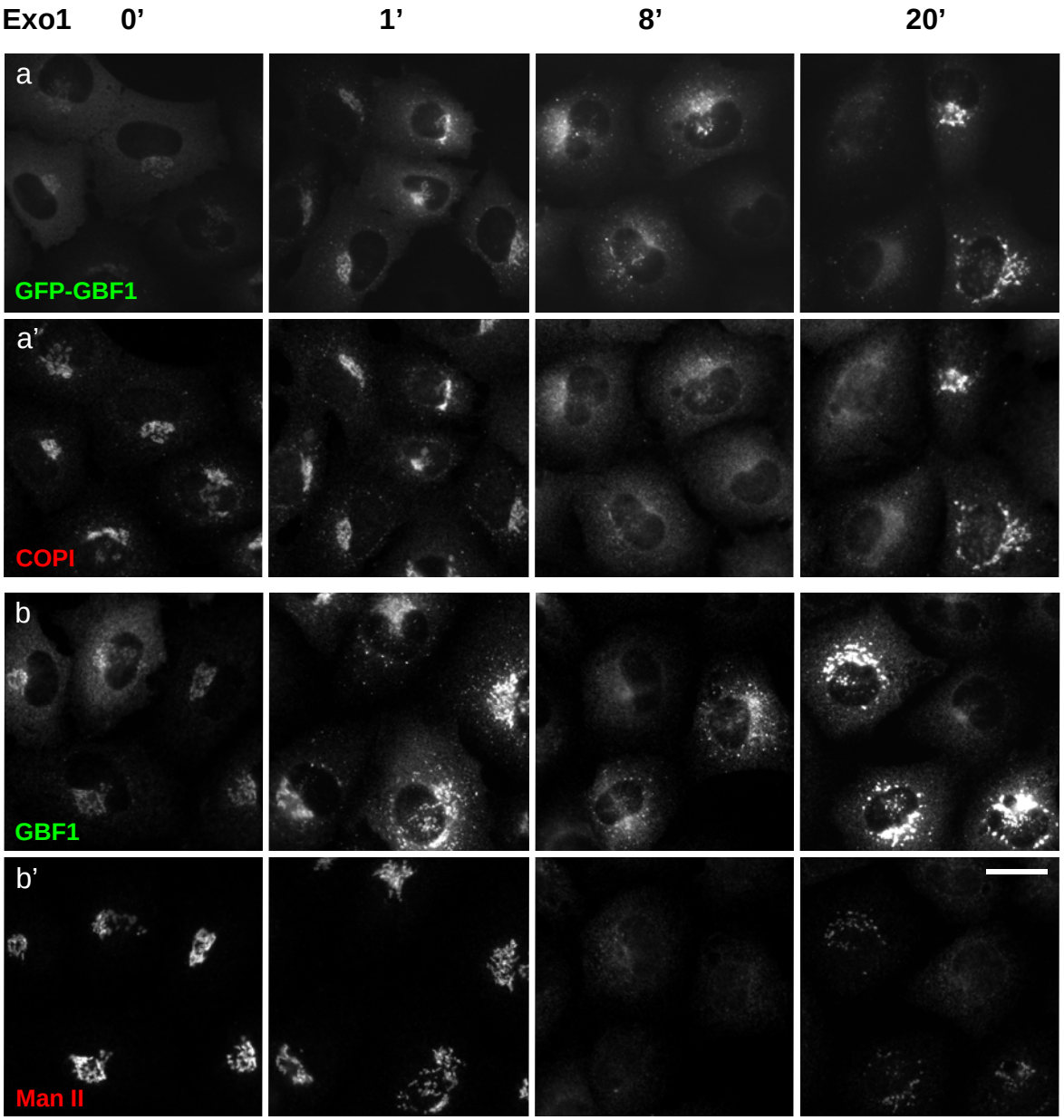

Figure 7.2 Overexpression of GBF1 compensates for the effect of Exo1.
NRK-GFP-GBF1 cells were treated with 100 µM Exo1 for the indicated times, fixed, and then processed for indirect immunofluorescence with antibodies directed against COPI (a’, red channel), GBF1 (b, green channel), and mannosidase II (b’, red channel). Bar, 20 µm.

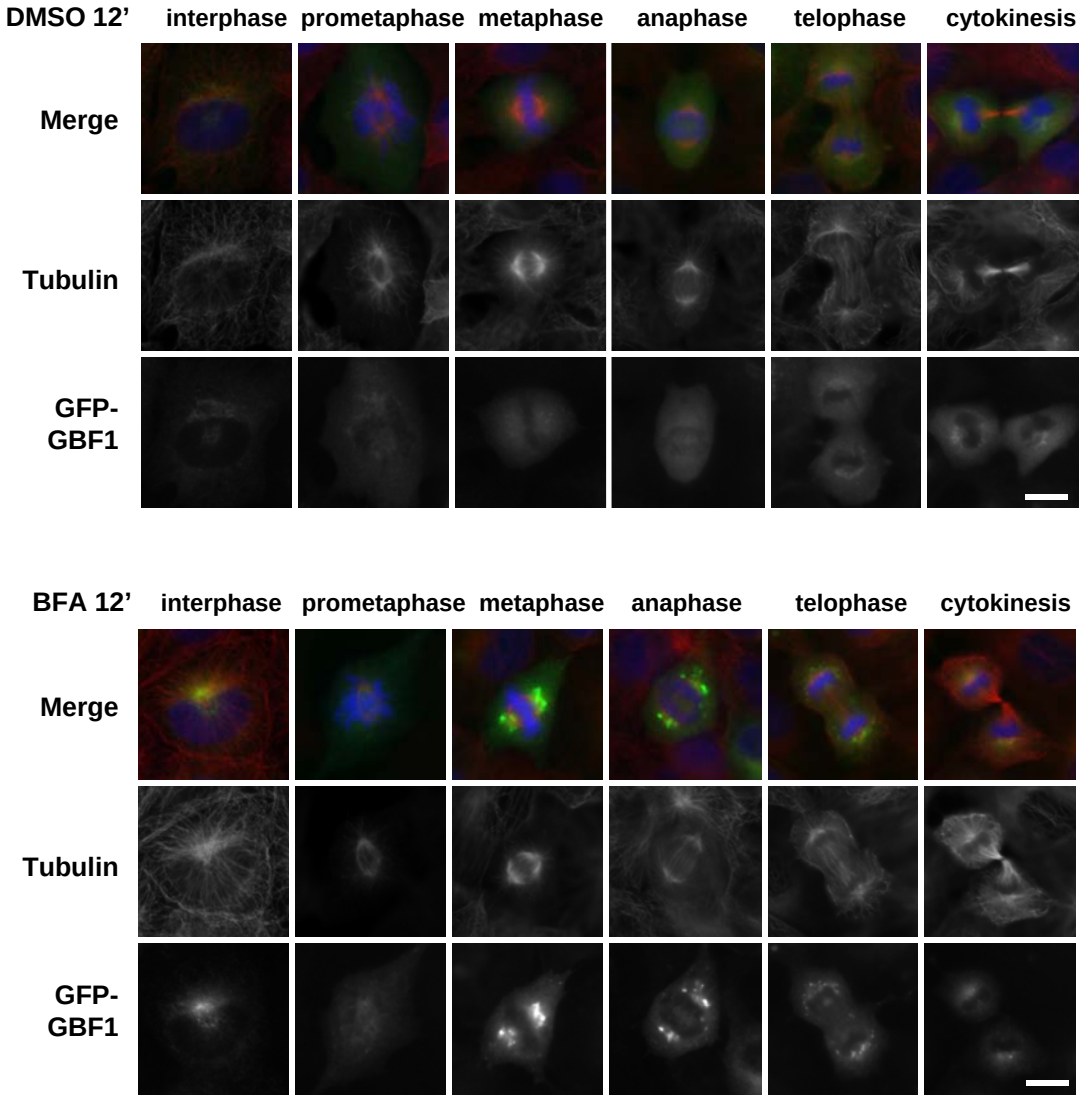

Figure 7.3 Microtubules for facilitating redistribution of Golgi enzymes following BFA treatment may be unavailable during mitosis.
NRK-GFP-GBF1 cells were treated with DMSO or 5 µg BFA/ml medium for 12 min, fixed, and then processed for indirect immunofluorescence with antibodies directed against tubulin (red channel) and staining with DAPI (merged images). Bar, 10 µm.

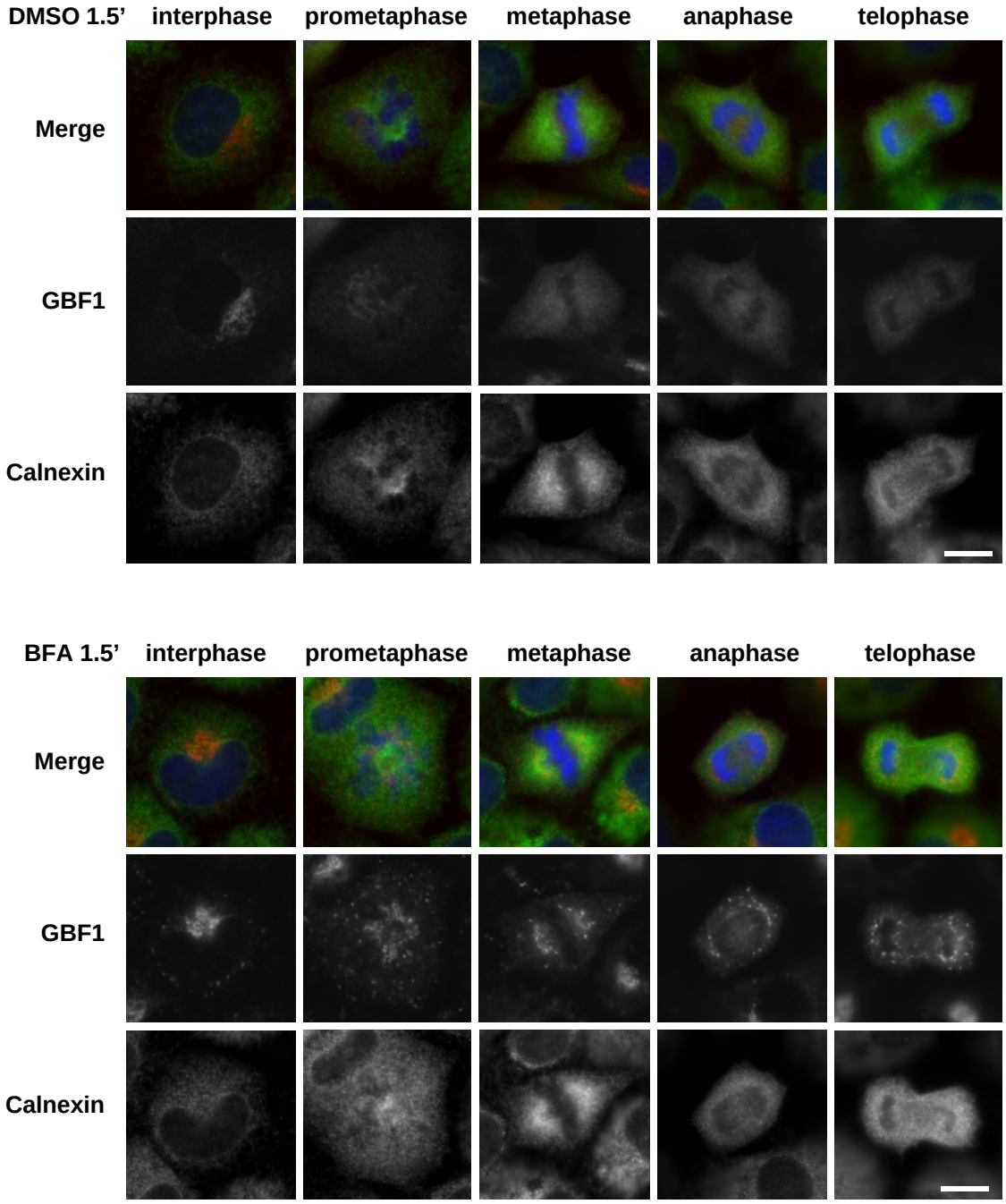

Figure 7.4 The ER marker calnexin does not concentrate on GBF1-positive mitotic structures after BFA treatment.
NRK were treated with DMSO or 5 µg BFA/ml medium for 1.5 min, fixed, and then processed for indirect immunofluorescence with antibodies directed against GBF1 (red channel) or calnexin (green channel) and staining with DAPI (merged images). Bar, 10 µm.

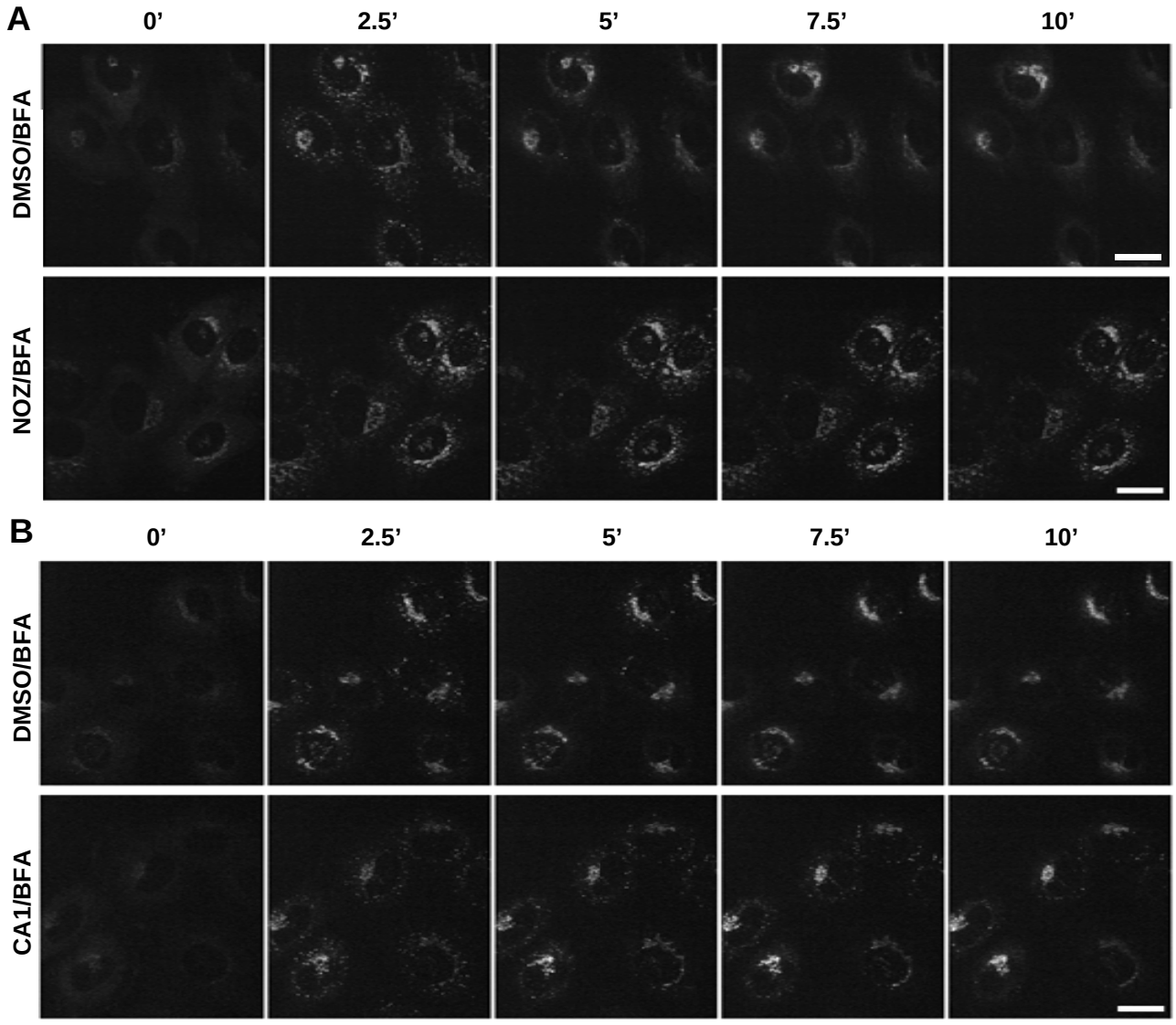

Figure 7.5 Nocodazole (NOZ) and coumermycin A1 (CA1) treatment stabilizes GBF1-positive peripheral puncta.

A) NRK cells stably expressing GFP-GBF1 were treated on ice for 15 min with either DMSO or 20 µg NOZ/ml medium. Following a 2 min warm-up at 37°C for DMSO and NOZ treated cells, live cells were examined at 37°C by time lapse-imaging. Z-stacks of 6 or 8 slices each 1 µm thick were acquired continuously after addition of 5 µg BFA/ml medium. Still images from projected stacks at indicated times are shown. Bars, 20 µm.

B) NRK cells stably expressing GFP-GBF1 were treated for 30 minutes at 37°C with DMSO or 70 µM CA1. Cells were examined and displayed as described in panel A above. Bar, 20 µm.

A version of the results for Figure 7.5A has been published in Zhao *et al.*, 2006 Journal of Cell Science, *119*: 3743-53.